THE STRUCTURE OF THE NON-POLAR PHASE OF $RbHSO_4$

THE STRUCTURE OF THE NON-POLAR PHASE OF $RbHSO_4$

By

JOHN PATRICK ASHMORE, B.Sc.

A Thesis

Submitted to the Faculty of Graduate Studies in

Partial Fulfilment of the Requirements

for the Degree

Doctor of Philosophy

McMaster University

May 1971

DOCTOR OF PHILOSOPHY (1971) McMASTER UNIVERSITY
Physics Hamilton, Ontario

TITLE: The Structure of the Non-Polar Phase of $RbHSO_4$

AUTHOR: John Patrick Ashmore, B.Sc.
(University of Western Ontario)

SUPERVISOR: Professor H.E. Petch

NUMBER OF PAGES: viii, 131

SCOPE AND CONTENTS:

An x-ray and neutron diffraction study of $RbHSO_4$ has been carried out at 23°C as a step towards understanding its ferroelectric behaviour at lower temperatures. The results of this study show a pseudo orthorhombic, ordered structure consisting of HSO_4^- and Rb^+ ions which can be arranged in a lattice similar to that of NaCℓ. Hydrogen bonds in which the protons are acentrically ordered are found to link the sulphate groups together. A comparison with the structure of NH_4HSO_4 determined independently by Nelmes (1970), shows remarkable similarities. The structure is also in agreement with the results of nuclear magnetic resonance and infrared absorption experiments.

Also, some x-ray and neutron diffraction data has been collected at -40°C in the ferroelectric phase. Although attempts to refine the low temperature structure met with only partial success it can be stated that there are no large atomic displacements and the polar phase is therefore similar to that of the non-polar phase.

ACKNOWLEDGEMENTS

The author would like to thank Professor H. E. Petch for suggesting this project and for his guidance and help. I would also like to thank Dr. I. D. Brown for his many suggestions and Dr. C. Calvo who, in spite of a heavy schedule, provided many helpful suggestions during the final stages of the work.

I am grateful to Dr. W.C. Hamilton, Dr. C.K. Johnson, Dr. J.S. Stephens and Dr. J.S. Rutherford for the use of their computer programs.

Special thanks are due to my wife for her patience and understanding and also for her encouragement.

This research has been supported by the National Research Council of Canada. The author is grateful to his wife, The Ontario Government and the National Research Council of Canada for personal financial assistance.

TABLE OF CONTENTS

LIST OF FIGURES

LIST OF TABLES

CHAPTER I

(A) Discussion of Ferroelectricity

A ferroelectric material is one which exhibits a reversible spontaneous electric dipole moment. If an electric field is applied to a ferroelectric material and the resulting polarization is plotted as a function of the applied field a hysteresis curve will be observed. The existence of this curve is sufficient to indicate the presence of ferroelectricity. Because of the similarity between this hysteresis curve and the one found in ferromagnetism the effect has been called ferroelectricity.

Rochelle salt (sodium potassium tartrate tetrahydrate) was the first ferroelectric material to be discovered (Valasek, 1921). Fourteen years later KH_2PO_4 was discovered to be ferroelectric below $-150^{o}C$ (Busch and Scherrer, 1935) and in 1945 the ferroelectric properties of $BaTiO_3$ were discovered independently by von Hippel et al (1945) and Wul and Goldman (1946). By 1960 the number of known ferroelectrics had rapidly increased to 76 (Jona and Shirane, 1962). It is interesting to note that seventy five percent of these compounds contain hydrogen atoms.

With a few exceptions, most ferroelectrics lose their ferroelectric properties above some temperature called the Curie temperature. Among these exceptions are guanidine sulphate

hexahydrate (Holden et al, 1955; Remeika and Merz, 1956) and $LiH_3(SeO_3)_2$ (Pepinsky and Vedam, 1959). These compounds either melt or decompose before they lose their spontaneous polarization. At the Curie temperature ferroelectrics exhibit a discontinuity in the dielectric constant. This is most noticeable along the direction in which the spontaneous polarization is a maximum (this direction is called the polar axis).

In order for a material to be ferroelectric certain conditions must be placed on its symmetry. For spontaneous polarization to occur in a crystal it is necessary that the structure be polar, i.e. if a vector (representing an electric dipole) is associated with a point in the crystal the symmetry operations must be capable of generating a resultant non-zero vector. The possible combinations of symmetry operations give rise to 32 crystal classes or point groups. Out of these 32 point groups only 21 are non-centrosymmetric and only 10 of these are polar. These ten, sometimes referred to as the pyroelectric classes[1], are C_1, C_2, C_3, C_4, C_6, C_S, C_{2v}, C_{3v}, C_{4v}, C_{6v}. Spontaneous polarization is a "vector" quantity and is restricted to compounds which belong to one of the polar point groups. Phenomena

---

(1) A pyroelectric is a material which exhibits a spontaneous polarization when it is heated or cooled uniformly.

such as piezoelectricity in which an electrical charge is induced in the material by the application of a mechanical stress require only that the material be non-centrosymmetric. As a result a piezoelectric material can belong to any of the 21 non-centrosymmetric point groups. It follows then that a ferroelectric material is necessarily piezoelectric but that a piezoelectric material is not necessarily ferroelectric.

Above the Curie temperature the crystal becomes non-polar (sometimes this non-polar phase is referred to as the paraelectric phase in analogy with the paramagnetic phase of a ferromagnetic material) and can belong to any of the 22 non-polar point groups. When the material changes from a non-polar to a polar phase some symmetry element belonging to the non-polar phase is normally lost. The other symmetry elements remain so that the polar phase still resembles the non-polar phase. The polar phase is thus a "pseudosymmetric" structure in that it has some resemblance to the higher symmetry non-polar phase from which it originates.

Aizu (1966) has shown that for a given non-polar point group there are specific point groups to which the crystal must belong if it is to be ferroelectric. If the structure is not capable of easily losing the symmetry elements necessary to belong to one of these point groups no ferroelectric transition will occur.

There are two approaches to the study of ferroelectricity. One, the macroscopic approach, involves the measurement of the bulk properties such as the dielectric constant, switching times and specific heats of the materials. These experiments are complemented by macroscopic theories, an example of which is Devonshire's theory of the ferroelectric phase transition (Devonshire, 1949). Such theories are "thermodynamic" in their approach and while they are capable of describing the bulk properties of ferroelectrics they can give no explanation of the phenomena on an atomic level.

The other approach involves experiments of a microscopic nature. Crystallographic studies in conjunction with nuclear magnetic resonance and infrared experiments can provide insight into the microscopic aspects of ferroelectricity. As a result microscopic theories of ferroelectricity have been developed and attempts have been made to describe the ferroelectric mechanism on an atomistic level. Slater's theory of KH_2PO_4 (Slater, 1941), in which structural information is used to calculate the Curie temperature, is one such example. More recently Cochran's lattice dynamical theory has been most successful in describing the ferroelectric behaviour on a microscopic level, (Cochran, 1960, 1961). His theory shows that in "perovskite" crystals ($BaTiO_3$ for example) the onset of the ferroelectric properties is due to the instability of some vibrational mode in the crystal. This theory is capable of describing

ferroelectric behaviour of $BaTiO_3$ but it cannot describe the properties of more complex ferroelectrics such as KH_2PO_4 or Rochelle salt.

There are many ways of classifying the different types of ferroelectricity found in various compounds. Each classification has its particular merits and drawbacks and has been put forward with the purpose of emphasizing some aspect of the problem of ferroelectricity. In this study it suffices to divide the ferroelectrics into two broad categories; those that contain hydrogen atoms and those that do not. The philosophy behind such a categorization is that since the energy required to change the hydrogen bonding scheme is quite small it is possible that the hydrogen atom may play an important role in the ferroelectric behaviour of the material. This idea was substantiated experimentally by studies carried out on KH_2PO_4 in which it was shown that the hydrogen atoms do participate in the transition (Bacon and Pease, 1953, 1955). Work on other hydrogen containing ferroelectrics such as $NH_4(SO_4)_2$ (Schlemper and Hamilton, 1966) and Colemanite (Hainsworth and Petch, 1966) also indicated that the hydrogen atoms play an important role in the transition.

One of the objectives of a study of a hydrogen containing ferroelectric is to determine what changes occur in the structure of the compound at the transition and how these changes are related to the hydrogen atoms. This knowledge can then be used, in conjunction with other experimental data, to try to understand the nature of

ferroelectricity on a microscopic, atomistic basis. Such an understanding must be able to explain why the spontaneous polarization occurs, why it is reversible and why the ferroelectric properties disappear above the Curie temperature.

(B) Review of literature on $RbHSO_4$ and NH_4HSO_4

Early work by Pepinsky and Vedam (1960) revealed the ferroelectric nature of $RbHSO_4$ and also showed that it was isomorphous with NH_4HSO_4. The ferroelectric properties of NH_4HSO_4 were discovered first by Pepinsky, Vedam, Hoshino and Okaya (1958, hereafter referred to as PVHO) and were attributed to the N–H···O bonds as in the case of $NH_4(SO_4)_2$ (Matthias and Remeika, 1956). Pepinsky and Vedam (1960), were then surprised to find that $RbHSO_4$, which is isomorphous with the ammonium salt, was also ferroelectric. Because of the close similarity between these two compounds their properties will be discussed and summarized in this introductory chapter.

In the case of NH_4HSO_4, PVHO noted that there were two phase transitions at -3^oC and -119^oC. At -3^oC the compound underwent a transition from a paraelectric to a ferroelectric state. The spontaneous polarization appeared below -3^oC and remained until -119^oC where it vanished, implying that the crystal had either returned to a paraelectric state or had become anti-ferroelectric. The dielectric constant showed a large discontinuity at -3^oC and a small step

FIGURE 1

NH_4HSO_4 Dielectric constant and spontaneous polarisation vs temperature (PVHO)

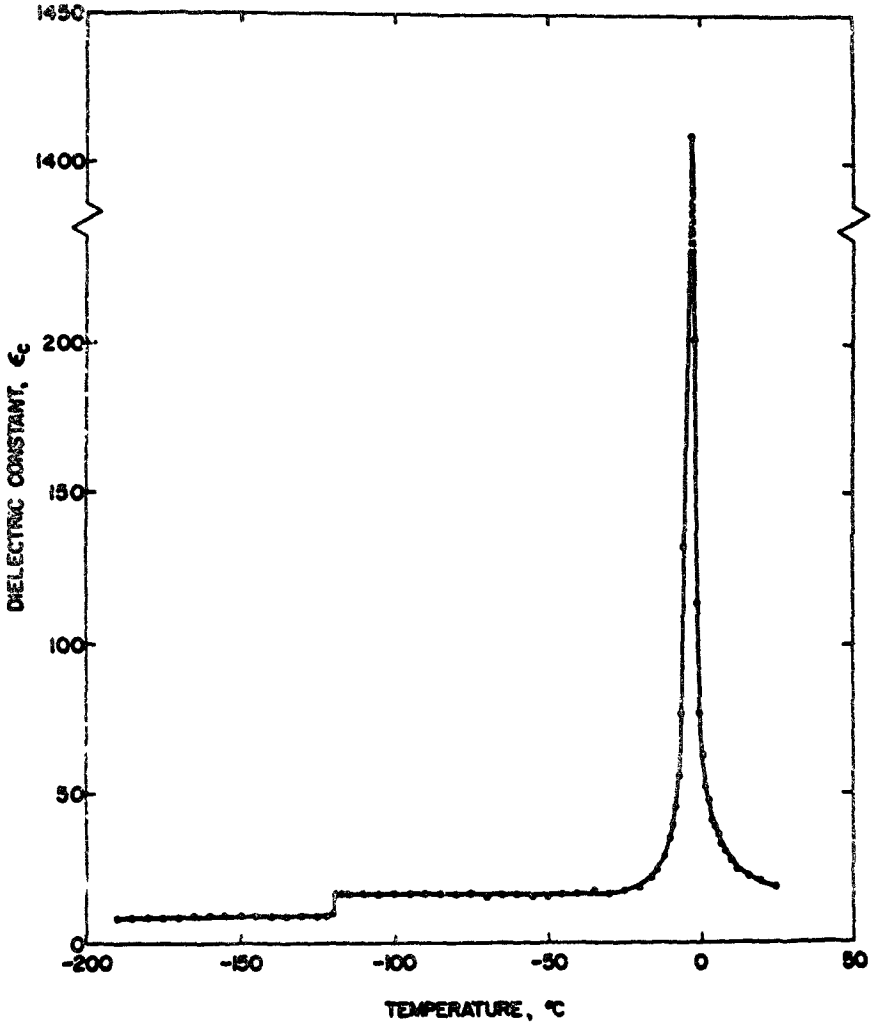
1450
1400
200
150
100
50
0
DIELECTRIC CONSTANT, ϵ_c
-200
-150
-100
-50
0
50
TEMPERATURE, °C

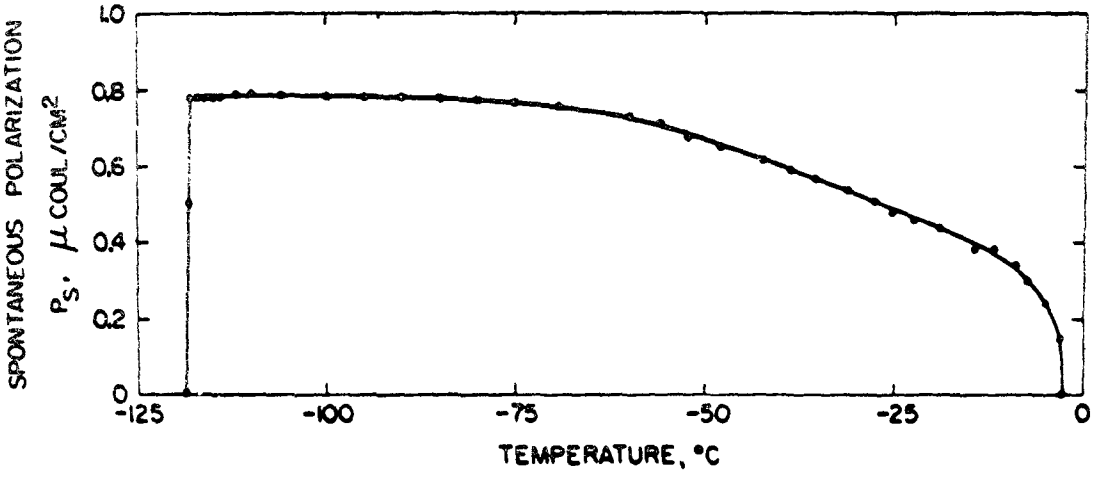
1.0
0.8
0.6
0.4
0.2
0
SPONTANEOUS POLARIZATION
P_S, μ COUL./CM^2
-125
-100
-75
-50
-25
0
TEMPERATURE, °C

discontinuity at -119°C. These points are illustrated in Fig. 1 which shows the small-signal dielectric constant at 10Kcs versus temperature and the spontaneous polarization versus temperature curve respectively. Because of the large dielectric constant and the shape of the P versus E curve just above the -3°C transition PVHO concluded that the upper transition must be second order. The large heat of transition (0.34 kcal/mole) at -119°C and the fact that the crystal shattered led the authors to conclude that this must be a first order transition. The specific heat curve shows a double peak at the -119°C transition which is reminiscent of the thermal behaviour of $NH_4(SO_4)_2$ (Vedam, Okaya and Pepinsky, 1958). PVHO also report the presence of thermal hysteresis at both transitions, the larger being at -119°C. In $RbHSO_4$ the appearance of a reversible spontaneous dipole moment below -15°C and the large discontinuity in the dielectric constant (small-signal at 10Kcs) show that the crystal has undergone a transition to a ferroelectric state. The dielectric constant and spontaneous polarization as a function of temperature for $RbHSO_4$ are shown in Fig. 2. The dielectric constants ϵ_a and ϵ_b, along the $\bar{a}$ and $\bar{b}$ axes, were found to have a value of 7 and 8 and to decrease uniformly with temperature to values of 5 and 6 at -119°C. The P_s versus temperature curve shows that P_s reaches a constant value of 0.65 μcoul/cm^2 below T = -119°C. An attempt to measure the heat of

FIGURE 2

$RbHSO_4$ Dielectric constant and spontaneous polarisation vs temperature (from Pepinsky and Vedam, 1960)

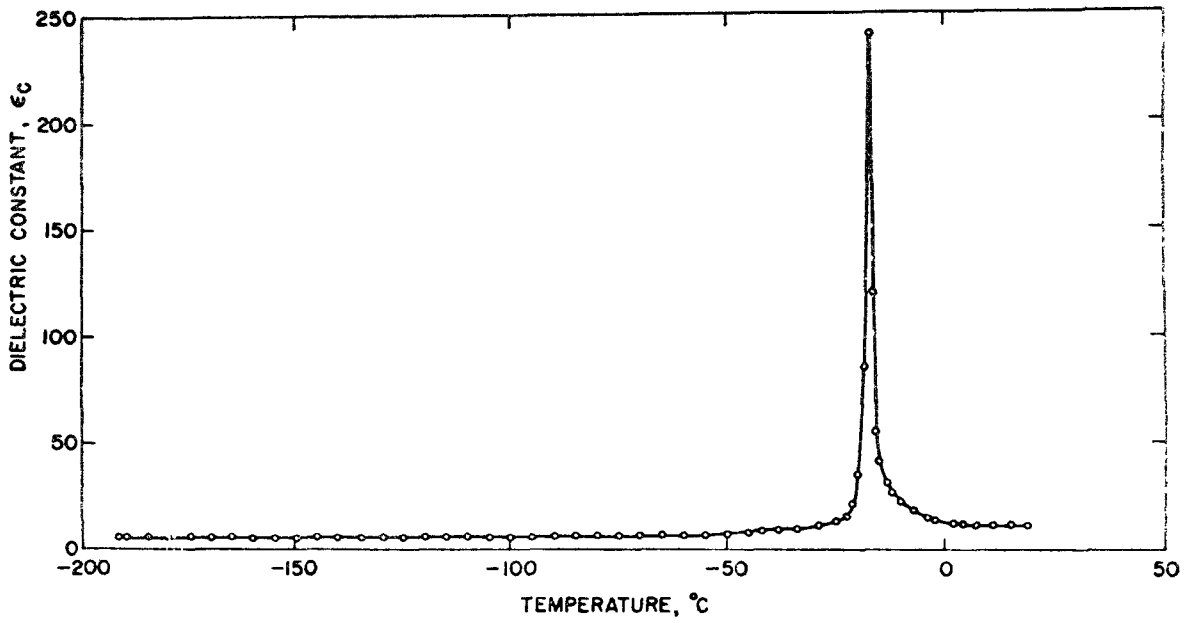
DIELECTRIC CONSTANT, ϵ_c
250
200
150
100
50
0
-200
-150
-100
-50
0
50
TEMPERATURE, °C

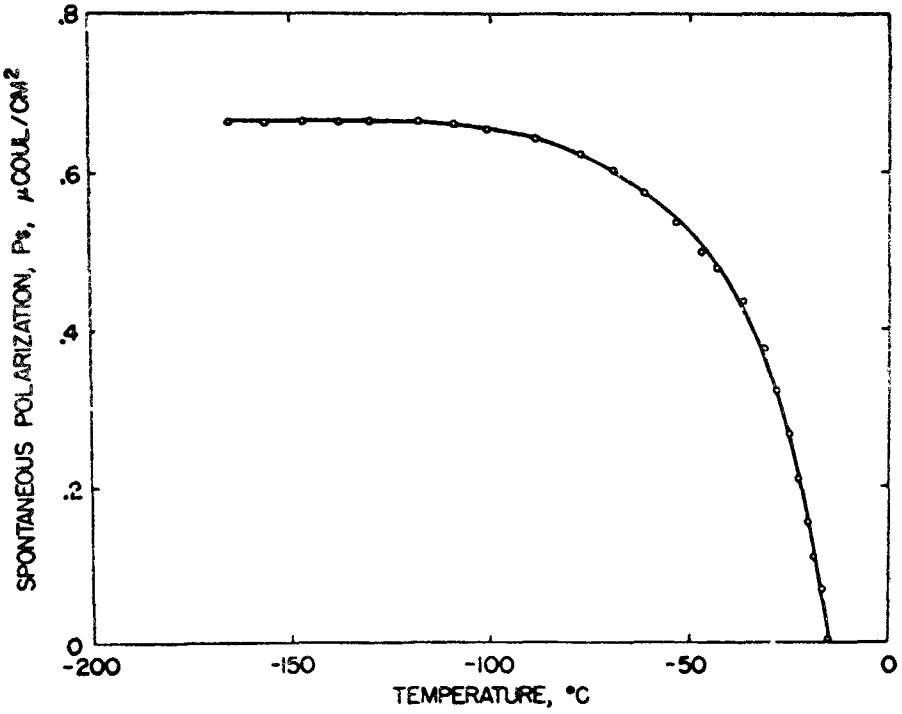
SPONTANEOUS POLARIZATION, P_s, μCOUL/CM^2
.8
.6
.4
.2
0
-200
-150
-100
-50
0
TEMPERATURE, °C

transition showed that it must be less than 25 cal/mole. These observations and the shape of the P versus E curve near the transition temperature indicate that it is a second order transition.

The earliest x-ray structure determination of $RbHSO_4$ was done by Bengtssen (1941). From h0ℓ, 0kℓ and hk0 rotation photographs he assigned an orthorhombic unit cell of dimensions $a = 24.61\text{Å}$; $b = 4.62\text{Å}$; $c = 14.80\text{Å}$ with symmetry Cmma and provided estimated coordinates of the Rb atoms. Later it was shown that $RbHSO_4$ is pseudo-orthorhombic with space group $B2_1/a$ and cell parameters $a = 24.61\text{Å}$; $b = 4.622\text{Å}$; $c = 14.87\text{Å}$; $\beta = 89.89^\circ$ (Pepinsky and Vedam, 1960). This can be shown to be equivalent to the monoclinic space group $P2_1/c$ with $a = 14.356\text{Å}$; $b = 4.622\text{Å}$; $c = 14.807\text{Å}$; with $\beta = 120.9^\circ$. (See Fig. 15). The latter authors also showed that NH_4HSO_4 and $RbHSO_4$ are isomorphous.

Recently a complete x-ray and partial neutron diffraction determination of the structure of the room temperature paraelectric phase of NH_4HSO_4 has been completed by Nelmes (1970). In order to compare these results with those of the present study a detailed discussion of the structure of NH_4HSO_4 will be postponed until Chap. 5.

Since the discovery of the ferroelectric properties of NH_4HSO_4 by PVHO several papers dealing with infra-red absorption studies (Myasnikova and Yatsenko, 1962), Raman scattering (Bazhulin, Myasnikova and Rakov, 1964) and nuclear magnetic resonance (NMR)

experiments (Burns 1961; Miller, Blinc, Brenman and Waugh, 1962) have been published. An inelastic neutron scattering experiment has been reported by Rush and Taylor (1965).

The basic purpose of these studies was to determine if there was any change in the dynamics of the NH_4^+ or $SO_4^=$ ions or the single hydrogen atom as the crystal underwent the ferroelectric transition. The infra-red experiments (Myasnikova and Yatsenko, 1962) and the Raman scattering experiments (Bazhulin, Myasnikova and Rakov, 1964) showed no significant change in the vibrational frequencies of the $SO_4^=$ ion in $RbHSO_4$ or NH_4HSO_4 as the crystal temperature was lowered through the transition temperature.

None of the preceding experiments show a significant change in the NH_4^+ spectra above and below the -3^oC transition. Rush and Taylor, (1965) noted that there was very little difference between the time of flight spectra around 260 cm^{-1} (a frequency corresponding to torsional motion of the NH_4^+ ion) at $T = 23^oC$ and at $T = -96^oC$ implying that the motion of the NH_4^+ ion does not change significantly at the -3^oC transition. They further report the splitting of the spectra around 260 cm^{-1} at $T = -148^oC$ (a temperature below the "lower transition" at $T = -119^oC$) indicating that some ordering of the NH_4^+ ions may occur at this transition. The proton spin-lattice relaxation experiments of Miller, Blinc, Brenman and Waugh (1962) showed no change in the relaxation times above and below the transition

temperature and thus were in agreement with the previous conclusions. In the ferroelectric phase the potential barrier hindering the reorientation of the NH_4^+ ion is still low (2 ± 0.5 kcal/mole)implying that the NH_4^+ ion reorientation frequency is still high. At T = -148°C these experiments show a noticeable change in the slope of the logarithm of the proton spin-lattice relaxation time versus 1/T plot indicating a change in the motion of the NH_4^+ ion at this temperature.

Below T = -3°C the infra-red absorption peak at 3165 cm^{-1} was observed to split into two components (Myasnikova and Yatsenko, 1962). The authors assigned this peak to the O-H stretching mode and attributed the splitting to the proton tunneling along the O–H· · · O bond.

There is general agreement that the $SO_4^=$ ion shows little change when the crystal temperature passes through the upper and lower transitions. Furthermore the authors of the preceding papers all agree that there is little difference in the dynamics of the NH_4^+ ion above and below the "upper transition" but that there is a change at the lower transition temperature.

Similar experiments have been performed on crystals of $RbHSO_4$. Infra-red experiments (Myasnikova and Yatsenko, 1962) showed little change in the spectra of the $SO_4^=$ as the crystal changed from a non-polar to a polar phase. Bazhulin, Myasnikova and Rakov (1964) noted, as in the case of NH_4HSO_4, a gradual change in the frequency and intensity of one of the vibrational frequencies of the $SO_4^=$ ion as the

temperature was lowered. The "hydrogen bond" peak at 3200 cm^{-1} is reported to split into two components when the crystal temperature is lowered at -15°C (Myasnikova and Yatsenko, 1962). As in the case of NH_4HSO_4 the authors suggest that the splitting could be due to proton tunneling along the O–H···O bond in the polar phase.

These suggestions are in agreement with the results of a recent proton magnetic resonance study (Silvidi, Falzone, and Roupe, 1969). The authors report no sudden change in the second moment near the transition temperature and further report that there is a gradual decrease in the second moment as the temperature is lowered. The second moment results imply that there is no change in the dynamics of the protons near the transition temperature. This is confirmed by the proton spin-lattice relaxation times measurements which also show no sudden change at T = -15°C. The authors report observing a large amount of hysteresis in the T_1 versus 1/T curve at temperatures below T = -15°C and suggest that this is evidence that some change which may contribute to the ferroelectric properties is being "frozen in".

(C) Purpose of this Research

Although a substantial amount of work had been done on NH_4HSO_4 and $RbHSO_4$, little progress had been made in interpreting the results in terms of an atomistic model of the ferroelectric behaviour of either material. The largest obstacle to further progress was a lack of knowledge of their structures. Through personal communication it was

known that a crystal structure determination of NH_4HSO_4 was planned by R. J. Nelmes under the supervision of Professor Cochran at the University of Edinburgh. It was decided to undertake a parallel investigation of $RbHSO_4$ in the hope that information about these two similar crystals would be complementary and help lead to an understanding of their ferroelectric behaviour.

The plan of this study was to use x-ray diffraction techniques to determine the basic structure of the heavy atoms in the paraelectric phase and then to use neutron diffraction to determine the hydrogen positions. It was considered essential to locate the hydrogen atoms as it was anticipated that they play an important role in the ferroelectric transition. In a number of ferroelectrics it has been possible to infer the mechanism of the ferroelectric behaviour from a knowledge of the paraelectric phase alone and it was hoped that this might be possible also in $RbHSO_4$.

CHAPTER II

THEORY

This chapter is not intended to be a detailed and rigorous description of the methods and theory of crystallography. There are several excellent books to which the reader can refer for more explicit details. Among these are: "Determination of Crystal Structures" by H. Lipson and W. Cochran (1966), "Crystal Structure Analysis" by M.J. Buerger (1960), and "The Theory of X-ray Diffraction in Crystals" by W.H. Zachariasen (1945). It is hoped that this chapter will acquaint the reader with the basics of crystallography and also provide definitions of certain quantities which will be used frequently throughout the thesis.

Both neutron and x-ray diffraction experiments were used in this study of $RbHSO_4$. While the two methods are similar there are some important differences which will be discussed at the appropriate time.

Ideally, a crystal can be considered to be made up of scattering elements[1], groups of which are related to translational symmetry. Such an array of scatterers can be related to a three dimensional array of points called a lattice so that identical points occur at $\bar{r}$ and $\bar{r} + \bar{s}$ where $\bar{r}$ is a vector from the origin to any point in the crystal and

---

(1) The fact that the scatterers are actually vibrating will be considered later in the discussion of the temperature factor.

$\bar{s} = u\bar{a} + v\bar{b} + w\bar{c}$ where $\bar{a}$, $\bar{b}$ and $\bar{c}$ are the primitive translation vectors and u, v, and w are integers. The volume defined by the vectors $\bar{a}$, $\bar{b}$, and $\bar{c}$ is repeated by the translational symmetry of the crystal and is called a unit cell. This cell, if chosen to be the smallest volume, belongs to one of the 14 possible space lattices or Bravais lattices. (These 14 space lattices originate from the 7 crystal systems).

Consider a parallel beam of monochromatic radiation whose direction of propogation is defined by a vector $\bar{K}_o$ (whose magnitude is $1/\lambda$; λ = the wavelength) and let this radiation be scattered into the direction $\bar{K}$ by a large three dimensional array of scatterers whose positions are described by the vector $\bar{t} = u\bar{a} + v\bar{b} + w\bar{c}$. The intensity distribution of the scattered radiation can be expressed by the function $|S|^2$ where

$$S = \frac{\sin 2\pi U(\bar{K} - \bar{K}_o).\bar{a}}{\sin 2\pi(\bar{K} - \bar{K}_o).\bar{a}} \times \frac{\sin 2\pi V(\bar{K} - \bar{K}_o).\bar{b}}{\sin 2\pi(\bar{K} - \bar{K}_o).\bar{b}} \times \frac{\sin 2\pi W(\bar{K} - \bar{K}_o.\bar{c}}{\sin 2\pi(\bar{K} - \bar{K}_o).\bar{c}}$$

and U, V, W are the number of scattering elements along $\bar{a}$, $\bar{b}$, $\bar{c}$. These numbers are very large and thus S is a rapidly oscillating function with many minima and maxima. The conditions for the maxima are given by:

$$\bar{a}.(\bar{K} - \bar{K}_o) = h$$

$$\bar{b}.(\bar{K} - \bar{K}_o) = k$$

$$\bar{c}.(\bar{K} - \bar{K}_o) = \ell.$$

These are the Laue equations and provide the conditions necessary for a maximum in the intensity of the scattered radiation. The quantities h k ℓ are integers and are commonly referred to as the Miller Indices.

Consider the vector $\bar{r}^* = K_1\bar{a}^* + K_2\bar{b}^* + K_3\bar{c}^*$ where K_1, K_2, K_3 are numerical constants and $\bar{a}^*$, $\bar{b}^*$, $\bar{c}^*$ are the basis vectors which will be defined more explicitly below. If this vector is to be a solution of the Laue equations it must satisfy them and hence substitution into these equations gives:

$$h = \bar{a}.\bar{r}^* = K_1\bar{a}.\bar{a}^* + K_2\bar{a}.\bar{b}^* + K_3\bar{a}.\bar{c}^*$$

$$k = \bar{b}.\bar{r}^* = K_1\bar{b}.\bar{a}^* + K_2\bar{b}.\bar{b}^* + K_3\bar{b}.\bar{c}^*$$

$$\ell = \bar{c}.\bar{r}^* = K_1\bar{c}.\bar{a}^* + K_2\bar{c}.\bar{b}^* + K_3\bar{c}.\bar{c}^*$$

The vector $\bar{r}^*$ will satisfy the first Laue equation if $\bar{a}.\bar{a}^* = \bar{b}.\bar{b}^* = \bar{c}.\bar{c}^* = 1$ and $\bar{a}.\bar{b}^* = \bar{a}.\bar{c}^* = \bar{b}.\bar{c}^* = \bar{a}.\bar{c}^* = 0$. This means that the basis vector $\bar{a}^*$ must be perpendicular to $\bar{b}$ and $\bar{c}$ and must have length = $1/d_{100}$ where d_{100} is the spacing between planes parallel to the a plane in real space. Similar conditions also apply to $\bar{b}^*$ and $\bar{c}^*$. It is possible to define a set of vectors which will satisfy these conditions. They are

$$\bar{a}^* = \frac{\bar{b} \times \bar{c}}{V} \; ; \; \bar{b}^* = \frac{\bar{c} \times \bar{a}}{V} \; ; \; \bar{c}^* = \frac{\bar{a} \times \bar{b}}{V}$$

where V = volume defined by $\bar{a}$, $\bar{b}$, $\bar{c}$ in the crystal space. It can be easily shown that the vector $K_1\bar{a}^* + K_2\bar{b}^* + K_3\bar{c}^*$ will satisfy the Laue equations and furthermore that K_1, K_2, K_3 will be integers equal to h, k, ℓ respectively. For all possible integers K_1, K_2, K_3 this vector

will generate a three dimensional array of points called a reciprocal lattice. Each of the points in this reciprocal space will correspond to a possible maximum in the distribution of the intensity of the scattered radiation from the crystal. Whenever the vector $\bar{K} - \bar{K}_o$ which is determined by the geometry of the experiment is equal to a reciprocal lattice vector $\bar{r}^*$ it will satisfy the Laue equations and the conditions for a maximum in the scattered intensity will be satisfied.

The vector $\bar{K}_o - \bar{K}$ has a magnitude of $\frac{2 \sin\Theta}{\lambda}$ where Θ is half the angle between $\bar{K}_o$ and $\bar{K}$. It can be shown that the reciprocal lattice vector $\bar{r}^* = h\bar{a}^* + k\bar{b}^* + \ell\bar{c}^*$ is parallel to the normal to a plane in real space whose orientation is specified by the indices $hk\ell$. This vector will have the magnitude $1/d(hk\ell)$ where $d(hk\ell)$ is the distance between successive planes whose orientations are given by $hk\ell$. When $\bar{K}_o - \bar{K}$ and $\bar{r}^*$ are coincident and equal the Laue equations will be satisfied. The magnitudes will be equal when $\bar{K}_o - \bar{K} = \bar{r}^*$ or $2d\sin\Theta = \lambda$. This is Bragg's law. It was originally derived on the assumption that the radiation could be considered to be "reflected" from planes of scatterers. For a given wavelength λ and a plane spacing $d(hk\ell)$ this equation gives the angle Θ necessary for a maximum in the intensity distribution. This maximum is called a Bragg peak.

The relative intensities $I_o(hk\ell)$ of these peaks can be measured by a photographic film or some type of radiation detector. These intensities must be measured in such a way that all the radiation

corresponding to each Bragg peak has been included in the measurement. The result is called an integrated intensity and will be represented by $I_R(hk\ell)$.

Information regarding the symmetry of the crystal can be obtained from the symmetry of the distribution of the scattered intensities in reciprocal space. In some cases certain classes of reflections (fixed hk and/or ℓ) are rigorously absent indicating the presence of symmetry elements containing a translational component.

In diffraction experiments it is often impossible to distinguish between $I_o(hk\ell)$ and $I_o(\bar{h}\bar{k}\bar{\ell})$. This equality is known as Friedl's law. As a consequence, all diffraction patterns will contain a centre of symmetry and thus it will not be possible to distinguish between centrosymmetric and non-centrosymmetric point groups. This means that it is only possible to place the crystal in one of the eleven distinguishable point groups called the Laue groups.

Before the intensity $I_R(hk\ell)$ can be used in a structure determination it is necessary to correct for certain effects which are dependent on the size and the shape of the crystal. Two such effects, absorption and secondary extinction, cause an attenuation in the diffracted radiation and thus the observed intensity is smaller than in the case where these effects are not present. In the case of x-ray diffraction, absorption which is due to the photoelectric effect, tends to dominate the attenuation while in the case of neutron diffraction it is the secondary

extinction that predominates. Secondary extinction is due to the interaction between the incident and the diffracted beams. While the absorption corrections for simple geometries and crystal shapes are straightforward, the corrections for secondary extinction are more complicated. In this study the latter corrections were made with the aid of the program ESAF (Hamilton, 1963). A discussion of the theory of secondary extinction and a description of the program may be found in Appendix A.

The intensities must also be corrected for the Lorentz and polarization effects both of which depend upon the manner in which the diffraction experiment was performed. The correction for the Lorentz effect takes into account the fact that different times are required for different reciprocal lattice points to pass through the "reflecting conditions". The correction for the polarization effect accounts for the fact that when an x-ray is scattered by an electron the amplitude of the scattered x-ray beam is proportional to $\cos\phi$ where ϕ is the angle between the electric vector of the incident x-ray and the direction of the scattered x-rays. In the case of neutron diffraction no polarization effect is present and hence no correction need be applied.

These corrected integrated $I_R(hk\ell)$ are proportional to the square of the structure factor $F_{\bar{H}}$ defined by:

$$F_{\bar{H}} = \sum_{n=1}^{N_s} S_n e^{2\pi i \bar{H}.\bar{r}_n}$$

where H represents the vector $h\bar{a}^* + k\bar{b}^* + \ell\bar{c}^*$ which describes the orientation of the plane $hk\ell$ and $\bar{r}_n$ is the vector $x_n\bar{a} + y_n\bar{b} + z_n\bar{c}$ describing the position of the scattering element "n" (with a scattering factor S_n) relative to an arbitrary origin. The summation is taken over all scattering elements within the unit cell. In the case of the space group $P2_1/c$ this expression becomes:

$$F_{hk\ell} = 4\sum_{n=1}^{N_s} S_n \cos 2\pi(hx_n + \ell z_n + \frac{k+\ell}{4}) \cos 2\pi(ky_n - \frac{k+\ell}{4})$$

and for P_c it is:

$$F_{hk\ell} = 2\sum_{n=1}^{N_s} S_n \left\{\cos 2\pi(hx_n + \ell z_n + \frac{\ell}{4}) \cos 2\pi(ky_n - \frac{\ell}{4}) + i \sin 2\pi(hx_n + \ell z_n + \frac{\ell}{4}) \cos 2\pi(ky_n - \frac{\ell}{4})\right\}$$

In the case of x-rays the photon is scattered by the electron "cloud" of the atom. Because the finite size of the electron "cloud" radiation scattered from different parts of the "cloud" will have slightly different phases with respect to each other. As a result the amplitude of the scattered radiation will be angularly dependent. The magnitude and distribution in $\sin\theta/\lambda$ of the scattering factor may be computed theoretically using the self consistent field approximation. In neutron diffraction the scattering mechanism is different. The neutron is scattered by the nucleus of the atom and because of the small size of the nucleus (10^{-12}cms) relative to the wavelength of the neutron ($1\text{Å} \simeq 0.025$eV) the scattering amplitude is not angularly dependent. Because of this, the scattering amplitude is constant for a given

nuclide and is referred to as the scattering length. Unfortunately present nuclear theory is not capable of calculating these scattering lengths and it is necessary to determine them experimentally.

Both elastic and inelastic scattering can be observed in neutron diffraction. This is possible because the energy of a thermal neutron is of the same order as that of a phonon. As a result it is possible for energy and momentum to be exchanged between the nucleus and the neutron resulting in a variation in both the energy and momentum of the scattered neutron. Because the energy of an x-ray photon is so much greater than that of the phonon inelastic scattering of x-rays is not so easily observed.

The expression for the structure factor was derived on the assumption that the atoms were stationary. In actual fact the atoms are vibrating at the rate of about 10^{12} cps and because of the high frequency of the x-ray photon the atom will appear to be stationary and will be displaced randomly from its position required by the crystal symmetry. In addition to this the whole crystal does not strictly obey the requirements of translational symmetry because it is actually composed of small volumes called domains. These domains are in themselves perfect but their orientations are distributed about some mean value so that the conditions of translational symmetry are not rigorously satisfied. Over a period of time many photons are incident on these domains and as a result it is necessary to average the atomic

positions over both space and time. The resulting effect is that the atom appears to occupy a larger volume in space than it really does. This causes a reduction in the measured intensities I_R as a function of the Bragg angle and the expression for the structure factor thus becomes:

$$F_{\bar{H}} = \sum_{n=1}^{N_s} S_n \exp 2\pi i (\bar{H}.\bar{r}_n) \exp -(B\sin^2\Theta/\lambda^2)$$

where λ is the wavelength of the incident radiation and Θ is the Bragg angle. The B is called the Debye-Waller factor and can be related to the thermal motion of the atoms by:

$$B = 8\pi^2\langle u^2\rangle$$

where $\langle u^2\rangle$ is the mean square amplitude of vibration of the atoms in a direction along the scattering vector.

A more general form of the temperature factor is the anisotropic temperature factor, in which the vibrational motion of the atom is approximated by an ellipsoid. The expression for a given atom is:

$$\exp - 2\pi^2(U_{11}h^2a^{*2} + U_{22}k^2b^{*2} + U_{33}\ell^2c^{*2} + 2U_{12}hka^*b^* + 2U_{13}h\ell a^*c^* + 2U_{23}k\ell b^*c^*)$$

where U_{ij} are the components of the mean square displacement of the atom in real space and are measured in Å^2. By an appropriate transformation it is possible to obtain from this expression the lengths and orientation of the axes of the thermal ellipsoid and hence the rms

displacements of the atoms along these directions.

The expression for the anisotropic temperature factor is sometimes written in terms of B_{ij} where $B_{ij} = 8\pi^2 U_{ij}$. Another common form can be obtained by taking the Fourier transform of the previous expression. This gives:

$$\exp - (\beta_{11}h^2 + \beta_{22}k^2 + \beta_{33}\ell^2 + 2\beta_{12}hk + 2\beta_{13}h\ell + 2\beta_{23}k\ell)$$

where $\beta_{11} = 2\pi^2 U_{11} a^{*2}$

$$\beta_{12} = 2\pi^2 U_{12} a^* b^*$$

In this thesis the first form of the temperature factor has been adopted.

Because of the three dimensional periodicity of the crystal it is possible to represent the distribution of the scattering elements in the unit cell by a Fourier series. This distribution is a continuous one and can be described by the scattering density function defined by:

$$\rho(r) = \sum_{\bar{H}} A_{\bar{H}} \exp - 2\pi i (\bar{H}.\bar{r})$$

where the summation is over all Miller indices $\bar{H}$ from $+\infty$ to $-\infty$ and $A_{\bar{H}}$ are the Fourier coefficients. It can be shown that these Fourier coefficients are related to the structure factors by $A_{\bar{H}} = F_{\bar{H}}/V$ where V is the volume of the unit cell. Thus the scattering density may be written as:

$$\rho(r) = \frac{1}{V} \sum_{\bar{H}} F_{\bar{H}} \exp - 2\pi i (\bar{H}.\bar{r}).$$

This expression is just the Fourier transform of:

$$F_{\bar{H}} = \sum_{n=1}^{N} S_n \exp \cdot 2\pi i \, (\bar{H}.\bar{r}).$$

The "solution" of a crystal structure requires the determination of the coordinates x, y, and z of the various atoms in the unit cell from the integrated intensities. Each $F_{\bar{H}}$ has associated with it an amplitude and a phase and can be written as:

$$F_{\bar{H}} = \sum_{n=1}^{N} S_n e^{i\phi_n}$$

where $\phi_n = 2\pi(\bar{H}.\bar{r}_n)$. Unfortunately since it is not possible to measure $F_{\bar{H}}$ but only $|F_{\bar{H}}|^2$ information about the phases and hence about the atomic positions normally cannot be obtained directly. This is referred to as the phase problem in crystallography. Depending on certain conditions there are several ways of overcoming this problem and of determining the phases. Because of the presence of a scatterer of x-rays with a high electron density (the rubidium atom) in $RbHSO_4$ it was possible to use the Patterson synthesis to determine the phases of some of the structure factors.

The Patterson synthesis may be defined in the following manner. The scattering density in a crystal at two points $\bar{r}$ and $\bar{r} + \bar{u}$, where $\bar{u}$ is an arbitrary vector, can be written as follows:

$$\rho(\bar{r}) = \sum_{\bar{H}} F_{\bar{H}} \, e^{-2\pi i \, \bar{H}.\bar{r}} \quad \text{and} \quad \rho(\bar{r}+\bar{u}) = \sum_{\bar{H}} F_{\bar{H}} \, e^{-2\pi i \, \bar{H}.(\bar{r}+\bar{u})}$$

The Patterson function P(u) is then defined in the following manner:

$$P(\bar{u}) = V \int_0^1 \rho(\bar{r}) \, \rho(\bar{r}+\bar{u}) d\bar{r} = \frac{1}{V} \sum_{\bar{H}} |F_{\bar{H}}|^2 \exp 2\pi i \, (\bar{H}.\bar{u})$$

where V is the volume of the unit cells. This is again a Fourier series with the coefficients $|F_{\bar{H}}|^2$ which are proportional to the integrated intensities I_R. The Patterson synthesis will be a maximum when the scattering density at $\bar{r}$ and $\bar{r}+\bar{u}$ are both a maximum together. A vector drawn from the origin of the Patterson map to a peak will correspond to a vector between two atoms in the crystal and the peak intensity will be proportional to the product of the scattering densities of the two atoms. If one atom in the compound is a particularly strong scatterer its contribution to the Patterson function will be easily identifiable.

If some of the atom positions are known, the remaining ones may be located with the aid of the difference synthesis. In the difference synthesis the structure factors and their phases are calculated on the basis of the known atomic positions. After these phases have been assigned to the "observed" structure factors $F_{\bar{H}}^{o}$ the scattering density maps for $F_{\bar{H}}^{o}$ and $F_{\bar{H}}^{c}$ may be calculated and the difference between them be defined as the difference synthesis:

$$D(\bar{r}) = \rho_o(\bar{r}) - \rho_c(\bar{r}) = \sum_{\bar{H}} \left(|F_{\bar{H}}^{o}| - |F_{\bar{H}}^{c}| \right) \exp 2\pi i(\bar{H}.\bar{r}_n)$$

where $F_{\bar{H}}^{o}$ and $F_{\bar{H}}^{c}$ are the observed and calculated structure factors respectively. If all the atoms are accounted for the synthesis will be "flat". For this reason the difference synthesis can be used as a final check to ensure that a structure is correct. If some atoms are left out of the structure factor calculation the difference synthesis map will indicate the most likely positions for the missing atoms. This property is most useful in determing the positions of light scatterers in x-ray diffraction and for locating hydrogen atoms in neutron diffraction experiments.

When a trial structure has been determined, the best set of atomic parameters may be obtained by using the method of non-linear least squares. In this method the quantity $R(P_i) = \sum_{\bar{H}}^{NO} W_{\bar{H}} \left[F_{\bar{H}}^{o} - F_{\bar{H}}^{c}(P_i) \right]^2$ is minimized with respect to the atomic parameters P_i. The quantity $W_{\bar{H}}$ is the relative weight which is assigned to each $F_{\bar{H}}^{o}$. This weight is chosen so that it reflects the accuracy with which the intensity $I_{\bar{H}}$ was measured.

After minimization of $R(P_i)$ a set of normal equations are obtained. These can be written in matrix notation as: $M\Delta P = G$ where ΔP is a column vector representing the necessary shifts in the parameters. P_i. M is the matrix whose elements M_{ik} are defined by:

$$M_{ik} = \sum_{H=i}^{NO} W_H \frac{\partial F_H^c(P_i)}{\partial P_i} \cdot \frac{\partial F_{\bar{H}}^c(P_i)}{\partial P_k},$$

and G is the column vector whose elements are:

$$G_K = \sum_{H=1}^{NO} \left\{ F_H^{\,o} \left[\frac{F_H^{\,c}}{|F_H^{\,c}|} \right] - F_H^{\,c}(P_i) \right\} \frac{\partial F_H^{\,c}(P_i)}{\partial P_k}$$

The agreement between the calculated and observed structure factors can be expressed by the two quantities:

$$R_W = \sqrt{\sum_{H=1}^{NO} W_H \left[|F_H^{\,o}| - |F_H^{\,c}| \right]^2 \Big/ \sum_{H=1}^{NO} W_H |F_H^{\,c}|^2}$$

$$R = \sum_{H=1}^{NO} \left| |F_H^{\,o}| - |F_H^{\,c}| \right| \Big/ \sum_{H=1}^{NO} |F_H^{\,c}|$$

where the sum j is over all observed reflections. The standard deviation $\sigma(P_i)$ in the parameters is given by:

$$\sigma(P_i) = \sqrt{\frac{\sum_{H=1}^{NO} W_H \left(|F_H^{\,o}| - |F_H^{\,c}| \right)^2}{NO - NV}} \cdot M_{ii}^{-1}$$

where NO is the number of observations and NV is the number of parameters to be adjusted. M_{ii}^{-1} is an element of the inverse matrix of M.

If all of the equations represented by the matrix equation $M\Delta P = G$ are not linearly independent then it is possible that the change in one parameter may bring about a change in another parameter. When this occurs the two parameters, say P_i and P_j, are said to be correlated. The severity of this correlation can be expressed with the correlation

matrix whose elements C_{ij} are related to the elements of the matrix M by:

$$C_{ij} = M_{ij}^{-1} \Big/ \sqrt{M_{ii}^{-1} M_{jj}^{-1}}.$$

When C_{ij} is equal to unity the parameters P_i and P_j are completely correlated. As the value of C_{ij} approaches zero, the amount of correlation decreases until $C_{ij} = 0$ where the parameters P_i and P_j are uncorrelated.

The effects of correlation can be reduced by using three dimensional data and by applying only a fraction of the calculated shifts for parameters that are correlated. If some parameters are strongly correlated they can each be refined in a separate cycle of refinement.

CHAPTER III

EXPERIMENTAL

(A) Growth of the Crystals

The crystals of $RbHSO_4$ were grown from an aqueous solution. Five hundred grams of powdered $RbHSO_4$ were dissolved into 500 millilitres of water and the solution was filtered three times to remove any suspended impurities. Further purification was accomplished by successive re-crystallization. The crystals used in the experiments were grown by means of the temperature lowering technique. The beaker containing the solution was placed in a large water bath, the temperature of which was controlled by a Haake Unitherm temperature control device, model number EDe. This device consists of a heater, a sensor and a small circulating pump and is designed to maintain the desired temperature of the bath to within $0.05^{o}C$. The Unitherm used here was modified so that the temperature of the bath could be lowered at different rates.

Seed crystals of about 3mm in size were obtained by lowering the temperature of the solution from 35 to $23^{o}C$ at the rate of $0.5^{o}C$ per hour. Selected seed crystals were suspended in the saturated solution and the temperature was lowered from 35 to $23^{o}C$ at the rate of $0.15^{o}C$ per hour. By this method some large crystals measuring up to 1.2cms in length were obtained. In addition, some smaller but

TABLE I

Summary of the Crystal Samples Used

Crystals used in X-ray Experiments:			
Sample Label	XR-1	XR-2	XR-3
Spindle Axis	c*	b*	b*
Shape	Spherical	Prism	Prism
Number of room temperature reflections measured	569	1143	-
Number of low temperature reflections measured	-	-	1484
Crystals used in Neutron Experiments: (all crystals were cylindrical)			
Sample Label	B-1	B-3	C-1
Cylinder Axis	b	c	c
Cylinder Height (cms)	1.201†	0.411	0.400
Cylinder Diameter (cms)	0.318	0.405	0.534
Number of room temperature reflections measured	290	780	105
Number of low temperature reflections measured	279	-	107

† Measurements are $\pm$ 0.005 cms.

excellent crystals were taken from the sides of the beaker and used either as seeds to grow larger crystals or for x-ray diffraction purposes.

Measurements of the cell parameters and the density indicated that the crystals were $RbHSO_4$ and that no hydrated compound had been formed. The larger crystals used for the neutron diffraction experiments were cut into cylinders by means of an air-abrasive apparatus. The dimensions of the crystals are given in Table 1.

(B) The Room Temperature X-ray Data

The room temperature data were collected on an integrating precession camera using Mo radiation with a Zr filter. A micro-densitometer was used to measure the intensities on the films. The h0ℓ, h1ℓ, h2ℓ, and 0kℓ data were collected with crystal XR-1. After collection of this data, the crystal, because of its hydroscopic nature, was damaged by high humidity. A second crystal, XR-2, was mounted and sprayed with a protective coating of clear plastic. Data of the type 0kℓ, 1kℓ, 2kℓ, hk0, hk1, hk2, ℓkℓ, 1 + ℓ, k, ℓ, 2 + ℓ, k, ℓ, were collected with this crystal. A summary of all data collected is given in Table II.

The films were indexed on the basis of the monoclinic unit cell, space group $P2_1/c$, described by Pepinsky and Vedam (1960). The absence of odd k reflections along 0k0 confirmed the existence of the two fold screw axis parallel to the b axis. The presence of the c

TABLE II

Summary of Data Collected

Room Temperature X-ray Data (T = 23°C):

Sample Label	XR-1	XR-2		
Data Collected	h0ℓ	0kℓ	ℓ, k, -ℓ	hk0
	h1ℓ	1kℓ	1+ℓ, k, -ℓ	
	h2ℓ	2kℓ	2+ℓ, k, -ℓ	
	0kℓ	3kℓ		
		4kℓ		
Number of reflections measured	569	1143		

Total Number of Unique Reflections

Observed	=	699
Unobserved	=	611
Unreliable	=	16
Total	=	1326

Low Temperature X-ray Data (T = -35°C):

Sample Label	XR-3		
Data Collected	0kℓ	hk0	ℓ, k, -ℓ
	1kℓ	hk1	1+ℓ, k, -ℓ
	2kℓ	hk2	2+ℓ, k, -ℓ
	3kℓ		
	4kℓ		
Number of reflections measured	1484		

Total Number of Unique Reflections

Observed	=	897
Unobserved	=	261
Unreliable	=	54
Total	=	1212

TABLE II

Continued

Room Temperature Neutron Data (T = 23°C)

Sample Label	B-1	B-3	C-1
Data Collected	h0ℓ	hkℓ (3 dimensional)	hk0
Maximum θ	62°	35°	63°
Number of reflections measured	295	705	105

Total Number of Unique Reflections

Observed	= 233
Unobserved	= 152
Unreliable	= 15
Total	= 400

Low Temperature Neutron Data (T = -30°C)

Sample Label	B-1	C-1
Data Collected	h0ℓ	hk0
Maximum θ	52°	53°
Number of reflections measured	279	107

Total Number of Unique Reflections

Observed	= 350
Unobserved	= 22
Unreliable	= 14
Total	= 386

glide perpendicular to b was confirmed by the absence of the odd reflections along the c axis. It was observed that on the h0ℓ film the strong reflections satisfied the conditions h = 2n; ℓ = 4 n and h = 2n + 1; ℓ = 4n + 2. Only one reflection, the $10\bar{6}$, violated this condition. Since reflections of the type -(h + ℓ)kℓ and hkℓ appeared to be equal in intensity there was a strong orthorhombic-like character in this film and also, to a lesser extent, in the h1ℓ and h2ℓ films. The breakdown of this pseudo-orthorhombic character was best observed in the h2ℓ film where the equivalence between hkl and -(h + 1)kℓ reflections did not hold. Examples of this are $52\bar{9} > 42\bar{9}$: $32\bar{8} > 52\bar{8}$; $82\bar{1}\bar{1} > 32\bar{1}\bar{1}$ and $72\bar{1}\bar{1} < 42\bar{1}\bar{1}$.

The data were all corrected for the Lorentz and polarization effects. The linear absorption coefficient is 77 cm^{-1} (due mostly to the rubidium atoms whose mass absorption coefficient is 90 cm^2/g) but since the crystals were less than 0.15 mm in size no absorption corrections were made.

(C) The Room Temperature Neutron Data

The neutron data were collected on a modified Picker X-ray semi-automatic diffractometer located at the McMaster University "swimming pool" reactor. The electronics associated with the counting circuitry were modified to include two amplifiers with variable gain and adjustable baselines. Peak intensities were

measured with a BF_3 counter and the incident beam was monitored by means of a U^{235} fission counter.

A monochromatic beam of wavelength $\lambda = 1.207 \pm 006$Å was produced by Bragg reflection off the $\langle 111 \rangle$ planes of an aluminium crystal. Second order contamination was less than .06% of the monochromatized beam. At a power level of two Megawatts the flux at the monitor counter was 5×10^5 n/cm^2-sec.

Data were collected by means of the continuous θ-2θ scan technique with typical scan rates of $(1/4^\circ)$/minute or $(1/8^\circ)$/minute. An equal amount of time was spent in measuring the background and the peak intensity. The peak intensity, accumulated monitor counts and the background were recorded for each reflection. The integrated intensities were calculated for each reflection.

The integrated intensities, I_o, were corrected for the Lorentz effect and were scaled to the standard reflection which was repeated every 50 reflections. Standard deviations, σ, were calculated on the basis of counting statistics. Reflections where $I_o < 3\sigma$ were considered to be unobserved and were assigned a value equal to 3σ with a standard deviation of σ.

After absorption corrections were applied the integrated intensities were transformed into structure factors with the aid of the program ESAF written by W. C. Hamilton (Hamilton, 1963). This program can be used to apply absorption and extinction corrections

for an arbitrarily shaped crystal. At this stage it was used to calculate the absorption correction only. The method of correcting for secondary extinction will be discussed in Chapter IV, Section C.

Due to the small absorption cross section of atoms in $RbHSO_4$ the major contribution to the effective linear absorption coefficient arises from the spin incoherent cross section for hydrogen. In most compounds this cross-section is found to have a value of 30 barns (Bacon, 1962). Using this value for the spin incoherent cross section for hydrogen in $RbHSO_4$ gives an effective linear absorption coefficient of 0.15 cm^{-1}. This value was used in the program ESAF.

Projection data of the type h0ℓ and hk0 were collected from the crystals B-1 and C-1. In order to protect the crystals from the high humidity in the reactor building the crystals were coated with a non hydrogenous oil called Fluorolube. This oil produces little incoherent scattering so it can be used without causing any appreciable increase in the background.

When it was discovered that the hydrogen atoms could not be completely resolved in the two projections, three dimensional data were collected with crystal B-3.

The collection of three dimensional data requires that the crystal orientation be known accurately. The procedure for determining these angles will be discussed briefly. Since it was known that the cylindrical axis of the crystal was coincident with the b axis of the

crystal, it was only necessary to determine the positions of the a^* and c^* axes. This was fairly easy since the 004 and 400 reflections were both strong. With these approximate setting angles the orientations were calculated for all reflections within a hemisphere up to $\Theta = 25^\circ$. These calculations were made with the program PICK 2 written by W. C. Hamilton. Out of this hemisphere 30 strong reflections were located and their accurate setting angles determined.

For the determination of these angles the BF_3 counter was equipped with 2 pairs of shutters; a horizontal and a vertical pair. The upper or lower half of the aperture could be blocked off with the vertical pair and the left and right sides of the aperture could be blocked off with the horizontal pair. The angles 2Θ, χ, and ϕ were adjusted so that the intensities in the left or right and top or bottom halves of the aperture were equal. The procedure was repeated until the intensity of the peak was maximized. The setting angles for these reflections, the cell parameters and the instrumental zeroes of the Θ, χ, ϕ angles were refined by least squares using the program PICK 2. The refinement converged after three cycles. The final parameters were used to calculate the orientation angles for all reflections up to $2\Theta = 80^\circ$.

Data were collected and treated in the same manner as described for the projection neutron data.

(D) The Low Temperature X-ray Data

The low temperature x-ray data were also collected on an integrating precession camera using $M_oK\alpha$ radiation. The crystal was sprayed with a plastic coating to protect it from condensation. Cooling was accomplished by blowing a stream of cold nitrogen over the crystal. The flow of nitrogen was controlled by a Variac which regulated the amount of power dissipated in a small resistor located inside the storage dewar of liquid nitrogen. This dewar was connected to a pipe which directed the stream over the crystal. A "tee" junction in the pipe made it possible to change dewars without disturbing the temperature of the sample.

The temperature was monitored by a fine copper-constantan thermocouple located at the exit of the pipe which was 2mm from the crystal. In order to minimize icing problems, the camera and the top of the generator were enclosed in a greenhouse constructed of plastic sheeting. Before the sample was cooled an electric field of 1600V/cm was applied parallel to the c axis of the crystal by means of two parallel copper plates connected to three 300 V batteries connected in series. In order to ensure that the sample was single domain the crystal was cooled to a temperature below T_c and then warmed to a temperature above T_c in the presence of the 1600V/cm electric field. This procedure, which is referred to as poling was repeated three times. The crystal was cooled at the rate of 1^oC/minute.

The temperature was monitored at the exit of the pipe and also on the side of the crystal opposite the pipe. With these two readings it was possible to estimate the crystal temperature to be $-35 \pm 2^{o}C$. When this temperature had been attained the electric field was slowly reduced to zero and the copper plates were then removed. The second thermocouple was removed and the output of the first thermocouple was monitored on a chart recorder. The temperature during the entire run of 4 weeks was constant to $\pm 5^{o}C$.

The appearance of the 030 and 050 reflections confirmed the loss of the two fold screw axis and hence confirmed that the crystal had undergone a phase transition to the ferroelectric phase. The films appeared to be quite similar to those taken at room temperature, implying that the changes in the heavier atom positions were small. The films were indexed by comparison with the room temperature data and Lorentz and polarisation corrections were applied.

(E) The Low Temperature Neutron Data

The principle used in cooling the sample was basically the same as in the x-ray case. The nitrogen stream was directed over the crystal which was enclosed in a double walled aluminum shield mounted in such a manner that it did not interfere with the crystal's rotation. This shield protected the crystals from the humidity and ensured that they were in a constant temperature environment. The temperature was monitored at a point just above the crystal. The

temperature gradient along the crystal was estimated to be about $2^{\circ}C/cm$. While it was being cooled, the crystal was subjected to an electric field of 1200V/cm. After the crystals had been poled and cooled to $-30^{\circ}C$ the electric field was removed and the temperature was monitored continuously on a chart recorder. The temperature was constant to within $5^{\circ}C$ throughout the entire run.

Data were collected with crystals B-1 and C-1 using the continuous Θ-2Θ scanning technique. Reduction of the data proceeded along the lines described in Section 3 of this chapter. The appearances of the 030 reflection confirmed that the crystal had undergone a phase change to the ferroelectric state.

(F) Determination of the Cell Parameters

The room temperature cell parameters were determined from hk0 and 0kℓ precession films using a standard crystal of TiO_2 for calibration. After calibration the distances measured on the film were used to least squares refine the cell parameters. The beta angle was obtained from the spindle settings of the precession camera.

The low temperature cell parameters were determined by taking two exposures; one with the crystal at room temperature and the other at low temperature. Calibration of this film was accomplished by using the room temperature $RbHSO_4$ parameters as the standard.

The cell parameters determined by the author and those determined by Pepinsky and Vedam (1960), and Bengtssen (1941), are listed in Table III.

TABLE III

Cell Parameters of $RbHSO_4$

Cell Parameters are given for the monoclinic unit cell $P2_1/c$ except for the results of Bengtssen. In this case the orthorhombic cell has been used and the axes have been interchanged in order to conform with the labelling used below.
Distances are in Å and angles are in degrees.

Room Temperature (T = 23°C):

	a	b	c	β
This study	14.354(14)	4.618(7)	14.808(13)	120° 55′ ± 10′
Pepinsky and Vedam (1960)	14.356(5)	4.622(5)	14.807(5)	121° 0′ ± 1°
Bengtssen (1941)	12.30	4.61	14.78	90° 0′

Low Temperature (T = -35°C):

This study	14.333(15)	4.616(8)	14.798(14)	120° 25′ ± 10′

CHAPTER IV

The Structure of the Paraelectric Phase of $RbHSO_4$

A) Determination of the structure by x-ray diffraction.

Because of the short b axis it was expected that the resolution of all atoms would be the greatest in the (010) projection and thus the initial x, z coordinates of the rubidium atoms were obtained from a Patterson synthesis projected on (010) shown in Fig. 3. The origin of the unit cell was placed at a point "a" in the projection so that the vector $\overline{\text{II}}$ joined two rubidium atoms related either by a centre of symmetry or by a two fold screw axis. This defined the x, z coordinates[1] of one of the Rb atoms. By means of the superposition method (Buerger, 1959) the second Rb atom was located and a consistent set of Rb-Rb vectors obtained.

These positions for the rubidium atoms were used to calculate the $RbHSO_4$ h0ℓ structure factors and their relative phases. The paraelectric phase of $RbHSO_4$ is centrosymmetric and thus these relative phases must be $\pm$ 1. The scattering curves used for the Rb^+,

---

(1) Throughout this thesis the atomic positions will be designated by the fractional coordinates x, y and z relative to the unit cell defined by the vectors a, b and c. The positions of the peaks in the Patterson synthesis will be designated by fractional coordinates u, v and w of the cell.

FIGURE 3

Patterson Synthesis Projected onto (010)

(Contours are in arbitrary units)

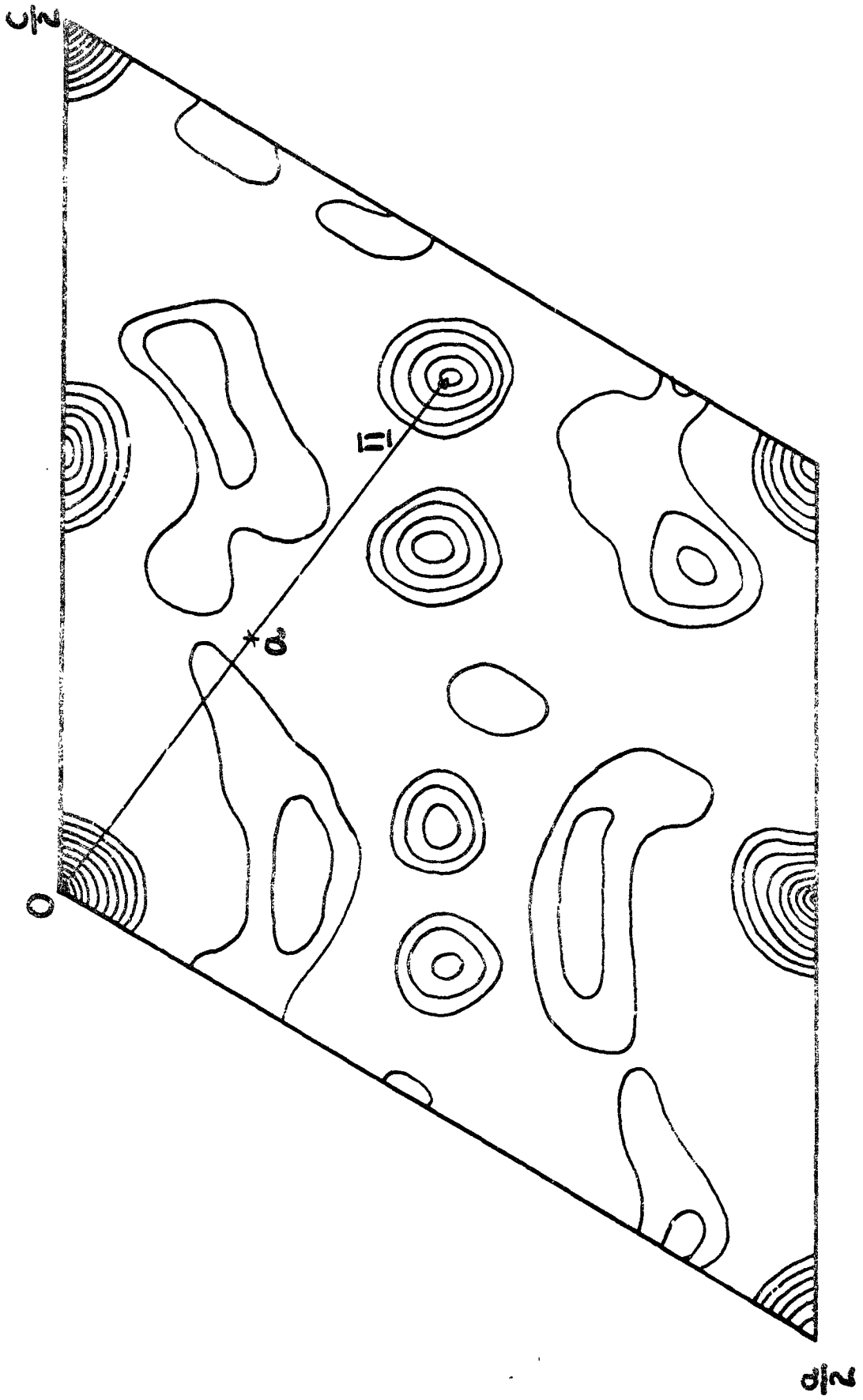
c/2
O
a
a/2

S^{o}, and 0^{-} atoms were the mean atomic scattering factors calculated from self-consistent field wavefunctions (International Tables for X-ray Crystallography, 1962). The Rb^{+} scattering curve was corrected for anomalous dispersion. A Fourier synthesis was calculated using the calculated phases and the observed structure factors with a cut-off eliminating those reflections for which F_o/F_c was greater than 2. This synthesis showed, in addition to the peaks due to the Rb atoms, peaks at x = 0.13, z = 0.18 and x = 0.37, z = 0.08. Around each of these peaks were smaller unresolved peaks. The larger peaks were attributed to the sulphur atoms and the unresolved peaks to the oxygen atoms of the sulphate anions. The Rb-S vectors associated with these sulphur positions were consistent with the Patterson synthesis. Using the Rb and S atoms to determine the phases, a Fourier and a difference synthesis were calculated. The difference synthesis showed little scattering density at the positions of the Rb and S atoms indicating that the trial structure was consistent with the data.

Around each sulphur atom site, the difference synthesis showed three peaks, two of which had approximately equal scattering density and the third with twice the density. An oxygen atom was placed in the positions of each of the smaller peaks and two more were placed at the third peak so that they overlapped in projection. The scale factor, atomic positions and isotropic temperature factors were least squares

refined and after the equivalent of 5 cycles the unweighted R factor ($R = \sum_{j=1}^{NO} \frac{|F_j^o| - |F_j^c|}{|F_j^c|}$) dropped from 0.22 to 0.14. In these initial stages of refinement unit weights were used and only observed reflections were included in the refinement. Refinement did not proceed as fast as expected because of correlations between the two sets of pseudo symmetrically related atoms (see Section B of this chapter) in the asymmetric zone and also between the x and z coordinates of the same atom. These correlation problems were overcome by using partial shifts (i. e. by applying only a fraction of the calculated shift in each parameter) and by varying strongly correlated parameters in different cycles of refinement. The problem became less severe when more data were included in the refinement.

At this point, a map of the vectors between the rubidium and oxygen atoms of the trial structure was constructed and compared with the Patterson synthesis. The agreement between the two showed that the structure was compatible with the observed structure factors.

The y coordinates were determined by means of a Patterson synthesis projected onto the (100) plane (see Fig. 4). In this projection there is a large degree of overlap so that individual peaks cannot be resolved. This made it difficult to obtain an unambiguous set of y coordinates directly from the Patterson synthesis.

FIGURE 4

Patterson Synthesis Projected onto (100)

(Contours are in arbitrary units)

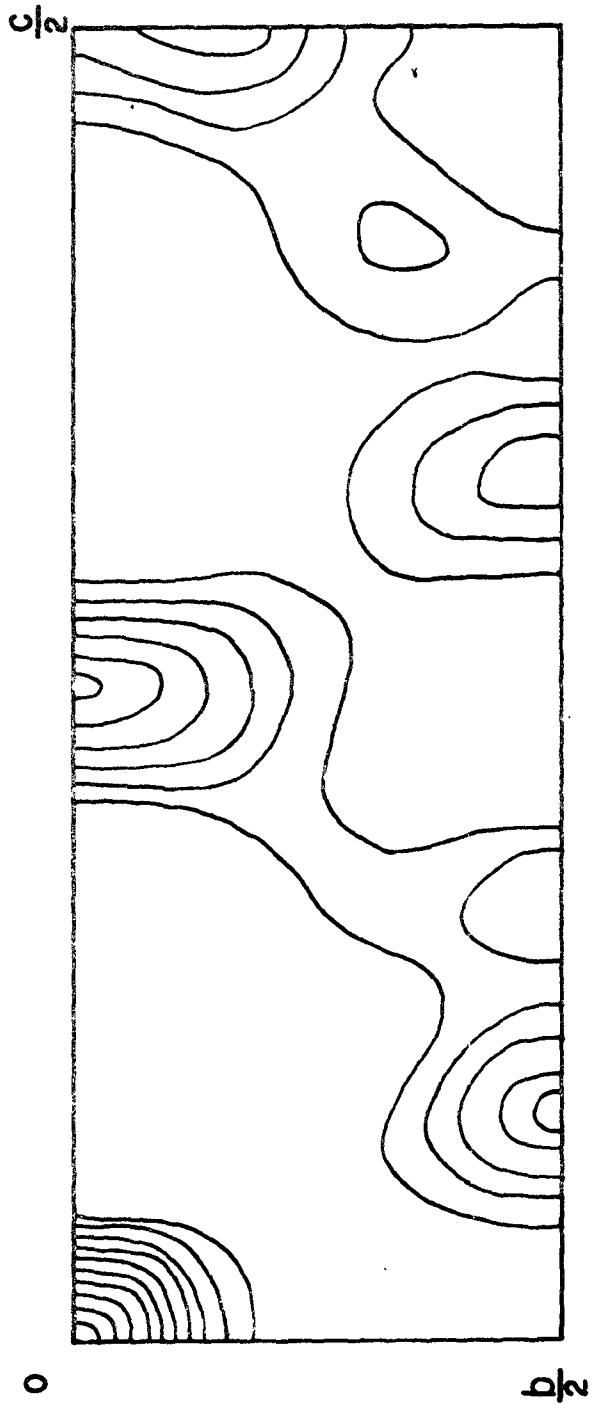
c/2
0
a/2

There is a peak in the Patterson synthesis at w = $\frac{1}{2}$ and close to v = 0 which can be associated with vectors between atoms related by the c glide. Thus, since this peak is close to v = 0, it was concluded that both rubidium atoms must lie close to the two glide planes at y = 3/4 and y = $\frac{1}{4}$ in the unit cell. Furthermore, since the rubidium and sulphur atoms alternate at equal intervals along the c axis, there should be some Rb-S vectors at w = $\frac{1}{4}$. Again the peaks in the Patterson synthesis at w = $\frac{1}{4}$ are close to v = 0 and it was concluded that each sulphur must have its y coordinates approximately equal to y coordinate of one of the adjacent rubidium atoms.

Some of the peaks located along v = $\frac{1}{2}$ correspond to vectors between atoms related by the two fold screw axis parallel to the b axis. The elongation along v of the peaks at v = $\frac{1}{2}$ was attributed to vectors joining atoms which are close to v = $\frac{1}{4}$ and are related by the centre of symmetry.

In the space group $P2_1/c$ there are two possibilities for the placement of the origin. It may be placed at the 2_1 axis or at the centre of symmetry. Since the projection down a 2_1 axis and the projection of an inversion centre are both two fold axes this problem did not arise in the solution of the h0ℓ projection. However, in order to determine the y coordinates it became necessary to resolve this ambiguity. As stated earlier the peaks at v = $\frac{1}{2}$ were due to the centre of inversion and/or the 2_1 axis. The peaks that are associated with

atoms related by the 2_1 axis must be localized at v = $\frac{1}{2}$ while the peaks due to atoms related by the centre of symmetry have no such restriction and as a result tend to be elongated parallel to the v axis. By considering the shape of the peaks at v = $\frac{1}{2}$ it was possible to determine that the centre of inversion was located at the origin of the cell.

Because of the number of overlapping peaks in the Patterson projected onto (010) , it was not possible to determine the actual coordinates of the atoms but only that they were close to the glide planes at y = 1/4, 3/4. While it was possible to estimate how far the rubidium atoms were away from the glide plane it was not possible to determine on which side of the glide planes the atoms were located. At this point a "brute force" method was employed. The coordinates of each configuration of the Rb atoms that were consistent with the Patterson synthesis were read into the least squares program and the scale and the y coordinates of the Rb atoms were varied for two cycles. Two of these configurations showed a noticeably lower R value. For each of these two arrangements the procedure was repeated for the various configurations of the sulphur atoms. The scales and the y coordinates of both the Rb and S were varied. The R factor for two of these configurations was considerably lower than the others. A further refinement which included h1*l*, h2*l*, 0k*l*, hk0, reflections gave a lower R factor for the configuration where all the Rb and S atoms were

on the same side of the glide planes. This configuration of rubidium and sulphur atoms was then used for the three dimensional trial structure. The y coordinates of the oxygen atoms were calculated from the best x, z coordinates on the assumption that they formed a perfect tetrahedron about the sulphurs.

Each sulphate group has two orientations which will give the same appearance when projected down the b axis. This means that there are four possibilities for the orientations of the sulphate groups within the asymmetric zone. When all the reflections were included in the least squares calculation the refinement converged for only one of the configurations.

A new weighting scheme was introduced at this stage of the refinement. A graph of $\langle \Delta^2 \rangle$, the square of the difference between the observed structure factor F_o and the calculated structure factor averaged over a range of values of F_o was plotted against F_o and the curve was fitted to the functional form $\langle \Delta^2 \rangle = A + BF_o + CF_o^2$ where A, B and C are constants whose values must be determined. The weights used were $W = 1/(A + BF_o + CF_o^2)$. Reflections which could not be observed on the films were given a value F_{lim} which represented twice the average background as measured by the micro densitometer in the vicinity of the reflection. If $F_{lim} > F_c$ the unobserved reflections were given zero weight in the refinement. If $F_{lim} < F_c$ then the reflection was given the weight $(F_{lim} - f.F_c)$ where f is an arbitrary

multiplier which is set equal to 0.5 in the earlier stages of refinement. Due to the correlations mentioned earlier only a fraction of the calculated parameter shifts were applied in each cycle of refinement. After the equivalent of two complete cycles of refinement the weighted R_w for all reflections decreased from 0.17 to 0.12. Refinement of the anisotropic temperature factors components with the positional parameters and the averaging of common reflections in the data set yielded a final R_w of 0.07. The average shift/error was 0.02 and

$\sum \frac{\langle \Delta^2 \rangle}{NO - NV} = 0.993$ (where the summation if over all $\langle \Delta^2 \rangle$ and NO is the number of structure factors used in the refinement and NV is the number of parameters varied). The final parameters and their standard deviations are listed in TableIV and the structure is illustrated in Fig. 5. A finalFourier synthesis is shown in Fig. 6 and the observed and calculated structure factors are listed in Appendix B.

(B) Preliminary Discussion of the Structure

This preliminary discussion will briefly describe the overall features of the structure and those aspects of it which may be useful in the discussion of models of the hydrogen bonding. A more complete discussion of the structure can be found in Chapter V.

In Fig. 5, the two crystallographically independent rubidium atoms in the asymmetric zone of the unit cell with space group $P2_1/c$ have been labelled Rb1 and Rb2. The sulphur atoms which have

FIGURE 5

Structure of the Paraelectric Phase

of $RbHSO_4$ projected onto (010).

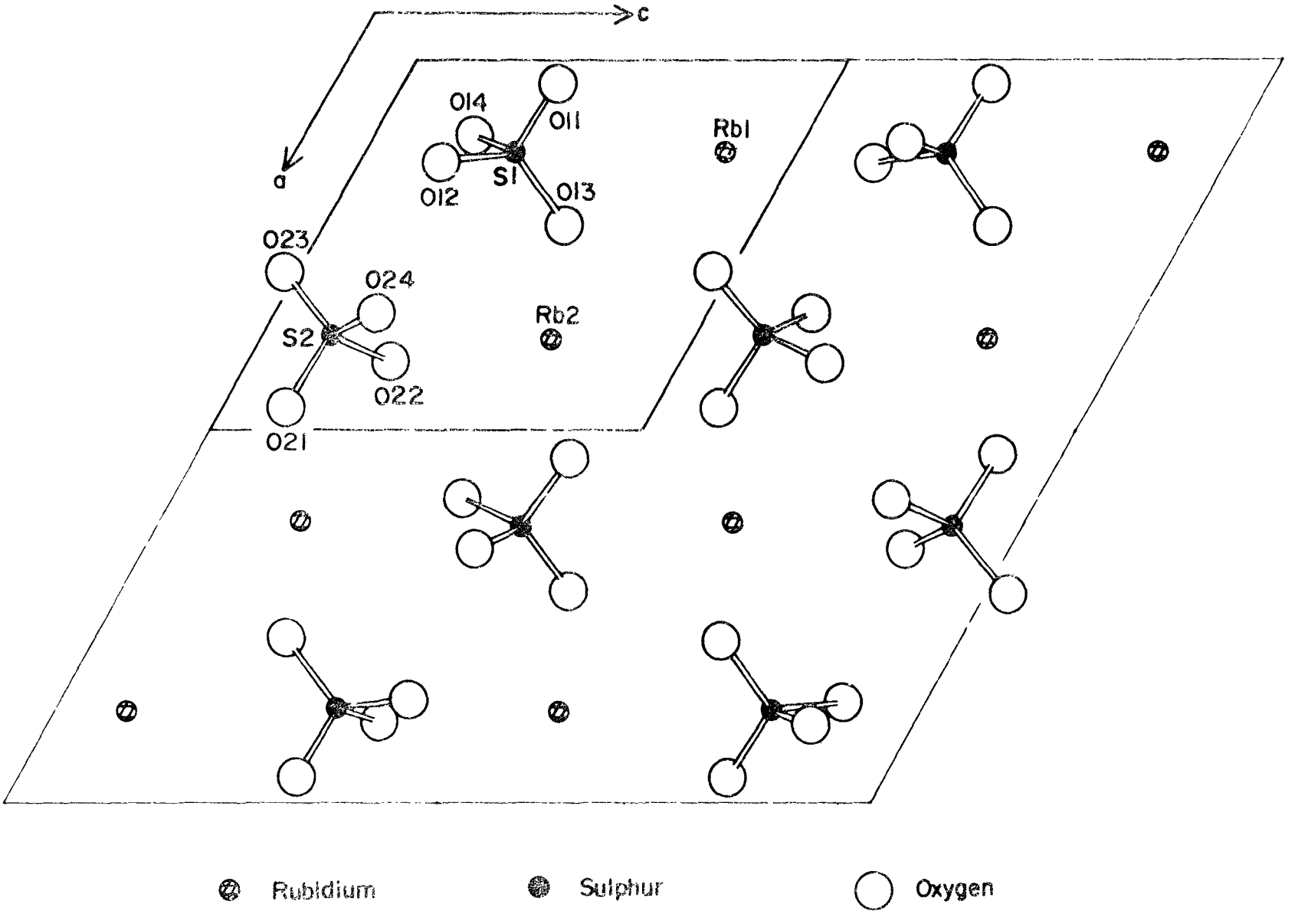
c
a
O14
O11
S1
O12
O13
Rb1
O23
O24
S2
Rb2
O22
O21
Rubidium
Sulphur
Oxygen

FIGURE 6

$RbHSO_4$: Fourier synthesis of the x-ray data collected at room temperature.

(Contours are in arbitrary units. The zero contour has been omitted.)

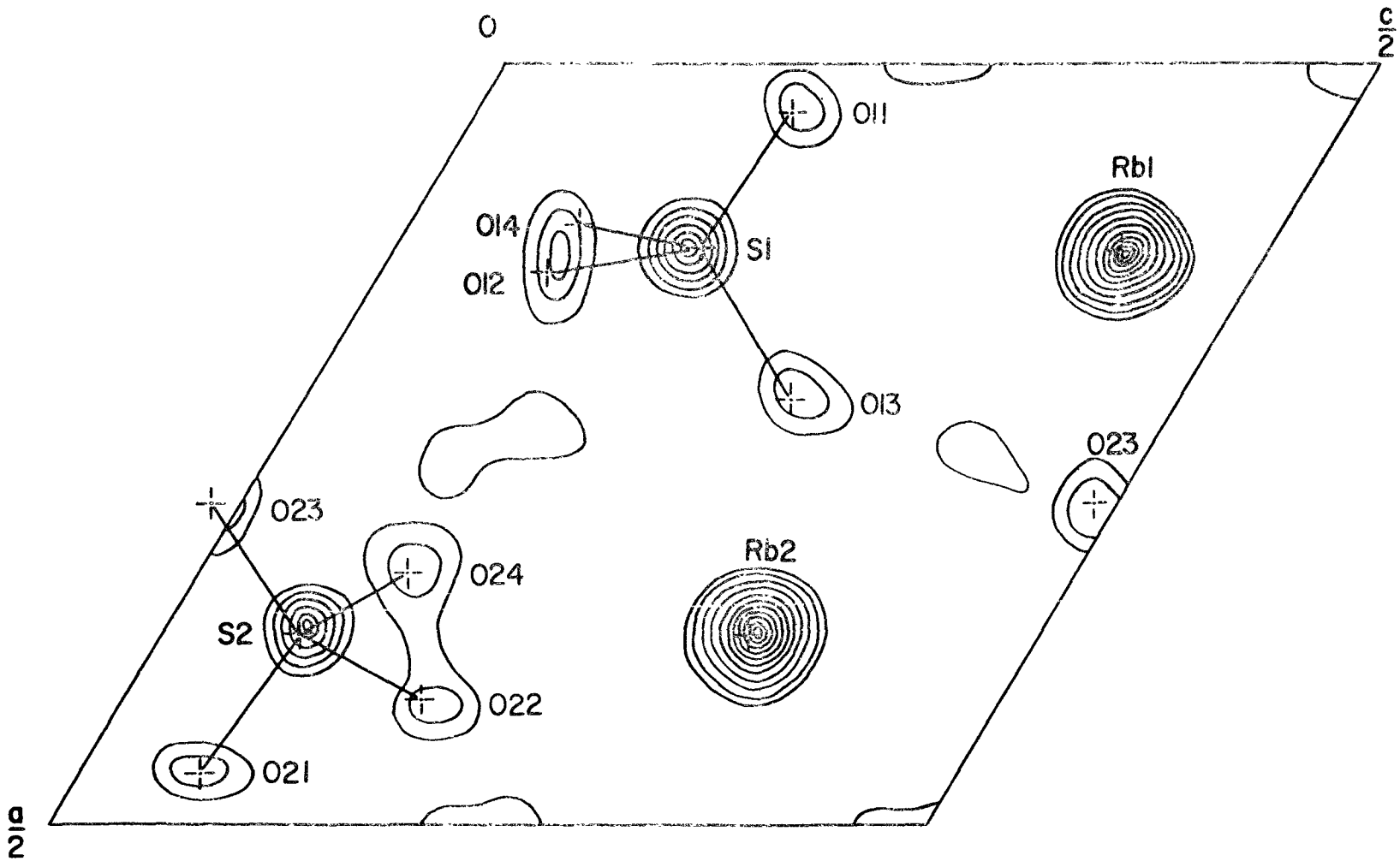
0
c/2
011
Rb1
014
012
S1
013
023
023
024
Rb2
S2
022
021
a/2

Table VII shows that in each sulphate group one S-O distance is significantly longer than the others. The oxygen atoms (012 and 022) involved in these long bond distances are both less than 2.60Å from another oxygen (014 and 024 respectively) suggesting that hydrogen bonding is occuring between 012 and 014 and between 022 and 024. The details of the hydrogen bonding and the S-O distances will be discussed more fully in Chapter V.

(C) Determination of the Hydrogen Positions in the Paralectric Phase of $RbHSO_4$ by Neutron Diffraction.

After the absorption correction had been applied to the h0ℓ and hk0 observed intensities, the atomic parameters were refined with these intensities using for the initial parameters those obtained from the x-ray refinement. The coherent scattering lengths used in the refinement were; S = 0.31×10^{-12} cms; O = 0.577×10^{-12} cms and H = -0.378×10^{-12} cms (Bacon, 1962). The scattering length for rubidium was taken to be 0.68×10^{-12} cms (Copely, 1970). After two cycles of refinement R_w settled at 0.26. A Fourier synthesis projected onto (010) showed regions of negative scattering density close to 014 and 012 and close to 022 and 024 implying that the hydrogen atoms were situated somewhere between 014 and 012 and between 024 and 022. This was confirmed by a difference synthesis (Fig. 7) involving only the heavy atoms. A Fourier synthesis projected onto (001) also showed negative regions near these oxygens but due to the extensive amount of

FIGURE 7

$RbHSO_4$: Fourier difference synthesis of neutron data collected at room temperature. Contours are in arbitrary units. The dotted contour is the zero contour. Dashed contours represent negative scattering densities.

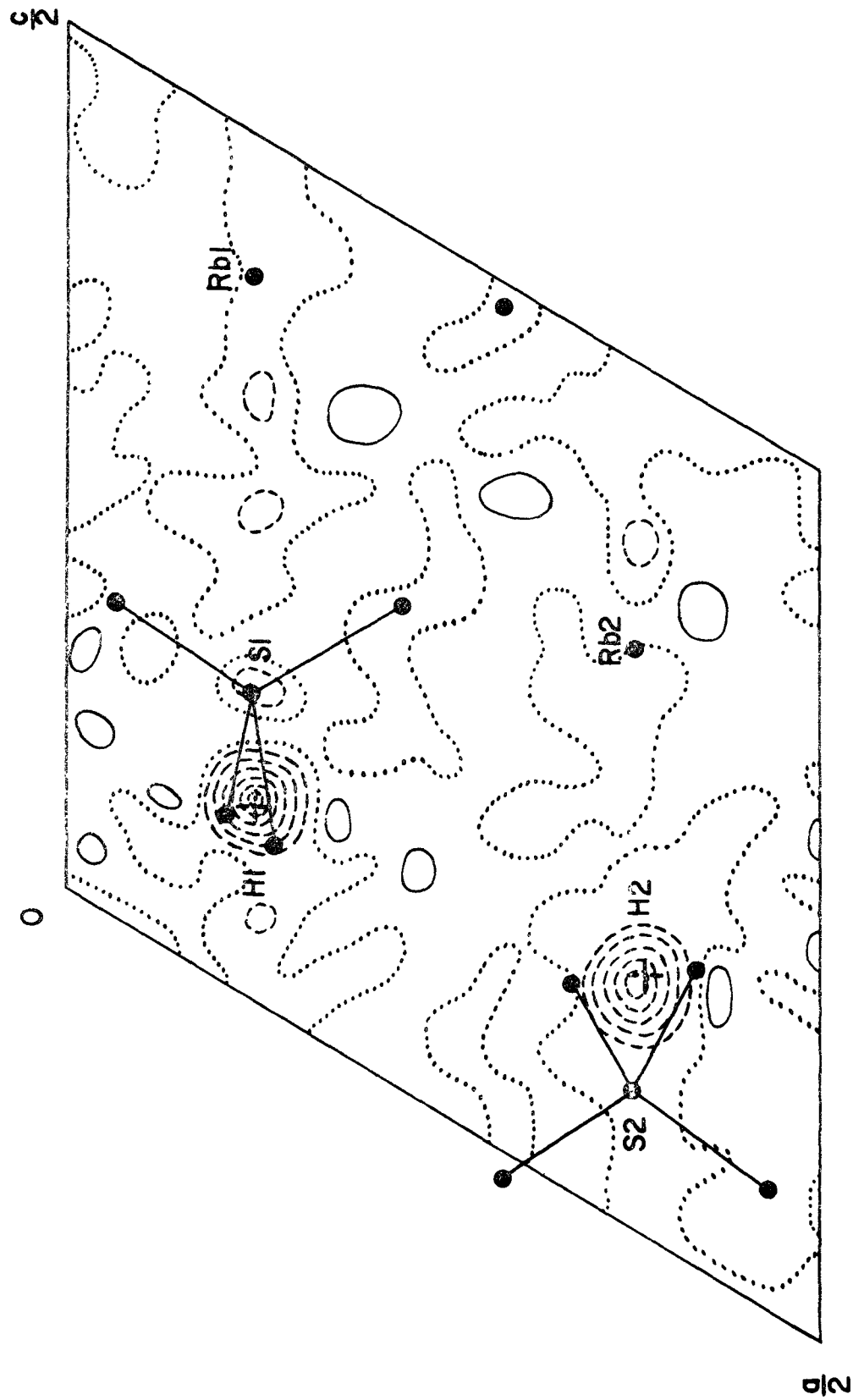
c/2
Rb1
Si
Rb2
H1
H2
S2
0
a/2

overlap of the atoms it was not possible to accurately determine the y coordinates of the hydrogens from this synthesis. These negative regions, indicating the presence of a hydrogen atom, confirmed that the hydrogen bonding occurs between 012 and 014 (+b) and between 022 and 024 (+b) as implied by the O-O distances. By using that fact that the x-ray structure showed the lengthening of only one S-O distance in each sulphate group a model was constructed in which the hydrogen atom H1 was on the line joining the two oxygens 012 and 014 (+b) at a distance of 1Å from 012 and hydrogen H2 was on the line joining 022 and 024 (+b) at a distance of 1Å from 022. After one cycle of refinement the R_w factor was 0.14. Three other models in which the hydrogens were placed at a distance of 1Å from the various oxygens involved in the hydrogen bonding all gave higher R_w values.

A fifth "disordered" model which consisted of two pairs of half hydrogen atoms was also tried. One pair, H1A and H1B were placed between 014 and 012 and the other pair, H2A and H2B were placed between 022 and 024. The R_w factor in this case was 0.17 but upon refinement of the atomic coordinates and population parameters of the atoms it dropped to 0.15. At this point the population parameters favoured the "acentrically ordered" model of the hydrogen atoms in which H1 was bonded to 012 and H2 was bonded to 022, in agreement with the earlier conclusions. The acentrically ordered model was adopted and the refinement was continued.

Some correlation problems involving the y coordinates of the atoms were encountered in the refinement of the h0ℓ and 0kℓ data. Considering the amount of overlap of the atoms in the (100) projection this is not surprising. The strongest correlations were observed between the y coordinates of S1 and S2, between 012 and 014, and between 022 and 024. These correlation coefficients were -0.67, 0.85, and 0.70 respectively. The effects of these correlations were minimized by refining the correlated parameters in different cycles of the least squares refinement. Fortunately the addition of three dimensional data which became available in the later stages of refinement solved the problem.

After the equivalent of one cycle of refinement an extinction correction was applied using the program ESAF written by W.C. Hamilton (1963). First a graph of $\ln (F_o^2/F_c^2)$ was plotted against I_c for all observed reflections from crystal B-I. A similar graph was also plotted for crystal C-I. The extinction parameter, which is proportional to the slope of the line through these points was determined for each crystal and these values were used in the program ESAF. After the application of these corrections further refinement yielded an R_w of 0.10. The procedure of determining the extinction correction was repeated and after another cycle of refinement the R_w dropped to 0.08. Since F_o'/F_c did not vary as a function of I_o', where the prime indicates the values corrected for extinction, no further

extinction correction was made. A final cycle of refinement showed no improvement in the R_w and the refinement was terminated.

At this time the three dimensional neutron diffraction data became available. After the intensities had been corrected for absorption, the Lorentz effect and reduced to structure factors, they were used in a refinement of the best set of atomic parameters obtained from the projection data. An initial refinement in which only the scale was varied resulted in an R_w factor of 0.27. The extinction corrections were made using a three dimensional version of ESAF (Hamilton, 1963) in the manner described earlier. A total of four cycles of corrections had to be applied before F'_o / F_c was made invariant to I'_o. The least squares refinement was continued for three more cycles until the average shift over standard deviation of the parameters was less than 0.1. The R_w factor at this point was 0.13.

The atomic positions and bond lengths are listed in Tables IV, VII and XIII. The anisotropic temperature factors are listed in Table V, and the principal axes of the thermal ellipsoids are listed in Table VI.

TABLE IV

Atomic Parameters of the Room Temperature (T = 23°C) phase of $RbHSO_4$ as determined by neutron and x-ray diffraction.
All Standard deviations are x 10^4. The anisotropic temperature factors from the x-ray refinement are listed in Table V.

		Neutron Diffraction	X-ray Diffraction
Rb1	x	0.1237 (3)	0.1233 (2)
	y	0.1401 (12)	0.1405 (4)
	z	0.4160 (3)	0.4160 (2)
	U	0.0220 (10)	-
Rb2	x	0.3750 (3)	0.3749 (2)
	y	0.7015 (12)	0.7018 (4)
	z	0.3360 (3)	0.3360 (2)
	U	0.0270 (10)	-
S1	x	0.1247 (6)	0.1246 (5)
	y	0.2183 (30)	0.2171 (8)
	z	0.1740 (7)	0.1741 (5)
	U	0.0210 (19)	-
S2	x	0.3718 (6)	0.3715 (5)
	y	0.7592 (32)	0.7614 (9)
	z	0.0788 (7)	0.0787 (5)
	U	0.0250 (19)	-
011	x	0.0318 (3)	0.0318 (10)
	y	0.1123 (16)	0.1096 (30)
	z	0.1773 (4)	0.1790 (10)
	U	0.0310 (12)	-
012	x	0.1414 (5)	0.1370 (10)
	y	0.0072 (23)	0.0160 (30)
	z	0.1006 (5)	0.0955 (10)
	U	0.0520 (18)	-

		Neutron Diffraction	X-ray Diffraction
013	x	0.2226 (4)	0.2223 (20)
	y	0.1946 (16)	0.2032 (40)
	z	0.2744 (4)	0.2775 (20)
	U	0.0350 (13)	-
014	x	0.1056 (6)	0.1031 (20)
	y	0.4860 (25)	0.4893 (20)
	z	0.1180 (6)	0.1185 (20)
	U	0.067 (2)	-
021	x	0.4668 (3)	0.4662 (20)
	y	0.6894 (14)	0.6914 (33)
	z	0.0737 (4)	0.0709 (18)
	U	0.0270 (12)	-
022	x	0.4097 (4)	0.4064 (11)
	y	0.9974 (16)	0.9963 (26)
	z	0.1659 (4)	0.1652 (10)
	U	0.0320 (12)	-
023	x	0.2856 (3)	0.2848 (13)
	y	0.8848 (16)	0.8838 (27)
	z	-0.0167 (4)	-0.0171 (11)
	U	0.0270 (12)	-
024	x	0.3344 (4)	0.3392 (11)
	y	0.5296 (16)	0.5205 (25)
	z	0.1162 (4)	0.1167 (9)
	U	0.0300 (13)	-
H1	x	0.1289 (6)	-
	y	0.8158 (21)	-
	z	0.1129 (6)	-
	U	0.0240 (16)	-
H2	x	0.3840 (6)	-
	y	0.1913 (22)	-
	z	0.1390 (6)	-
	U	0.0350 (19)	-

TABLE V

X-ray Room Temperature Data (T = 23°C).
Anisotropic Temperature Factors
Functional form $\exp -2\pi^2(U_{11}(ha^*)^2+2U_{12}ha^*kb^*+\ldots$

	U_{11}	U_{22}	U_{33}	U_{12}	U_{13}	U_{23}
Rb1	0.02075	0.02435	0.02609	0.00063	0.01139	-0.00128
Rb2	0.02352	0.02974	0.02509	-0.00091	0.01228	0.00117
S1	0.02568	0.01436	0.02053	-0.00021	0.01343	-0.00208
S2	0.01785	0.01757	0.02026	0.00214	0.00882	-0.00052
011	0.02283	0.04554	0.03355	-0.00658	0.01565	-0.00426
012	0.04881	0.03506	0.02394	-0.01666	0.02492	-0.01399
013	0.04043	0.08565	0.04097	-0.01171	0.01695	-0.01476
014	0.12024	0.01293	0.09282	0.00478	0.07602	0.02172
021	0.03065	0.05303	0.05770	0.01532	0.02793	0.00529
022	0.03914	0.02219	0.01958	0.00578	0.00858	-0.00119
023	0.02369	0.03398	0.01087	0.00730	-0.00272	0.00262
024	0.03038	0.02222	0.01378	-0.00897	0.00740	-0.00360

TABLE VI

X-ray Room Temperature Data (T = 23°C)
Principal Axes of the Thermal Ellipsoids

The RMS displacements are in Å and are listed in order of increasing size for each atom.
The direction cosines are taken with respect to the axes a, b, and a x b respectively.

ATOM	RMS(Å)	cos α	cos β	cos γ
Rb1	0.143	-0.916	0.214	-0.340
	0.155	0.001	-0.847	-0.532
	0.168	0.402	0.487	-0.776
Rb2	0.153	0.945	0.212	0.251
	0.158	-0.184	-0.292	0.939
	0.175	-0.272	0.933	0.237
S1	0.115	-0.206	0.911	0.356
	0.139	-0.510	-0.412	0.755
	0.160	0.835	-0.027	0.550
011	0.140	-0.955	-0.221	-0.199
	0.182	0.247	-0.221	-0.943
	0.218	0.165	-0.950	0.265
012	0.112	0.306	-0.389	-0.869
	0.163	-0.679	-0.729	0.086
	0.245	-0.667	0.564	-0.488
013	0.183	-0.440	-0.282	-0.853
	0.221	-0.895	0.060	0.442
	0.301	0.073	-0.957	0.279
014	0.066	0.196	0.933	-0.302
	0.258	0.716	-0.347	-0.606
	0.354	-0.670	-0.097	-0.736
S2	0.124	-0.628	0.761	-0.161
	0.138	-0.391	-0.488	-0.780
	0.150	0.672	0.428	-0.604

021	0.130	-0.917	0.388	-0.097
	0.233	0.325	0.583	-0.745
	0.250	-0.232	-0.714	-0.660
022	0.138	0.078	-0.508	-0.858
	0.144	-0.254	0.822	-0.510
	0.225	-0.964	-0.257	0.065
023	0.085	0.313	-0.169	0.935
	0.178	-0.395	0.872	0.290
	0.215	0.864	0.460	-0.206
024	0.110	-0.136	-0.429	-0.893
	0.141	0.418	0.792	-0.445
	0.200	-0.898	0.434	-0.072

TABLE VII

T = 23°C - Sulphate Bond Lengths and Angles

The arithmetical unweighted average will be referred to in the discussion.
Bond lengths are in Å; errors are given in brackets x 10^2 Å.

Atoms	Neutron	X-ray	Average
S1 - 011	1.45 (1)	1.46 (2)	1.455
- 012	1.57 (2)	1.57 (2)	1.570
- 013	1.43 (1)	1.45 (2)	1.440
- 014	1.44 (2)	1.45 (2)	1.445
S2 - 021	1.44 (1)	1.46 (3)	1.450
- 022	1.56 (1)	1.55 (2)	1.555
- 023	1.44 (1)	1.44 (2)	1.440
- 024	1.42 (1)	1.43 (2)	1.425
011 - 012	2.42 (1)	2.43 (3)	2.425
- 013	2.38 (1)	2.39 (3)	2.385
- 014	2.42 (1)	2.42 (3)	2.420
012 - 013	2.38 (1)	2.47 (3)	2.425
- 014	2.32 (2)	2.30 (2)	2.310
013 - 014	2.45 (1)	2.46 (3)	2.455
021 - 022	2.39 (1)	2.43 (3)	2.410
- 023	2.41 (1)	2.40 (3)	2.405
- 024	2.41 (1)	2.38 (2)	2.395
022 - 023	2.41 (1)	2.40 (2)	2.405
- 024	2.36 (1)	2.36 (2)	2.360
023 - 024	2.41 (1)	2.40 (2)	2.405
012 - 014 (b)	2.50 (2)	2.54 (2)	2.520
022 - 024 (b)	2.64 (1)	2.57 (2)	2.605

Sulphate angles in degrees; errors are given in brackets in degrees.

	Neutron	X-ray	Average
011 - S1 - 012	107 (1)	107 (1)	107.0
011 - S1 - 013	112 (1)	110 (2)	111.0
011 - S1 - 014	114 (1)	113 (2)	113.5
012 - S1 - 013	105 (1)	110 (2)	107.5
012 - S1 - 014	101 (1)	100 (1)	100.5
013 - S1 - 014	117 (1)	117 (1)	117.0
021 - S2 - 022	105 (1)	108 (1)	106.5
021 - S2 - 023	113 (1)	112 (1)	112.5
021 - S2 - 024	114 (1)	111 (1)	112.5
022 - S2 - 023	106 (1)	107 (2)	106.5
022 - S2 - 024	104 (1)	105 (1)	104.5
023 - S2 - 024	112 (1)	114 (1)	113.0

CHAPTER V

Discussion of the Structure of the Paraelectric Phase of $RbHSO_4$

(A) Comparison of the X-ray and Neutron Diffraction Results

Comparison of the atomic coordinates shown in Table IV shows that most of the atom positions determined in the x-ray and neutron experiments are in agreement. Some discrepancies occur in the coordinates of the even numbered oxygens (those involved in the hydrogen bonding). The coordinates of the oxygen atoms determined by neutron diffraction should be more precise than those obtained from the x-ray experiments because of the higher relative scattering cross section of the oxygen nucleus for thermal neutrons. This fact is illustrated by the standard deviations obtained in the two experiments. In the x-ray case the average standard deviations for the rubidium atoms were $\pm$ 0.003Å and $\pm$ 0.02Å for the oxygen atoms while the refinement of the neutron data yielded average standard deviations of $\pm$ 0.007Å for the oxygens and $\pm$ 0.007Å for the rubidium atoms.

Caution should be exercised in using the standard deviations for purposes of close comparison. The standard deviations obtained by least squares analysis outlined in Chapter III are only meaningful when the error in the observed structure factor is of a random nature. In diffraction experiments several systematic errors are present and

these are not taken into account in the actual least squares refinement. Examples of these are absorption, secondary extinction and possible instrumental errors. While attempts can be made to correct the intensities for absorption and secondary extinction, some systematic errors will undoubtedly remain. The presence of these systematic errors means that the standard deviations obtained from the least squares refinement will be "too optimistic".

Table VII shows that the pertinent bond lengths with the exception of 012-013 and 022-024(b) are in reasonable agreement. The former exception can be attributed to the discrepancies in the y coordinates of both 012 and 013 while the latter can be attributed to the large error in the y coordinate of 024. Because the neutron diffraction temperature factors are isotropic only qualitative comparisons can be made between the two sets of results. Both sets of results indicate a large temperature factor for 014 but in the neutron results the temperature factor of 012 also is larger than the average while in the x-ray case it is the temperature factor of 013 that is larger.

(B) Discussion of the overall features of the structure

It was mentioned in the preliminary discussion of the structure in Chapter IV, Section B, that each rubidium atom is surrounded by six sulphate groups which if regarded as points lie at the vertices of a distorted octahedron, oriented so that the four fold axis of the octahedron lies in the a-c plane parallel to the c axis. Ideally each Rb ion can share

an edge with each of the six surrounding HSO_4^- anions leading to a possible coordination number of twelve. The rubidium ions are arranged about the sulphate groups so that each sulphate group is surrounded by six rubidiums. The structure is held together by these strong Rb-O interactions.

Such a configuration of the Rb and S atoms can be considered to approximate that of the NaCl structure. In this idealized structure the positions of the sulphates are at 1/8, 1/4, 1/8 for S1 and 1/8, 3/4, 3/8 for S2 and the positions for the rubidiums are at 1/8, 1/4, 3/8 for Rb1 and 3/8, 3/4, 3/8 for Rb2. The average deviation from these idealized positions is 0.30Å with the largest deviation occurring in the Rb1 y coordinate which is 0.123 ($\simeq$1/8) rather than 0.25. Reference to Figs. 5 and 8 will illustrate the orientation of the idealized NaCl cell with respect to the $P2_1/c$ cell. The transformations are $\bar{a} = \bar{B} + \bar{C} - \bar{A}$, $\bar{b} = 1/2\ (\bar{C}-\bar{B})$ and $\bar{c} - 2\bar{A}$ where the capital letters refer to the unit cell parameters of the NaCl cell and the lower case letters refer to those of the $P2_1/c$ cell.

In Fig. 8 the atoms are labelled so as to illustrate their positions relative to the NaCl cell. It can be seen that the one edge of the NaCl cell is parallel to the $\bar{c}$ axis while the b axis is parallel to one of the face diagonals. The $\bar{A}$ axis is parallel to the 24.6Å axis in the large orthogonal cell.

FIGURE 8

Diagram of the NaCℓ cell as related to $RbHSO_4$.

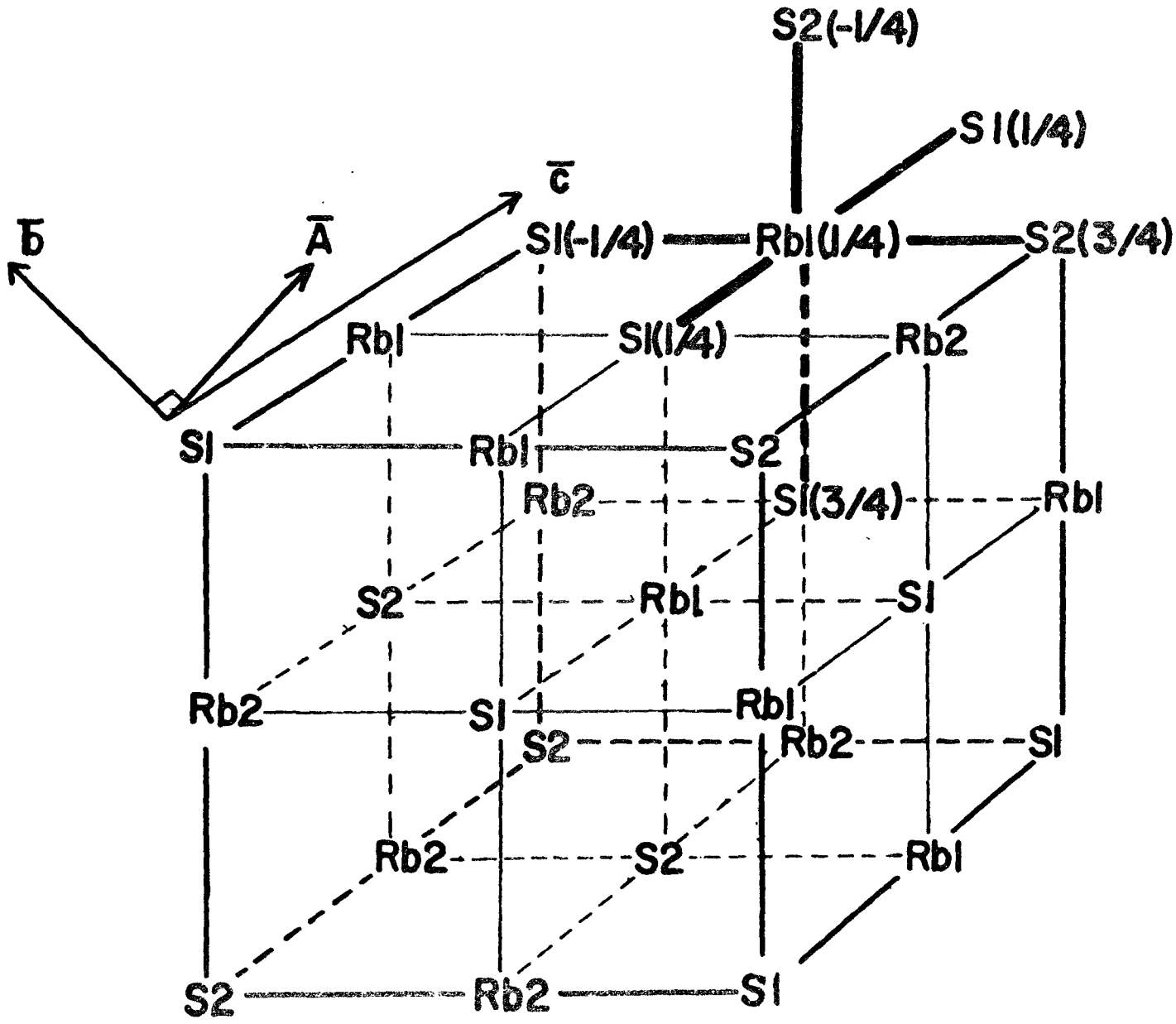
S2(-1/4)
S1(1/4)
c̄
b̄
Ā
S1(-1/4)
Rb1(1/4)
S2(3/4)
Rb1
S1(1/4)
Rb2
S1
Rb1
S2
Rb2
S1(3/4)
Rb1
S2
Rb1
S1
Rb2
S1
Rb1
S2
Rb2
S1
Rb2
S2
Rb1
S2
Rb2
S1

The structure deviates from the idealized NaCl structure in a number of ways. Obviously the oxygen atoms of the sulphate groups reduce the octahedral symmetry about the sulphur atoms to no higher than tetrahedral. In addition, it can be seen that Rb1 and Rb2 have coordination numbers of 10 and 9 respectively instead of 12. As a result the sulphate tetrahedron S1 shares only three (out of a possible six) of its edges with the rubidium atoms while S2 shares only four. A comparison of the axial ratios of the structure, in terms of $\bar{a}$, $\bar{b}$ and $\bar{c}$ (3.2:1:3.2) to the predicted ratios for the NaCl structure ($\sqrt{6}$: 1 : $\sqrt{8}$) shows that the cell is distroted from that of the ideal NaCl structure. It will be shown below that this distortion can be attributed to the hydrogen bonding along the b axis which causes the b axis to contract.

(C) Detailed Discussion of the Structure.

Comparison of the coordinates of the two sulphate groups shows that they appear to be related by a centre of symmetry at (1/4, 1/2, 1/8) or a two fold screw axis parallel to b at (1/4, y, 1/8). The two rubidium atoms are also consistent with the existence of either of these two symmetry operations.

A study of the detailed geometry of the two sulphates shows that the two are not identical and cannot be symmetry related by either a two fold screw axis operation or the centre of symmetry. Table VII lists the pertinent bond lengths and angles and Figs. 9 and 10 illustrate the two sulphate tetrahedra. With the exception of the short 012-014

FIGURE 9

$RbHSO_4$

$T = 23^{\circ}C$

Geometry of the Sulphate Group S1

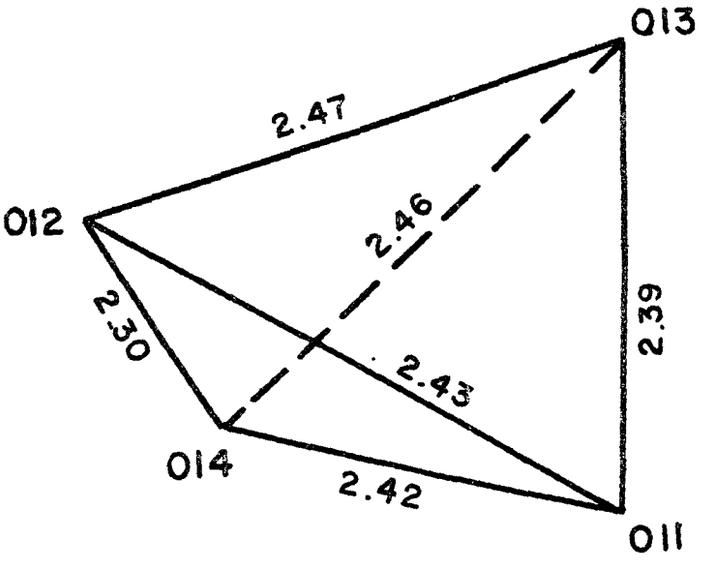
013
2.47
012
2.46
2.30
2.39
2.43
014
2.42
011

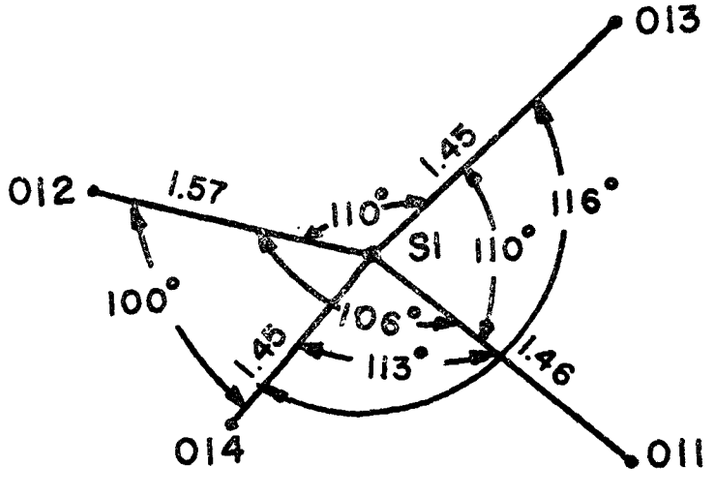
013
012
1.57
1.45
110°
116°
S1
110°
100°
106°
1.45
113°
1.46
014
011

FIGURE 10

$RbHSO_4$

T = 23°C

Geometry of the Sulphate Group S2

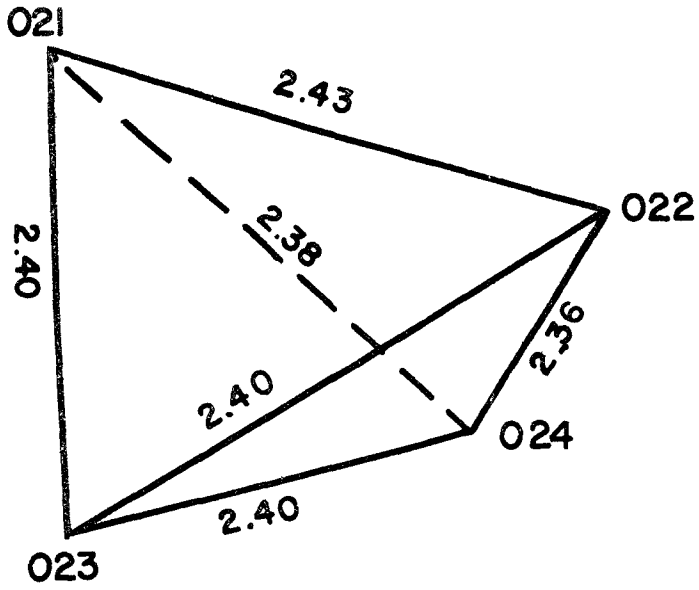
021
2.43
022
2.40
2.38
2.36
2.40
024
2.40
023

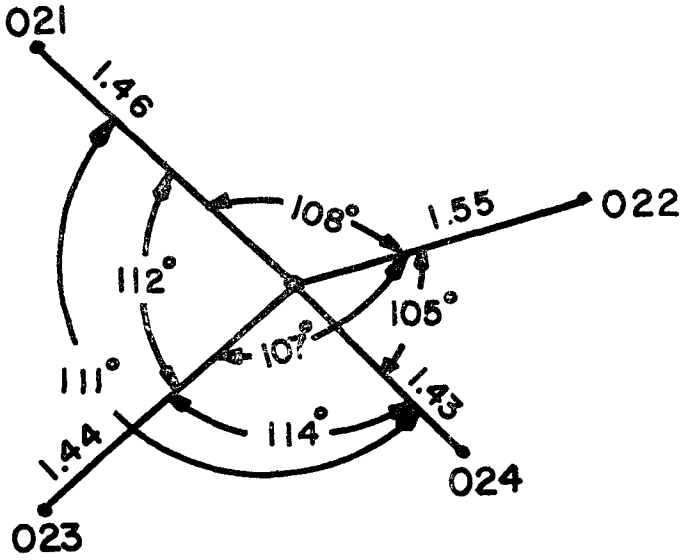
021
1.46
108°
1.55
022
112°
105°
107°
111°
1.43
114°
1.44
024
023

distance, the O-O distances of the S1 group are all within two standard deviations of the average value of 2.41Å. In the case of the S2 group all of the O-O distances are well within two standard deviations of the average value of 2.40Å indicating that the faces of the tetrahedron are regular. The average S-O distances and the O-S-O angles for S1 and S2 groups are 1.48Å, 1.47Å and 109.2°, 109.5°, respectively. These distances and angles agree with those quoted in the literature and the angles are close to those of the ideal tetrahedral angle of 109.46°.

In Table VII it can be seen that in each sulphate group one S-O distance is considerably longer than the average of the group and the remaining three S-O distances are all smaller than the average. A similar effect has been found in $KHSO_4$ (Cruickshank, 1964; see also Loopstra and MacGillavry, 1958), $NaHSO_4$ (Pringle and Broadbent, 1965) and more recently in NH_4HSO_4 (Nelmes, 1970). The S-O lengths for these acid sulphates are shown in Table VIII. The degree of lengthening of one of the S-O bonds is the same as in the case of $RbHSO_4$ and in all of these cases can be attributed to the presence of a hydrogen atom which covalently bonds to one of the oxygens in the sulphate group to form an HSO_4^- anion.

It can also be seen from Table VIII that the average of the O(H)-S-O angles is less than the average of the O-S-O angles. This is also true in the case of $RbHSO_4$. For the S1 group where the long bond is the S1-012 bond, the average of the angles subtended at S1 by 012

TABLE VIII

Sulphate Geometries Reported in other Acid Sulphates

Distances are in Angstroms and angles in degrees.

$NaHSO_4.H_2O$ (Pringle and Broadbent, 1965)

S - 01	= 1.43 (1)	01 - S - 02	= 113 (1)
- 02	= 1.48 (1)	02 - S - 04	= 112 (1)
- 03	= 1.61 (1)	01 - S - 04	= 113 (1)
- 04	= 1.44 (1)	03 - S - 01	= 109 (1)
		03 - S - 02	= 101 (1)
		03 - S - 04	= 108 (1)

$(NH_4)HSO_4$ (Nelmes, 1970)

S - 01	= 1.43 (2)	01 - S - 02	= 113 (1)
- 02	= 1.42 (2)	01 - S - 03	= 112 (1)
- 03	= 1.44 (2)	02 - S - 03	= 115 (1)
- 04	= 1.55 (2)	04 - S - 01	= 109 (1)
		04 - S - 02	= 108 (1)
		04 - S - 03	= 101 (1)

$KHSO_4$ (Cruickshank, 1964)

S - 01	= 1.55	02 - S - 04	= 106
- 02	= 1.48	02 - S - 03	= 110
- 03	= 1.47	03 - S - 04	= 113
- 04	= 1.45	01 - S - 02	= 104
		01 - S - 04	= 112
		01 - S - 03	= 110

and the other oxygens is 105° which is less than the ideal tetrahedral angle of 109.46°. The angles subtended at S1 by the other oxygens have an average value of 113°. In the case of the S2 group the averages are 107° and 112° respectively. A similar situation occurs in $KHSO_4$ (Cruickshank, 1964) and NH_4HSO_4 (Nelmes, 1970).

The lengthening of one S-O bond and the angular effect mentioned above suggest that either the tetrahedron is distorted so that the O-O distances in the tetrahedron are unequal or that the sulphur atom has been shifted from its central position in the tetrahedron. In the S2 group the lengths of the edges of the tetrahedron indicate that it is undistorted and thus the lengthening of the S2-022 bond must be due mostly to the movement of the central S2 sulphur away from 022. In the case of S1 the situation is not so clear. The short 012-014 distance indicates some distortion in the sulphate groups and thus it would appear that the lengthening of the S1-012 bond may be due to a shift of the S1 sulphur from its central position and/or a distortion in the sulphate tetrahedron resulting in unequal O-O distances.

Only two oxygen-oxygen distances between adjacent sulphate groups are less than 3Å. In the case of the S1 groups the distance between 012 and 014 (+b) which is in the adjacent S1 group located one unit cell above S1 is 2.54 ± 0.02Å. The situation is similar for the S2 group where the distance between 022 and 024 (+b) which is in the adjacent S2 group is 2.57 ± 0.02Å. (The neutron diffraction results give

2.63 ± 0.01Å for this distance). These distances correspond to values found for oxygen-oxygen distances which involve a hydrogen bond (Hamilton and Ibers, 1968). Typical O—H···O distances are between 3.00Å and 2.40Å (Hamilton and Ibers, 1968). The shorter distances correspond to a strong and symmetrical bond where the hydrogen atom is equidistant from both oxygens. The weakest and most asymmetrical bonds are correspondingly longer. Distances of 2.5 to 2.6Å correspond to a moderately strong hydrogen bond.

The neutron diffraction results confirm that the hydrogen bonding occurs between 012 and 014 and between 022 and 024 and that the hydrogen atom is acentrically ordered in both bonds. The bond lengths associated with the hydrogen bonding are also shown in TableIX. The hydrogen bonding geometry for both H1 and H2 is illustrated in Figs. 11 and 12. The bond lengths imply that hydrogen H1 is strongly bonded to the oxygen 012 and weakly bonded to 014. The hydrogen bond can thus be represented diagramatically by 012—H1····014 with an 012—H1 distance of 0.94Å and an H1····014 distance of 1.57Å. Similarly the hydrogen bonding scheme for H2 can be represented by 022—H2····024 where 022—H2 is 0.97Å and H2····024 is 1.68Å. Both values for O—H and for the H····O distances are within the range of values found in the literature (Hamilton and Ibers, 1968).

Qualitatively it would be expected that the longer O—H distance would be associated with the shorter O—H···O distance (Hamilton and

TABLE IX

T = 23°C - Interatomic Distances and Angles involving Hydrogen Atoms

Bond lengths are in Å; errors are given in brackets x 10^2.

H1—012	0.94 (1)	H2—022	0.97 (1)
H1···014(b)	1.57 (2)	H2···024(b)	1.68 (1)
H1—$Rb1^{I}$(-a)	3.52 (1)	H2—$Rb1^{II}$(-c)	3.57 (1)
—$Rb1^{II}$(-c)	3.57 (1)	—Rb2(-a)	3.75 (1)
—$Rb1^{II}$(b-c)	3.82 (1)	—Rb2	3.81 (1)
—Rb2	3.41 (1)	—$Rb2^{I}$	3.29 (1)
—H2	4.52 (1)	—H1(-b)	3.89 (1)

Angles are in degrees; errors are given in brackets in degrees.

012—H1···014	172 (1)	022—H2···024	167 (1)
S1 —012—H1	110 (1)	S2 —022—H2	114 (1)
S1 —014···H1	152 (1)	S2 —024···H2	125 (1)

FIGURE 11

$RbHSO_4$: T = 23°C

Detail of hydrogen bonding between

012 and 014.

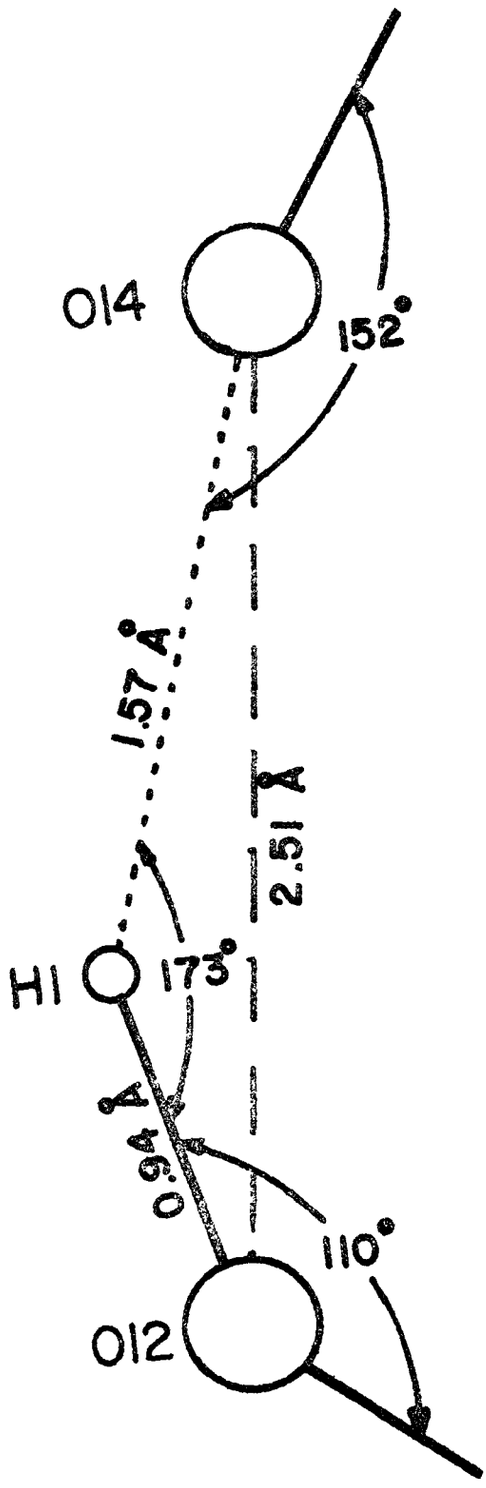
O14
152°
1.57 Å
2.51 Å
H1
173°
0.94 Å
110°
O12

FIGURE 12

$RbHSO_4$: T = 23°C

Detail of hydrogen bonding between

022 and 024.

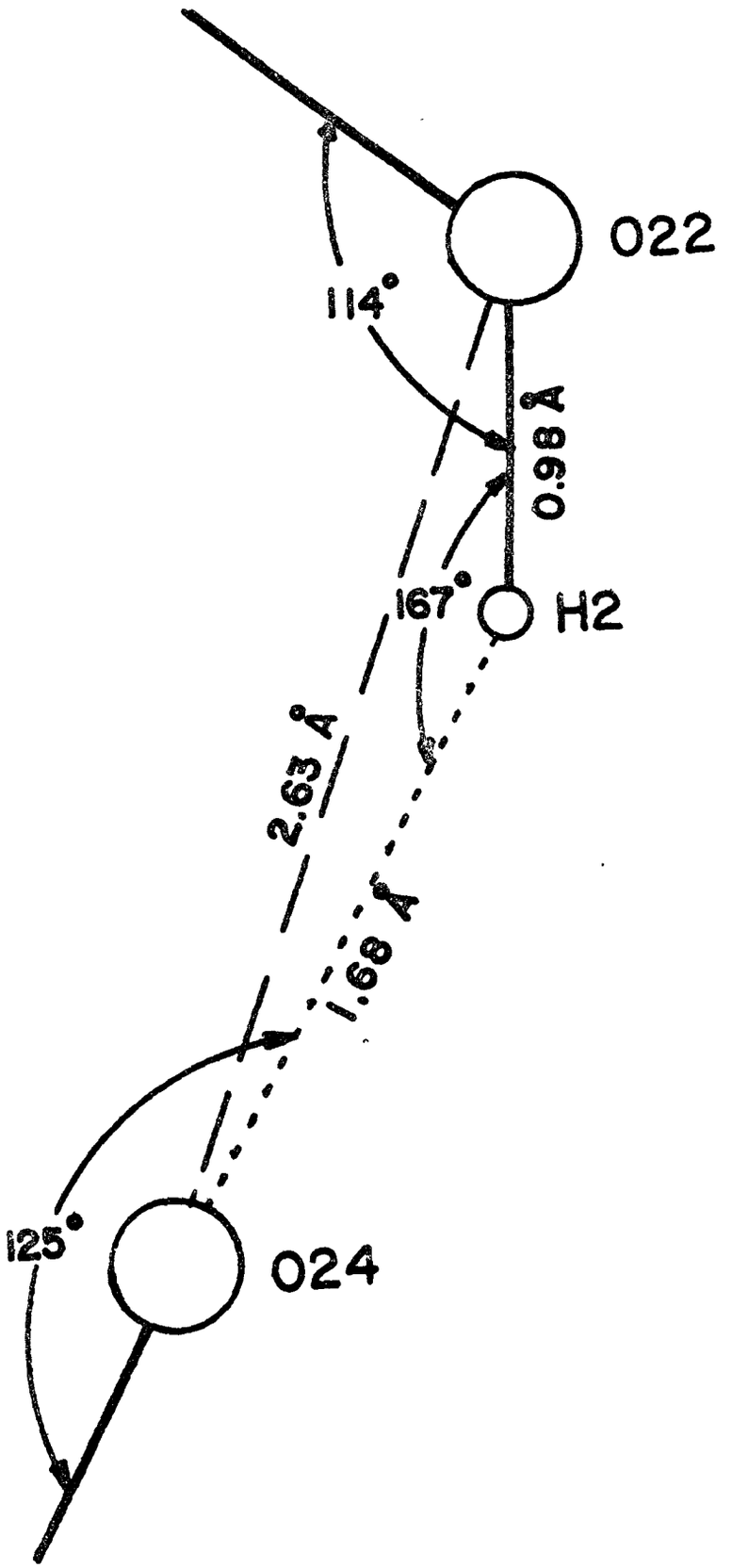
O22
114°
0.98 Å
167°
H2
2.63 Å
1.68 Å
125°
O24

Ibers, 1968). This is not found to be so in either of the two hydrogen bonds. However, in view of the standard deviations, it is probably not significant. It would also be expected that the longer S—O bond would be associated with the shorter O—H bond. This is found to be the case in both of the sulphates but again the standard deviations are too large to attach any significance to the fact.

The angle subtended at H1 by 012 and 014 is 173 ± 3^{o} indicating that the hydrogen bond is bent. In the case of H2 this 022-H2-024 angle is 167 ± 2^{o} indicating that the bond is more bent. These angles are also within the range of values found in the literature (Hamilton and Ibers, 1968).

It is appropriate at this point to discuss the structure of NH_4HSO_4 determined by Nelmes (1970). The atomic coordinates for all heavy atoms are in remarkably good agreement with those for $RbHSO_4$. Consequently there is good agreement between the bond lengths and angles (see Table X). There are, however, some discrepancies in the hydrogen bond geometries in the two structures. While Nelmes finds the hydrogen atoms H1 and H2 strongly bonded to 012 and 022 respectively, the O—H and O—H···O distances and the O—H····O angles differ considerably from those found in $RbHSO_4$.

The neutron diffraction data for the NH_4HSO_4 consists of (h0ℓ) reflections only and as a result the y coordinates for the hydrogen atoms had to be determined by calculation (Nelmes, 1970). It would seem

TABLE X

Comparison of the bond lengths and angles in $RbHSO_4$ with those in the isomorphous NH_4HSO_4 (Nelmes, 1970).

The unweighted average is given for $RbHSO_4$ bond lengths. Bond lengths are given in Å; errors are in brackets x 10^2 Å for $RbHSO_4$ and x 10^3 Å for NH_4HSO_4.

Atoms	$RbHSO_4$	NH_4HSO_4
S1 —011	1.46 (1)	1.430 (2)
—012	1.57 (2)	1.546 (3)
—013	1.44 (1)	1.419 (2)
—014	1.45 (2)	1.441 (3)
S2 —021	1.45 (1)	1.440 (2)
—022	1.56 (1)	1.557 (2)
—023	1.44 (1)	1.441 (2)
—024	1.43 (1)	1.455 (2)
012—014 (b)	2.52 (2)	2.514 (6)
H1 —012	0.94 (1)	0.760 (40)
H1 ...014 (b)	1.57 (2)	1.790 (40)
022—024 (b)	2.61 (1)	2.598 (5)
H2 —022	0.97 (1)	0.690 (30)
H2 ···024 (b)	1.68 (1)	1.920 (30)

Bond angles are in degrees; errors are in brackets and are in degrees.

011—S1—012	107 (1)	109 (.1)
011—S1—013	111 (1)	112 (.1)
011—S1—014	114 (1)	112 (.1)
012—S1—013	108 (1)	108 (.1)
012—S1—014	101 (1)	100 (.1)
013—S1—014	117 (1)	115 (.1)

012—H1···014	172 (1)	160 (4)
022—H2···024	167 (1)	172 (6)
021—S2—022	107 (1)	106 (.1)
021—S2—023	113 (1)	113 (.1)
021—S2—024	113 (1)	112 (.1)
022—S2—023	107 (1)	108 (.1)
022—S2—024	105 (1)	109 (.1)
023—S2—024	113 (1)	113 (.1)

reasonable that these discrepancies in the angles may be due to the lack of accurate y coordinates and hence are probably not significant.

The geometry of the hydrogen bonds and the lack of any large anisotropic temperature factors for the hydrogen atoms suggests that in $RbHSO_4$ the hydrogen atom is acentrically ordered. A similar conclusion has been reached by Nelmes (1970) for the hydrogen bonding in NH_4HSO_4.

Baur (1970) has studied 2400 tetrahedral groups in a variety of crystal structures and has developed an empirical method of predicting the bond length and bond angles from the electrostatic bond strengths of the various cations. It is interesting to compare the results from this study with those predicted by this empirical method. The electrostatic bond strength, measured in valence units (v.u.), that is received by an anion from various cations is given by $Px = \sum_i Z_i/CN_i$ where Z_i is the formal charge and CN_i is the coordination number of each cation. The individual anion - cation distances d(A-X) within the polyhedra are related to the bond strength by $d(A\text{-}X) = \langle d(A\text{-}X) \rangle + b\Delta Px$ where b is an empirical constant, ΔPx is the difference between the individual Px and $\langle Px \rangle$, the mean for the polyhedron, and $\langle d(A\text{-}X) \rangle$ is the mean cation - anion distance for a given coordination number.

Baur has studied a large number of sulphate compounds and has obtained values of 0.128 for b and 1.473Å for $\langle d(A\text{-}X) \rangle$.

The electrostatic bond strength of each of the oxygen anions was calculated by assigning formal charges of +6 to the sulphur ion and +1 to the rubidium ions and by using the coordination numbers of 4 for the sulphur and 9 and 10 for the rubidium ions Rb1 and Rb2 respectively. The bond strengths of the hydrogen bonds were given values of 0.83 v.u. for the donors (012 and 014) and 0.17 v.u. for the acceptors (022 and 024).

The results listed in Table XI show the observed and predicted bond lengths are in good agreement.

A qualitative explanation of the lengthening of the S-O(H) bond can be made as follows. In the sulphate group the bonding occurs through σ orbitals arising from sp^3 hybridisation and from two systems of strongly bonding π orbitals formed from the $3d_{x^2-y^2}$ and $3d_{z^2}$ orbitals of the sulphur atom and the $2p\pi$ and $2p\pi^1$ orbitals of the oxygen atoms, (Cruickshank, 1961). The length of the single S-O bond of 1.69Å is shortened to 1.49Å by this bonding.

When a hydrogen atom is bonded by say O^1, the $2p\pi$ molecular orbital of O^1 overlaps with the s orbital of the hydrogen atom to form a σ bond between them. The formation of this σ bond will increase the electron density between O^1 and H while the loss of one oxygen $2p\pi^1$ bond with the S(3d) orbital will increase the number of electrons at O^1. The result is that the S—O bond will be lengthened. The remaining three $2p\pi^1$ orbitals associated with the other oxygen atoms will join with the $S(3d^1)$ orbital to form one of the systems of π orbitals. Since

TABLE XI

S-O distances based on empirical data compiled by Baur (1970).

The distances are calculated from bond strengths using the empirical equation $d(A\text{-}X) = \langle d(A\text{-}X) \rangle + 0.128\ (\Delta Px)$ where ΔPx is the deviation of the individual Px values from the mean.

	Observed Distances (Å)	Bond Strength (v. u.)	Deviation of Px from ΔPx (v. u.)	Predicted Bond Length (Å)
S1-011 =	1.46	1.80	+0.18	1.46
-012 =	1.57	2.60	-0.62	1.56
-013 =	1.44	1.82	+0.16	1.46
-014 =	1.45	1.70	+0.28	1.44
		Mean = 1.98		
S2-021 =	1.45	1.83	+0.18	1.45
-022 =	1.56	2.72	-0.71	1.56
-023 =	1.44	1.81	+0.20	1.44
-024 =	1.43	1.71	+0.30	1.43
		Mean = 2.01		

the $S(3d^1)$ orbital is now only shared between the sulphates there will be a strengthening of these bonds accompanied by a corresponding decrease in the S-O distances. The other set of orbitals that combines with the S(3d) orbitals are not affected by the hydrogen atom bonding to O^1.

Fig. 8 shows that Rb1 is surrounded by six sulphate groups, four of which are of the type S1 and two S2. The rubidium polyhedron shares edges with four of the sulphate tetrahedra S1, $S1^{11}$, $S2^{11}$, $S1^1(-b)$ and the corners of two, $S2^{11}(-b)$ and $S1^1$, so that it forms bonds with a total of 10 oxygens.

The rubidium oxygen distances are listed in Table XII. The average Rb1-O distance is $3.05 \pm .009$Å with the smallest being 2.91Å and the largest 3.21Å. There are no other Rb1-O distances less than 3.5Å. The Rb1-O distances involving oxygen atoms participating in the shared edges of the polyhedra have an average value of 3.10Å while the distances of corner sharing oxygens 011^1 and $023^{11}(b)$ are shorter with an average of 2.94Å. The former distances range from 3.06Å to 3.21Å while the latter range from 2.91Å to 2.97Å. The angles subtended at Rb1 by the oxygens belonging to the shared edges are all smaller than the angles between other oxygens in the polyhedron suggesting that the sulphates sharing edges with the rubidium atom are further away than those that share a corner. The angles subtended at the sulphur atoms by these oxygens do not show any systematic

TABLE XII

T = 23°C - Rubidium-Oxygen Distances

Bond lengths are in Å; errors are given in brackets x 10^2 Å.

Atoms	Neutron	X-ray	Average
Rb1 - 011	3.07 (1)	3.05 (2)	3.060
- 011^{1}	2.91 (1)	2.90 (2)	2.905
- 011^{1}(-b)	3.11 (1)	3.12 (2)	3.115
- 012^{11}	3.08 (1)	3.02 (2)	3.040
- 013	3.09 (1)	3.05 (3)	3.070
- 014^{1}(-b)	3.15 (1)	3.10 (3)	3.125
- 014^{11}	3.19 (1)	3.22 (2)	3.205
- 023^{11}	3.15 (1)	3.14 (1)	3.145
- 023^{11}(b)	2.97 (1)	2.97 (2)	2.970
- 024	3.05 (1)	3.08 (2)	3.065
Rb2 - 021^{1}(a)	2.98 (1)	3.00 (2)	2.990
- 021^{1}(a-b)	3.07 (1)	3.07 (2)	3.070
- 021^{11}(b)	3.10 (1)	3.06 (3)	3.080
- 022	3.12 (1)	3.10 (2)	3.110
- 022^{1}(a-b)	3.25 (1)	3.30 (2)	3.275
- 023^{11}(b)	3.07 (1)	3.07 (2)	3.070
- 024	3.10 (1)	3.13 (2)	3.115
- 013	3.01 (1)	2.98 (2)	2.995
- 013(b)	2.96 (1)	2.99 (2)	2.975

differences from other O—S—O angles in that $O11^{1}(-b)—S1^{1}(-b)—O14^{1}(-b)$ is 114^{o} while $O12^{11}—S1^{11}—O14^{11}$ is 101^{o}.

Rubidium Rb2 is also surrounded by six sulphate groups four of which are type S2 and two of which are type S1. The Rb2 polyhedron shares edges with three S2 tetrahedra $S2^{1}(a-b)$, S2 and $S2^{11}(+b)$ and the corners with $S2^{1}(a)$, S1 and S1(b) so that it bonds to only 9 oxygens. The average Rb2—O distance to oxygens on the shared edges is 3.12Å with the largest being 3.28Å and the smallest 3.07Å.

Again, the distance to the "corner" oxygens is smaller with an average of 3.00Å with distances ranging from 2.98Å to 3.00Å. The angles subtended at Rb2 by the oxygens belonging to the shared edges of the sulphate groups are all smaller than other O—Rb2—O angles and again the angles subtended at the sulphur atoms show no systematic deviation from the mean.

There are four hydrogen atoms within 4.0Å of each rubidium atom (Table IX). In the case of Rb1 there are three H1 hydrogens and one H2. The distances vary from 3.52Å to 3.82Å. Rubidium Rb2 has three neighbouring H2 hydrogen atoms and one H1. In this case the distances vary from 3.29Å to 3.81Å. Two of these distances, Rb2—H1 (3.29Å) and Rb2—H2 (3.41Å), are noticeably shorter than the others.

The environments of Rb1 and Rb2 are clearly different. Rb1 has 10 neighbouring oxygens and no hydrogen atoms closer than 3.5Å

while Rb2 has 9 neighbouring oxygens and two hydrogen atoms within 3.41Å. The environments of the rubidium atoms are illustrated in Fig. 13. The 10 neighbouring oxygens of Rb1 are indicated by open circles while the 9 neighbours of Rb2 are illustrated by solid circles. It can be already seen that the environments of the two rubidium atoms with respect to the hydrogen atoms are different. Hydrogens H1A and H2A are arranged so that they lie on the same side of the c glide plane at y = 1/4 while in the case of Rb2 the hydrogen atoms H2A and H1B are arranged so that they lie on opposite sides of the glide plane at y = 1/4. The environment of Rb1 can explain why the Rb1 y coordinate is at 1/8 rather than 1/4 (as it is in the case of Rb2[1]). Electrostatic repulsion between the positive H1A and H2A hydrogens and the positive Rb1 ion causes the Rb1 to move away from them and hence from its "ideal" position at y = 1/4, No such movement along the b axis occurs in the case of Rb2 because the hydrogen atoms H2A and H1B are on opposite sides of the ion so that there is no net force along the direction of the b axis.

Table V shows the anisotropic temperature factors determined by the x-ray experiment. Because no absorption corrections were made the thermal factors are probably too large. However, the relative magnitudes of these quantities will be correct for each atom. Two oxygen atoms 013 and 014 both in the sulphate group S1 have noticeably larger temperature factors. The components U_{11} and U_{33} of 014 are

FIGURE 13

$RbHSO_4$: T = 23°C

Detail of rubidium environments. The projection is down the c axis. The O prefixes have been omitted from the labels of the oxygen atoms for reasons of clarity.

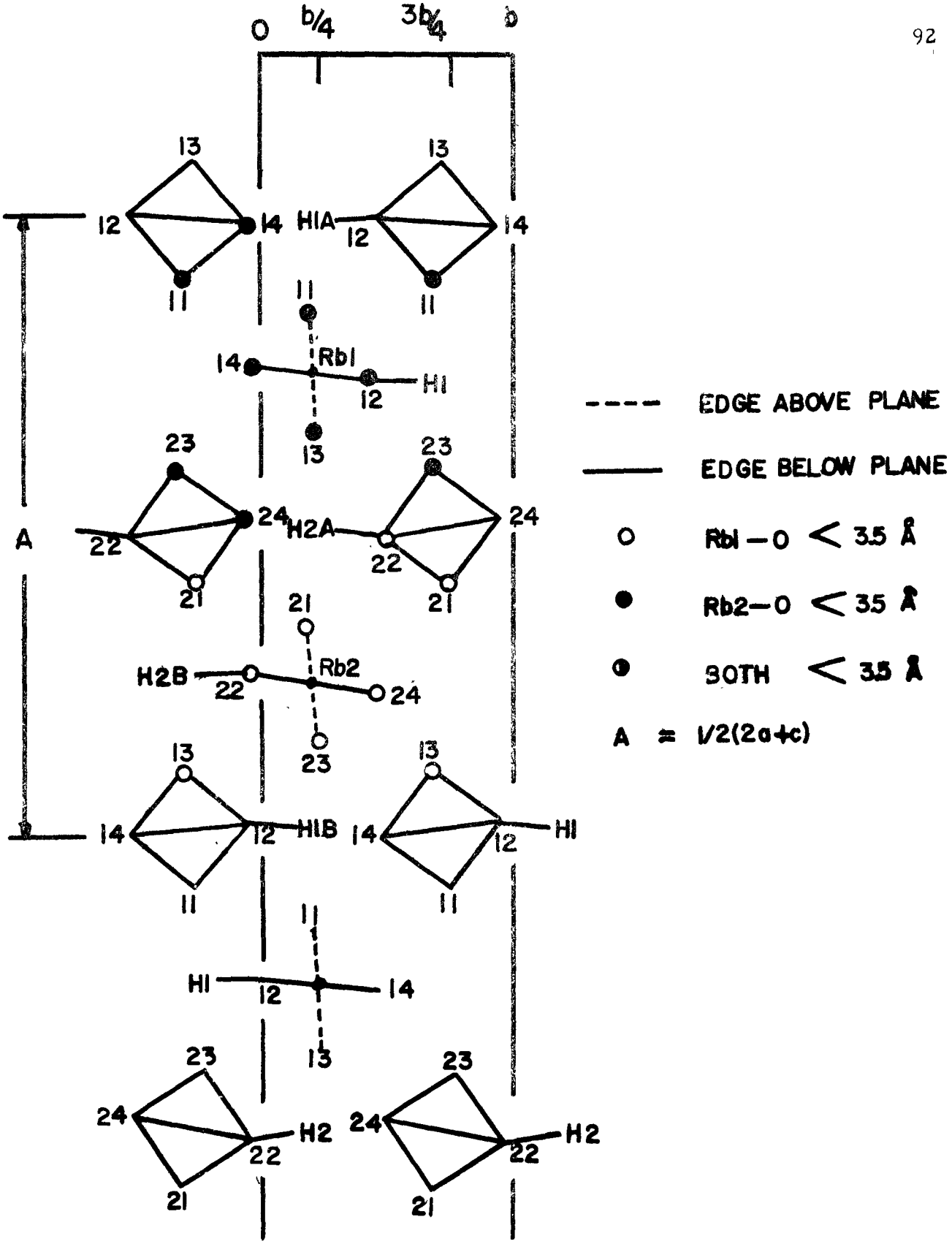
0
b/4
3b/4
b
A
13
12
14
H1A
11
Rb1
H1
23
24
H2A
22
21
Rb2
H2B
H1B
H2
EDGE ABOVE PLANE
EDGE BELOW PLANE
Rb1 — O < 3.5 Å
Rb2 — O < 3.5 Å
BOTH < 3.5 Å
A = 1/2(2a+c)

three to four times larger than average and the U_{22} component of 013 is two times the average value. The lengths (RMS values) and direction cosines of the semi-major axes of the thermal ellipsoids of both sulphate groups are given in Table VI. The cosines are taken with respect to $\bar{a}$, $\bar{b}$, $\bar{a} \times \bar{b}$.

From this table it is clear that the longest axis of the thermal ellipsoid of 013 is parallel to the b axis and is perpendicular to the S1-013 bond. In the case of 014, the largest axis of the ellipsoid is again in a plane perpendicular to the S1-014 bond. The drawing in Fig. 14 made by the computer program ORTEP (Johnson, 1965) illustrates the large thermal parameters on these two atoms. The neutron diffraction results show that the isotropic temperature factors of 014 and 012 are much larger than the average while that which corresponds to 013 is only slightly larger than the average (see Table IV). The fact that both the x-ray and neutron diffraction temperature factors of 014 are large implies that this is a real effect and cannot be attributed to any systematic error. A similar effect involving the temperature factors of atoms corresponding to 013 and 014 has been observed in NH_4HSO_4 by Nelmes (1970).

It is possible to attribute the large thermal factors to two phenomena; motional or static disorder in the crystal. The temperature factors of the atoms 013 and 014 correspond to displacements of these atoms of 0.5Å which means that if the sulphate group were vibrating it

FIGURE 14

Diagram of thermal ellipsoids of

atoms of the two sulphate groups.

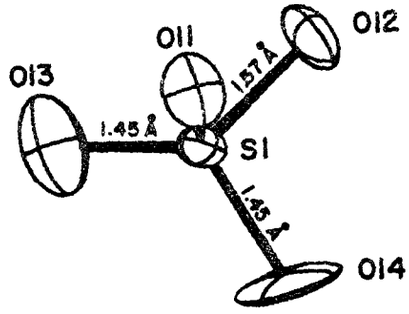
O11
O12
O13
1.57 Å
1.45 Å
S1
1.45 Å
O14

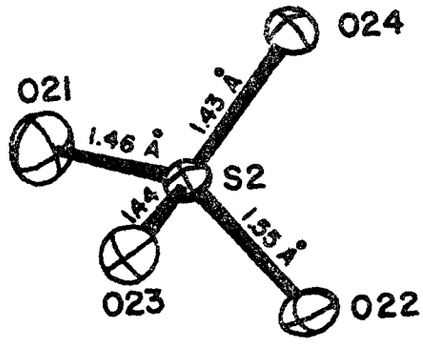
O24
O21
1.43 Å
1.46 Å
S2
1.44
1.55 Å
O23
O22

would have to have an amplitude of 20 degrees. Since an oscillation of this size would require considerable energy it would appear unlikely that the large thermal factors are due only to large amplitude vibrational motion of the S1 groups.

The temperature factors for the oxygens belonging to the S2 sulphates do not show such a large effect. Oxygen atom 021 has the largest thermal ellipsoidal axis length (.25Å). Due to the large errors on the temperature factors for the oxygen atoms and the smaller variations found in their values it is not possible to determine whether or not the S2 groups are disordered. If there is disorder in these groups it is certainly less than that found in the S1 group.

The temperature factors in the rubidium and the sulphur atoms are of reasonable size and show no large anisotropy indicating that these atoms are not disordered and do not exhibit any unusual dynamical behaviour.

The temperature factors of both hydrogen atoms are similar in size to those of the oxygen atoms. Anisotropic refinement of the hydrogen atom temperature factors did not reveal any large anisotropy, in agreement with the acentrically ordered model for the hydrogens.

(D) Discussion of the Idealised NaCl Structure.

It was mentioned in Section (B) that the structure could be considered to be similar to the NaCl structure. In this idealised sodium chloride structure each rubidium atom is surrounded by six sulphate

groups thus forming bonds with a possible total of 12 oxygen atoms. Each oxygen would bond to three rubidium atoms. The sulphate groups would have to be oriented so that there would be a pseudo two fold axis of the sulphate approximately along the b axis and a second such axis along c. In this configuration the hydrogen bonds would be nearly parallel to the diagonal of the face perpendicular to the c axis. Symmetry would further require that the hydrogen bonds be symmetric. Thus in this idealised structure all distinction between Rb1 and Rb2, between the sulphate groups S1 and S2 and between H1 and H2 would be lost.

The actual structure differs from this idealised structure in a number of ways. It was mentioned above that the axial ratios indicate that the b axis has contracted. The hydrogen bonds are parallel to this axis and it thus appears that the b axis has contracted in order to strengthen these bonds.

The acentrically ordered hydrogen bonding scheme does not conform with the requirements of the ideal structure. It will be shown below that it is this hydrogen bonding scheme that gives rise to two unrelated rubidium ions and two HSO_4 groups in the asymmetric zone.

The environments of the two rubidium atoms differ in the number of neighbouring oxygen atoms. This difference can be attributed to the presence of hydrogen bonding between 012 and 014 and between 022 and 024. According to Pauling's electroneutrality principle (Pauling, 1960) the oxygens to which the hydrogens are bonded (012 and 014) would be

"over bonded" if they also formed bonds with three rubidium atoms. In order to avcid this overbonding the sulphates are reoriented so that strong Rb1-012 and Rb1-022 bonds no longer exist (See Fig. 13). In the case of Rb2 this reorientation takes place so that the bond to 012 is greater than 3.5Å and the bond to 022 is noticeably longer (3.28Å) than the average (3.05Å). It should be noted that Rb2 does not bond to the other two oxygens participating in the hydrogen bond (024 and 014).

These facts have been summarised in Table XIII. The number of possible bonds to the rubidium atoms for each oxygen have been listed so that the "long bonds" due to the electroneutrality principle are listed in the lower half of the tables while those in the upper half correspond to Rb-O distances less than 3.22Å. It can be seen that 011, 013, 021 and 023 have the maximum number of three Rb atoms all within a distance of 3.20Å. Oxygens 014 and 024 which are involved in the hydrogen bonding each have two rubidium atoms within 3.20Å while oxygens 012 and 022 (also involved in hydrogen bonding) each have only one rubidium within 3.20Å. The second Rb2-022 distance in the table is 3.26Å and as a result this bond will be weakened.

As mentioned in Section (C) the deviation of the y coordinate of Rb1 (y = 1/8) from its ideal value of 1/4 can be attributed to the configuration of the hydrogen atoms about Rb1. This configuration is such that the electrostatic repulsion between Rb1 and the hydrogens causes Rb1 to shift the ideal y coordinate from 1/4 to 1/8.

TABLE XIII

Summary of Rb-O distances arranged for each oxygen atom.

The distances are the unweighted averages of the distances obtained by neutron and x-ray diffraction experiments.
All distances greater than 3.50Å are indicated by *.

011	012	013	014
Rb1 (3.06)	Rb1 (3.04)	Rb1 (3.07)	Rb1 (3.13)
Rb1 (2.91)		Rb2 (3.00)	Rb1 (3.21)
Rb1 (3.12)		Rb2 (2.98)	
	Rb1*		Rb2*
	Rb2*		

021	022	023	024
Rb2 (2.99)	Rb2 (3.11)	Rb1 (2.97)	Rb1 (3.07)
Rb2 (3.07)	Rb2 (3.28)	Rb1 (3.15)	Rb2 (3.12)
Rb2 (3.08)		Rb2 (3.07)	
	Rb1*		Rb2*

As a result of the coordination numbers of 9 and 10 for Rb1 and Rb2 the sulphate S1 shares only three (out of a possible six) of its edges with the rubidium polyhedra and S2 shares only four. The degree of distortion and the difference in the temperature factors of the two sulphate groups provide further evidence that the two sulphate groups are not identical.

Thus as a result of the acentrically ordered hydrogen bonding there are two cyrstallographically independent molecules of $RbHSO_4$ in the asymmetric zone.

(E) Discussion of the Pseudo Symmetry

Bengtssen (1941) reported the space group of $RbHSO_4$ to be Abmm with a = 4.60, b = 14.8 and c = 24.6Å with the number of molecules per unit cell, z = 16. This is equivalent to the space group Cmma with a = 14.8, b = 24.6 and c = 4.60Å listed in the International Tables (1962).

This study is in agreement with the work of Pepinsky and Vedam (1960) which showed that the room temperature phase of $RbHSO_4$ was actually monoclinic with space group $B2_1/a$ where a = 24.61, b = 4.62, c = 14.81Å and $\beta = 89.8^{\circ}$ and z = 16. This can also be written as $P2_1/c$ with a = 14.36Å and $\beta = 121^{\circ}$ and z = 8.

As noted earlier the photograph of the (010) zone shows the strong pseudo orthohombic nature of the structure. The intensity distribution implies that this pseudo symmetry must include a pseudo mirror plane

perpendicular to the 24.7Å axis and a pseudo n glide parallel to the 14.81Å axis. Presumably it was this pseudo symmetry that led Bengtssen to chose the space group Cmma.

Now that the symmetry and the structure are known it is interesting to ask how the structure deviates from the "ideal" orthorhombic case. The most obvious choice for such an "ideal" orthorhombic cell is based upon the orthogonal monoclinic cell with space group $B2_1/a$ where $\beta = 90^\circ$. The orthorhombic cell must contain all the symmetry elements found in $B2_1/a$ plus some additional symmetry or pseudo symmetry elements which may be associated with one of the orthorhombic space groups. Unfortunately while the cell $B2_1/a$ is orthogonal and appears to be orthorhombic in projection it does not have sufficient symmetry to be identified directly with any of the orthorhombic space groups. There are six centrosymmetric orthorhombic space groups (Bmmb, Bmam, Bmmm, Bmab, Bbmb, Bbab) that are face centered each possessing a sixteen fold general position. Since the number of formula units of $RbHSO_4$ in the $B2_1/a$ cell is sixteen there is one formula unit per general position. The transformation of the unit cell from the monoclinic $P2_1/c$ space group to the monoclinic $B2_1/a$ space group with $\beta = 90^\circ$ (the orthogonal cell) is given by $\overline{A} = 2\overline{a} - \overline{c}$; $\overline{B} = \overline{b}$; $\overline{C} = \overline{c}$ where the capital letters refer to the orthogonal cell and the lower case letters refer to the monoclinic $P2_1/c$ cell. This transformation will create additional A glide plane parallel to the $\overline{B}$ axis.

The indices will transform in the following manner; H = 2h - ℓ; K = k; L = ℓ where hkℓ refer to the indices based on the $P2_1/c$ cell and the capitals refer to those based on the orthogonal cell.

On the basis of systematic absences it is possible to show that four of the six space groups do not satisfy the symmetry requirements of the monoclinic cell. The space groups Bmmm and Bmam can be dismissed since they do not contain a 2_1 axis parallel to the $\bar{b}$ axis and therefore do not satisfy the conditions required by the $B2_1/a$ cell that for reflections of the type OKO, K must be even. Out of the remaining four space groups two, Bmmb and Bbmb, do not contain the c and a glide planes and thus violate the requirement that for HOL both H and L must be even. The remaining space groups Bmab and Bbab are consistent with the systematic absences required by the $B2_1/a$ cell.

Attempts to generate an approximation to the $B2_1/a$ structure from either of these two space groups failed because it was not possible to generate the pseudo symmetry related atoms of the $B2_1/a$ structure by the symmetry operations of Bbab or Bmab. It is therefore not possible to identify the space group $B2_1/a$ with a higher symmetry orthorhombic space group.

The structure of $RbHSO_4$ does have some pseudo orthorhombic character and it should be possible to find some unit that exhibits this pseudo symmetry and also to find the "ideal" orthorhombic space group. An alternative approach is to look for a pseudo cell that is a fraction of

the volume of the large $B2_1/c$ cell. From Table IV or Fig. 5 it can be seen that both the Rb1 and Rb2 positions and both the S1 and S2 positions are related by a pseudo centre of symmetry located at x= 1/8, y = 1/2, and z = 0 in the orthogonal $B2_1/a$ cell. Thus the pseudo cell would contain only two molecules of $RbHSO_4$ related by the pseudo centre of symmetry. Such a cell would have the dimensions a/8 x b x c/2 where a, b, and c are the dimensions of the $B2_1/a$ cell. The large orthogonal cell (a = 24.7Å, b = 4.62Å, and c = 14.81Å) will be composed of eight of these higher symmetry pseudo orthorhombic sub-cells.

Because of the symmetry of $B2_1/a$ this new cell must have two fold screw axes at $x = a^1$, $z = 0$; $x = a^1$, $z = c^1$; $x = 0$, $z = c^1/2$;and centres of symmetry at 0, 1/2, 0; 0, 1/2, 1; and 1, 1/2, 1, 2 (these are fractional coordinates of the new pseudo cell which is illustrated in Fig. 15). These symmetry elements together with the pseudo centre of symmetry will generate additional centres of symmetry and screw axes as shown in Fig.16 and two mirror planes parallel to the c plane at y = 1/4 and 3/4. An orthorhombic space group that includes all these symmetry operations is Pmmn.

The general positions in Pmmn are;

x, y, z; 1/2 - x, y, z; x, 1/2 - y, z; 1/2 - x, 1/2 - y, z;

x, y, z; 1/2 + x, y, z; x, 1/2 + y, z; 1/2 + x, 1/2 + y, z.

Since there are only two formula units in this unit cell the atoms must be located in special positions. The rubidium atom R and the sulphur atom

FIGURE 15

Comparison of the orthogonal

and oblique unit cells.

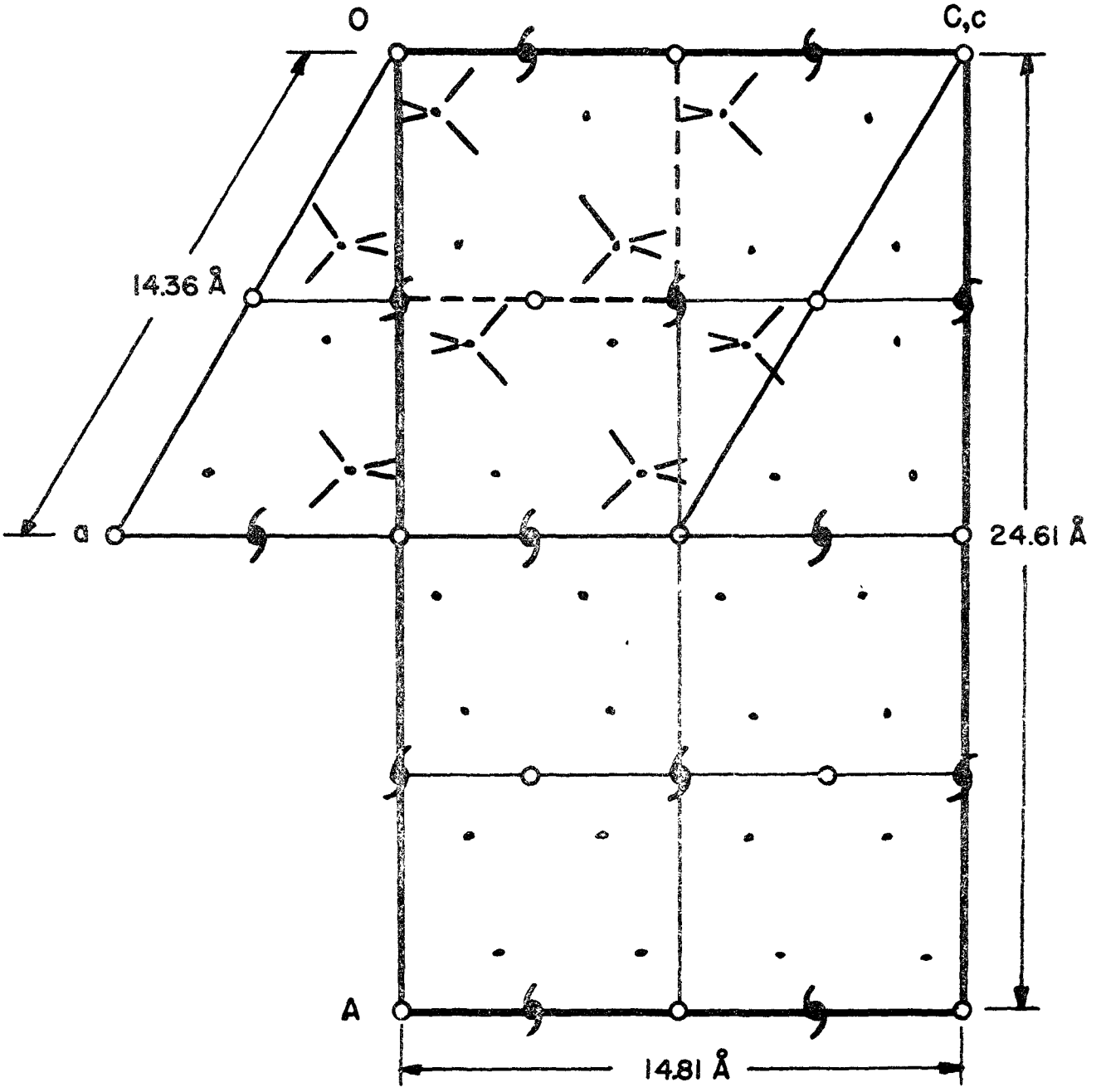
O
C,c
14.36 Å
a
24.61 Å
A
14.81 Å

FIGURE 16

Pmmn Details

(A) Symmetry of $B2_1/a$
The pseudo centre of symmetry is shown dotted.

(B) Symmetry of Pmmn.

(C) Configuration of the Atoms in Pmmn.

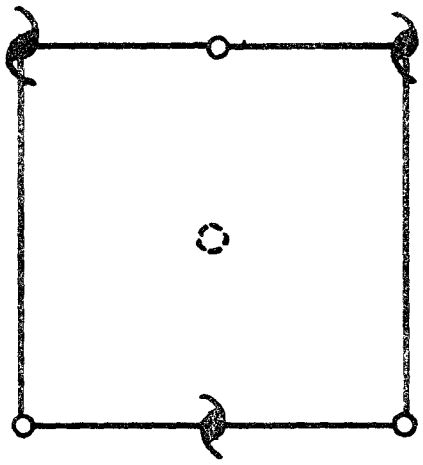

(A)

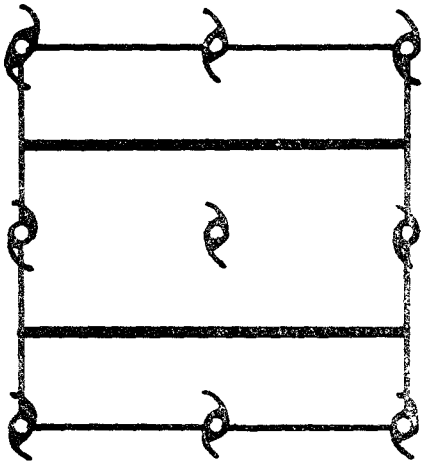

(B)

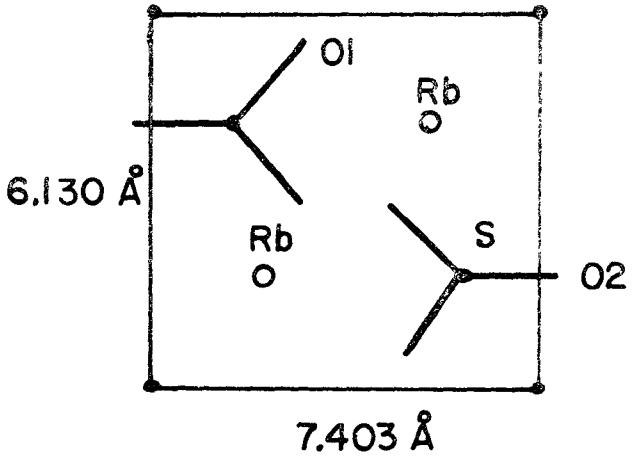

(C)

S will go into positions (a) at 1/4,1/4,z (and also 3/4,3/4,z) with z = 3/4 and 1/4 respectively. Only two oxygen atoms are needed to specify the oxygen positions in the sulphate tetrahedra since 011 and 013 as well as 012 and 014 will be related by the mirror planes and the two sulphate groups will be related by the pseudo centre of symmetry. The oxygen atoms 011, 013, 021 and 023 will be generated by special positions (f), (x, 1/4, z; x, 3/4, z; 1/2 - x, 1/4, z; 1/2 + x, 3/4, z) with x = 0.08 and z = 0.33. Oxygen atoms 012, 014, 022 and 024 will be generated by special positions (e), (1/4, y, z; 3/4, y, z; 1/4, 1/2 - y, z; and 3/4, 1/2 + y, z) with y = 0.07 and z = 0.05.

The constraints placed on the structure by the space group Pmmn will have a similar effect as those mentioned above in the discussion of the idealized NaCl structure. Briefly, the orthorhombic structure will require symmetrical hydrogen bonds and equivalence between atoms Rb1 and Rb2 and between the sulphate groups S1 and S2. The mirror planes at y = 1/4; 3/4 will require equivalence between oxygens 012, 014, 022 and 024. The mirror plane perpendicular to the a axis requires that 011, 013, 021 and 023 be equivalent. The deviations from this orthorhombic structure are similar to those discussed in the case of the idealized NaCl structure.

The orthorhombic pseudo symmetry implies the existence of a high temperature phase transition above which the structure would be completely described by the orthorhimbic space group Pmmn. It is

conceivable that at this higher temperature the hydrogen atoms should have sufficient energy to jump between two different equilibrium positions making it possible for the two pseudo symmetry related formular units of $RbHSO_4$ to become symmetry related.

Unfortunately $RbHSO_4$ melts at 208°C and it is therefore unlikely that this higher symmetry phase exists.

CHAPTER VI

The Structure of the Ferroelectric Phase

(A) Determination of the Structure

The low temperature structure differs from the room temperature phase in that it has lost the two fold screw axis and therefore has twice as many atoms in the asymmetric zone. The loss of the two fold screw axis was confirmed by the appearance of 030 and 050 reflections in the x-ray case and 030 in the neutron case. Initially the atoms were generated by applying the symmetry operations arising from the 2_1 axis to the coordinates of the atoms in the room temperature phase. It should be noted that in keeping with the convention used in the International tables the glide plane in the lower symmetry cell Pc was placed at the origin (in $P2_1/c$ it is placed at y = 1/4). The actual coordinate transformation applied to the room temperature coordinates is xyz $\longrightarrow$ - x, 1/4 + y, 1/2 - z.

Comparison of the Patterson synthesis projected onto (010) and (100) with those from the room temperature phase showed that the two phases were similar indicating that the coordinates of the Rb atoms do not change appreciably as the crystal undergoes the phase change. It was not possible to resolve the individual Rb-O vectors and hence no conclusions could be made regarding the oxygen positions.

In order to obtain some measure of the magnitude of the differences between the two structures, the x-ray data were refined with the final room temperature parameters with the symmetry of the space group $P2_1/c$. After two cycles of refinement the unweighted R reached a value of 0.22. This implies that the differences between the two structures are small and, in particular, that within one estimated standard deviation there is no significant change in the positions of the rubidium atoms. The final room temperature structure with the low temperature neutron data gave an R of 0.31 implying that the oxygen atoms' positions have changed.

It was noted that in the paraelectric phase the refinement with the room temperature neutron data showed that the temperature factors of 012 and 014 (0.052Å^2 and 0.067Å^2) were larger than the average of 0.030Å^2 for the other oxygens. In the case of x-ray diffraction it was oxygen atoms 013 and 014 that had larger temperature factors. The anisotropic temperature factor components U_{11} and U_{33} of oxygen atom 014 were noticeably larger than the average values for the other oxygen atoms (See Table V). On the assumption that this large value was due to some disordering of the sulphate group S1 the group was rotated from its position in the paraelectric phase about an axis parallel to the crystallographic c axis by an amount of 20 degrees. The sulphate group S2 was arbitrarily rotated by 20 degrees about an axis parallel to the b axis in order to destroy the centrosymmetric nature of the model.

These positions were used in a least squares refinement with the low temperature x-ray data. The R factor decreased to 0.20 and appeared to be relatively insensitive to the oxygen atom parameters. It was observed that some of the oxygen atom's coordinates changed in an erratic manner, resulting in S-O distances that varied from 1.28 to 1.71Å. On the basis of the least squares standard deviations the average error in the S-O distance was $\pm$ 0.08Å.

Reference to the correlation matrix showed that while most elements were less than 0.20, thirty-nine were greater than 0.40 indicating the existance of strong correlations.

In order to minimize the correlations, the geometry of the sulphate anions was fixed and the sulphates were refined as a group. In these refinements the orientations of the groups and their centres were allowed to vary. Those groups that were symmetry related in the room temperature phase were refined in different cycles of refinement. Various starting points, using different orientations of the sulphates, were tried. If it is assumed that the loss of the two fold axis must be due to a change in the orientation of the sulphates, it is possible to try different models based on the fact that in the low temperature phase there must be a spontaneous dipole moment along the c axis. In the room temperature phase the HSO_4^- ion will also have a dipole moment associated with it but, because of the symmetry of

the space group $P2_1/c$, the net dipole moment due to these HSO_4^- anions will be zero.

All the models refined to an approximation of the room temperature structure with an R of 0.16. Further refinement did not produce a significant change in the R value. The refinement of the individual oxygen and sulphur atoms resulted in an increased R factor and unreasonable bond lengths of 1.2 to 2.1Å.

Attempts to refine the low temperature neutron diffraction data resulted in similar problems. In this case 99 elements of the correlation matrix were greater than 0.40 and it was necessary to refine the sulphates as groups. Initially the hydrogen atoms were placed in the positions corresponding to those in the room temperature phase. Refinement of the sulphate groups and hydrogen atoms resulted in the R factor decreasing from 0.33 to 0.26. Extinction corrections were applied, as in the case of the room temperature neutron diffraction data. After three cycles of refinement and two cycles of extinction corrections the R factor was 0.16. Further refinements did not produce any significant improvement in the R factor and attempts to refine individual oxygen and sulphur atom parameters resulted in an increased R factor and unreasonable bond lengths.

(B) Discussion

Both the x-ray and neutron diffraction refinements are in qualitative agreement with each other and both result in the orientations

of the sulphate groups being approximately the same as those found in the room temperature structure. A comparison of the Rb-O distances obtained from the refinements with the low temperature and room temperature data shows some differences but because of the high standard deviations it is not possible to state whether these are significant.

It can be shown (Cruickshank, 1960) that the error in a positional parameter x is given by the expression $\sigma(x) = R/\bar{s}\sqrt{N/4P}$ where R is the R factor $\bar{s}$ is the r. m. s. reciprocal radius, $N = \sum_i f_i^2/f^2$ (where f_i is the form factor for each atom evaluated at $s = 2 \sin\theta/\lambda$ and f is the form factor of the atom under consideration) and P is the difference between the number of variables and the number of reflections. For the x-ray refinements the error in the oxygen and sulphur positions is approximately $\pm$ 0.02Å, resulting in an error of $\pm$ 0.08Å in the S-O bond length. In the case of the Rb-O distances the error will be $\pm$ 0.04Å. It is quite conceivable that the difference between the positional parameters of the paraelectric and ferroelectric structures is of the order of $\pm$ 0.02Å for the oxygen and sulphur atoms and as a result it is not possible to determine the structure of the ferroelectric phase with the data collected in these experiments. The relatively low R factors obtained when the room temperature positions were refined with the low temperature data support this idea.

There are several reasons why the refinement of the low

temperature structure failed to converge to a low R factor and a physically reasonable structure. In the case of the x-ray diffraction refinement it should be noted that due to the relatively large scattering power of the rubidium atom the refinement is not "sensitive" to the oxygen atom positions. The low temperature neutron data is insufficient to overcome the correlation problems encountered during the refinement of the individual atomic positions.

It is also possible that the crystal of $RbHSO_4$ consisted of more than one ferroelectric domain and since the diffraction experiment measured the spatial and temporal average of the atoms throughout the entire crystal the model of the structure of such a multi-domain crystal would have to take into account the number, size and orientations of these domains. Attempts were made to ensure that the samples used were single domain by "poling" the sample (see Chapter III , section C) but it was not possible to determine whether or not the samples were single domain at the time of the experiment. The fact that the samples were poled and that there were no large anisotropic temperature factors in the refinements with the low temperature data would suggest that the crystal was indeed single domain.

If the crystals were single domain then it must be the quantity or quality of the data that limits the refinement so that in order to determine the ferroelectric phase it will be necessary to measure more intensities with a greater precision than was attained in these experiments.

Collection of a complete hemisphere of data would minimize the correlation problems encountered in the refinements. It would be advantageous to use neutron diffraction since the relative scattering powers of the atoms are approximately the same. The collection of very accurate x-ray intensities ($\simeq$1%) could take advantage of the anomalous scattering of the rubidium atoms so that a sufficient number of phases could be determined. In addition the anomolous absorption could be used to determine the absolute positions of the atoms with respect to the direction of the spontaneous polarisation.

CHAPTER VII

Discussion and Conclusions

(A) Comparison of the Results with Other Experiments on $RbHSO_4$ and NH_4HSO_4

The similarity between the paraelectric structures of NH_4HSO_4 (Nelmes, 1970) and $RbHSO_4$ and between the Raman spectra (Bazhulin, Myasnikova, and Rakov, 1963; hereafter referred to as BMR, 1963) above and below the transition temperature, T_c, implies that the mechanism of the transition is the same in both compounds. If this is so, one may conclude that the Rb^+ and NH_4^+ ions play minor roles in the ferroelectric behaviour and that there is probably no significant change in the dynamical behaviour of the NH_4^+ ion at the -3^oC transition. Indeed, the results of the cold neutron scattering experiments (Rush and Taylor, 1965) and the NMR experiments (Miller, Blinc, Brenman and Waugh, 1962) confirm that there is little change in the motion of the NH_4^+ ion at the $T = -3^oC$ transition. However, at the lower transition ($T = -96^oC$) in NH_4HSO_4 both experiments reveal changes in motion of the NH_4^+ ion indicating that it plays some role in the -119^oC transition.

The existence of acentrically ordered hydrogen bonding, in which the hydrogen atom is covalently bonded to one of the oxygens of the

sulphate group, is revealed also by the results of the Raman scattering experiment (BMR, 1963) and the infrared experiments (Myasnikova and Yatsenko, 1962). This model of the hydrogen bonding is also in agreement with the NMR results of Silvidi, Falzone and Roupe (1969). A calculation of the second moment based on the proton and rubidium positions determined in this study provided a value of 0.60 gauss^2 (including both Rb-H and H-H interactions) while the value obtained experimentally by Silvidi, Falzone and Roupe (1969) was 0.51 ± 0.03 gauss^2 at room temperature.

In their infrared experiments, Myasnikova and Yatsenko (1962) noted splitting of the bands corresponding to O-H frequencies below T_c and have attributed this to "tunneling" of the protons. Silvidi, Falzone and Roupe (1969) observed that the second moment decreases with decreasing temperature and also attributed the effect to "tunneling". The above authors are unclear in their definition of "tunneling" but it is unlikely that quantum mechanical tunneling would predominate at -35°C where thermally activated processes would be important.

BMR (1963) have reported splitting in some of the bands associated with the vibrational modes of the sulphate group which they attribute to the distortion of the sulphate group. Such a distortion is consistent with the existence of a covalent bond between one of the sulphate oxygen atoms and a hydrogen atom.

While it has not been possible to determine the structure of the ferroelectric phase it can be concluded that the differences between it and the paraelectric phase are small. This is in agreement with the results of Raman experiments (BMR, 1963) which show little difference in the spectra above and below the transition. The results of the refinements of the low temperature structure show some of the hydrogen atoms moving closer to the rubidium atoms. This effect would be in agreement with the Raman experiments (BMR, 1963) which show a slight shift in frequency and intensity of one of the bands associated with the $SO_4^=$ group.

BMR (1963) report a small increase in the frequency of one of the vibrational modes of the $SO_4^=$ group below T_c. It is possible to attribute this increase in frequency to a change in the hydrogen bonding, which will effect the π bonding scheme in the sulphate group. The vibrational frequency of the S-O bond would be increased if it were strengthened. Such a strengthening of the S-O bond would suggest a weakening of the covalent bond between the hydrogen atom and one of the sulphate's oxygen atoms.

(B) Ferroelectricity

The lack of knowledge of the structure of the ferroelectric phase makes it difficult to postulate a model for the transition. The only evidence for an order-disorder type of transition is found in the large temperature factors of the two of the oxygen atoms belonging to one of

the sulphate groups. Without this disorder in the paraelectric phase the crystal would still not exhibit a spontaneous polarisation because the symmetry of the space group $P2_1/c$ is such that the dipoles associated with the HSO_4^- anions would compensate each other. Under this situation the paraelectric phase of $RbHSO_4$ resembles that of an antiferroelectric structure.

With the reduced symmetry at the phase transition, the HSO_4^- anions are likely to assume different orientations. Because this phase is polar along the c axis, these orientations must be such that a net dipole moment will exist parallel to the $\bar{c}$ axis and the resultant dipole parallel to the $\bar{A} = 2\bar{a} - \bar{c}$ axis must be zero. There will be no resultant dipole moment parallel to the $\bar{b}$ axis because the c glide related anions will compensate each other.

The changed orientation of the sulphate anions may be related to changes in the proton positions. It was pointed out earlier that below T_c some of the protons appeared to move closer to the rubidium atoms. Such a movement of the protons could be associated with the change in orientation of the HSO_4^- anions. Without a detailed knowledge of the structure it is not possible to say whether or not the protons are "tunneling" as suggested by Silvidi, Falzone and Roupe (1970).

(C) Conclusion

This work has been entirely successful in its main objective of solving the complete structure of $RbHSO_4$ in its paraelectric phase.

Unfortunately it has not been possible to derive the ferroelectric structure or to infer the ferroelectric mechanism simply from a knowledge of the paraelectric phase. Exploratory work indicated that a full 3-dimensional neutron diffraction study would be needed to solve the structure of the ferroelectric phase.

REFERENCES

Aizu, K. (1966) Phys. Rev. 146, 423.

Bacon, G.E. and Pease, R.S. (1953) Proc. Roy. Soc. (London) A, 220, 397.

Bacon, G.E. and Pease, R.S. (1955) Proc. Roy. Soc. (London) A, 230, 359.

Bacon, G.E. (1962) Neutron Diffraction, 2nd ed. Clarendon Press, Oxford.

Baur, W.H. (1970) Trans. Am. Crystallographic Association. 6, 129.

Bazhulin, P.A., Myasnikova, T.P. and Rakov, A.V. (1963) Sov. Phys. Solid State 5, 1299.

Bengtssen, E. (1941) Ark. Kemi. Min. 15B(7), I.

Buerger, M.J. (1959) Vector Space and its Application in Crystal Structure Investigation, J. Wiley & Sons, Inc. New York.

Bueger, M.J. (1960) Crystal Structure Analysis, J. Wiley & Sons, New York.

Busch, G. and Scherrer, P. (1935) Naturwiss. 23, 737.

Busing, W.R. and Levy, H.A. (1964) Acta Cryst. 17, 142.

Cochran, W. (1960) Advan. Phys. 9, 387.

Cochran, W. (1961) Advan. Phys. 10, 401.

Copely, J.R.D. (1970) Acta Cryst. A26, 376.

Cruickshank, D.W.J. (1964) Acta Cryst. 17, 682.

Cruickshank, D.W.J. (1961) J. Chem. Soc. p5486.

Darwin, C.G. (1922) Phil. Mag. 43, 800.

Devonshire, A.F. (1949) Phil. Mag. 40, 1040.

Hainsworth, F.N. and Petch, H.E. (1966) Can. J. Phys. 44, 3083.

Hamilton, W.C. (1963) Acta Cryst. 16, 609.

Hamilton, W.C. and Ibers, J.A. (1968) Hydrogen Bonding in Solids, W.A. Benjamin, Inc., New York.

Holden, A.N., Matthias, B.T., Merz, W.J., and Remeika, J.P. (1955) Phys. Rev. 98, 546.

Hoshino, S., Vedam, K., Okaya, Y. and Pepinsky, R. (1958) Phys. Rev. 112, 405.

International Tables for X-ray Crystallography. (1962) Kynoch Press, Birmingham.

Johnson, C.K. (1965) Oak Ridge National Laboratory Report ORNL - 3794.

Jona, F. and Shirane, G. (1962) Ferroelectric Crystals, MacMillan Company, New York.

Lipson, H. and Cochran, W. (1966) The Determination of Crystal Structures, 3rd Ed. G. Bell & Sons, London.

Loopstra, L.H. and MacGillavry, C.H. (1958) Acta Cryst. 11, 349.

Matthias, B.T. and Remeika, J.P. (1956) Phys. Rev. 103, 262.

Miller, S.R., Blinc, R., Brenman, M. and Waugh, J.S. (1962) Phys. Rev. 126, 528.

Myasnikova, T.P. and Yatsenko, A.F. (1962) Sov. Phys. Solid State, 4(3), 475.

Nelmes, R.J. (1970) Private Communication.

Pauling, L. (1960) The Nature of the Chemical Bond, Cornell University Press.

Pepinsky, R., Vedam, K., Hoshino, S., and Okaya, Y. (1958) Phys. Rev. 111, 1508.

Pepinsky, R. and Vedam, K. (1959) Phys. Rev. 114, 1217.

Pepinsky, R. and Vedam, K. (1960) Phys. Rev. 117, 1502.

Pringle, G.E. and Broadbent, T.A. (1965) Acta Cryst. 19, 426.

Remeika, J.P. and Merz, W.J. (1956) Phys. Rev. 102, 295.

Rush, J.J. and Taylor, T.I. (1965) Inelastic Scattering of Neutrons, International Atomic Energy Agency, Vienna 2, 333.

Schlemper, E.O. and Hamilton, W.C. (1966) J. Chem. Phys. 44, 4498.

Silvidi, A.A., Falzone, A.J., and Rouple, J.L., (1969) Solid State Common. 7, 359.

Slater, J.C. (1941) J. Chem. Phys. 16,

Valasek, J. (1922) Phys. Rev. 19, 478.

von Hippel, A., Breckenridge, R.G., Chesley, F.G. and Tisza, L. (1946) Ind. Eng. Chem. 38, 1097.

Zachariasen, W.H. (1945) Theory of X-ray Diffraction in Crystals, Dover Publications, New York.

Zachariasen, W.H. (1967) Acta Cryst. 23, 558.

APPENDIX A

The Secondary Extinction Coefficient

Extinction is the reduction of intensity of the incident beam of radiation due to Bragg reflection. If a crystal is oriented so that it is in the Bragg reflecting condition then as the beam of incident radiation penetrates the crystal some of this intensity will be scattered into the diffracted beam and in turn some of this diffracted beam will be scattered back into the incident beam. There will be a phase difference of 180^{o} between this twice reflected beam and the incident beam so that the two will interfere destructively, resulting in an attenuation of the beam. Such a process requires that the crystal be perfect so that the multiple scattering will be coherent. This attenuation, due to the coherent scattering, is called primary extinction and has been discussed by Darwin (1922) and Zachariasen (1945, 1967).

In reality crystals are composed of many small perfect blocks (which are referred to as mosaic blocks) slightly misoriented from some mean direction. Since the angular range of reflection for a perfect crystal is of the order of seconds of arc and the misorientation of the mosaic blocks is of the order of minutes of arc the incident beam will be able to penetrate much deeper into the crystal without suffering from attenuation due to primary extinction. Some of the misoriented mosaic

blocks will still be in the Bragg reflecting condition and as a result will scatter intensity out of the beam. A mosaic block located deeper in the crystal may be "shadowed" by one with the same orientation located closer to the surface upon which the x-ray beam is incident. The beam diffracted by this second block will have a random phase with respect to the beam diffracted by the first block and thus no interference (constructive or destructive) will occur. The result of this incoherence between the two diffracted beams is a reduction in the intensity of the diffracted beam. Such an effect is called secondary extinction. In ideal crystals, which are to some extent mosaic, it is customary to assume that the primary extinction is negligible and to make corrections only for the effects of secondary extinction. The theory and procedure discussed below follow that outlined by Hamilton (1957, 1963).

It is assumed that the boundary curve of the cross section of the crystal is convex so that the emergent beam from the crystal cannot re-enter the crystal. A coordinate system can be constructed so that one axis (M) is parallel to the incident beam and the other axis (N) is parallel to the diffracted beam. A general point in the crystal may then be represented by (m, n) in the coordinate system.

The rate of interchange of energy between the incident beam of power P_o at the point (m, n) inside the crystal and the diffracted beam of power P_H at (m, n) can be represented by the two equations:

$$\partial P_H/\partial M = -(\mu+\sigma)P_H + \sigma P_o$$

$$\partial P_o/\partial N = -(\mu+\sigma)P_o + \sigma P_H$$

where M and N represent the distances along the directions of the diffracted and incident beams respectively. The quantity μ is the linear absorption coefficient measured in cm^{-1} and σ is, in the case of neutron diffraction $QW(\Delta\theta)$ where $W(\Delta\theta)$ is the distribution function for the mosaic blocks and Q is the reflectivity defined by the equation $Q = \lambda^3 F_c^2/V_c^2 \sin 2\theta$ where λ is the wavelength of the neutron, θ is the Bragg angle, F_c is the structure factor and V_c is the volume of the unit cell. Normally it is assumed that $W(\Delta\theta)$ is represented by a Gaussian function with standard deviation η. In this treatment $W(\Delta\theta)$ is approximated by a step function defined by:

$$W(\Delta\theta) = 1/2\eta\sqrt{3} \qquad |\Delta\theta| \leq \eta/3$$

$$W(\Delta\theta) = 0 \qquad |\Delta\theta| > \eta/3.$$

In the case of a spherical or cylindrical sample the differential equations may be solved analytically. The appropriate boundary conditions are $P_o = P_o^o$ for points where the beam is incident on the crystal and $P_H = 0$ for points opposite to those where the diffracted beam emerges. In the program ESAF the boundary of the crystal is approximated by a series of planes. The differential equations can then be solved to give P_H and P_o for each point on a two dimensional grid constructed so that its axes are parallel to the directions of the incident and diffracted beams.

A numerical integration of P_H over the cross section of the crystal will provide a value of $P_H(m_s, n_s)$ at the surface of the crystal where the diffracted beam emerges. This value of P_H will be a function of the angle $\Delta\theta$ and can be written as $R(\Delta\theta)$.

The integrated intensity R_H can then be defined by:

$$R_H = \int_{-\infty}^{\infty} R(\Delta\theta)\, d(\Delta\theta) \;/\; P_o \int_{-\infty}^{\infty} W(\Delta\theta)\, d(\Delta\theta).$$

By using the expression for $W(\Delta\theta)$ mentioned above these integrals may easily be solved. The secondary extinction coefficient E_s may then be determined by:

$$E_s = I_o^H / I_c^H = R^H / QVA$$

where I_o^H, I_c^H are the observed and calculated intensities. Q is the reflectivity, V the crystal volume and A the pure absorption correction factor.

The extinction coefficient is a function of both the intensity I_c^H and the Bragg angle θ. Hamilton (1957) has shown that if $E_s > 0.70$ the variation in E_s as a function of Bragg angle is less than 3%. This condition is satisfied in the case of $RbHSO_4$ and hence the dependence of E_s upon the angle θ can be ignored. The extinction coefficient E_s is also a function of the intensity. Because the intensities have not been measured on an absolute scale it is not possible to apply the extinction correction until the appropriate scaling factor has been determined. This problem may be overcome by partially refining the structure and then plotting a graph of $\ln(I_o^H / I_c^H)$ versus I_c^H. Since $E_s = I_o^H / I_c^H = e^{-KI_c^H}$

the plot should give a straight line with slope K. This value for K can be used in the program ESAF to evaluate the correction factors for each reflection. Further refinement and repeated corrections can be made until the slope of the plot is zero.

PBFSO4 X-RAY DATA (T=23 C) UNOBSERVED REFLECTIONS ARE MARKED WITH * AND UNRELIABLE WITH U

H	L		FOBS	FCLC
		K = 0		
0	2	*	17	4
0	4		192	206
0	6	*	23	0
0	8		101	102
0	10	*	29	14
0	12		141	140
0	14	*	31	4
1	0	*	11	3
1	2	U	38	43
1	4	*	25	9
1	6		57	55
1	8	*	34	7
1	10		38	74
1	12	*	38	11
1	14		38	78
1	16	*	33	15
1	-6		129	124
1	-8	*	32	22
1	-10		86	84
1	-12	*	14	11
1	-14		45	52
2	4		180	192
2	6	*	31	8
2	8		186	182
2	10	*	18	11
2	12	*	20	5
2	14	*	21	7
2	16		58	53
2	-4	U	234	322
2	-6	*	11	3
2	-8		154	147
2	-10	*	16	5
2	-12		31	29
2	-14	*	20	2
2	-16		61	67
3	0	*	18	10
3	4	*	20	7
3	6		74	73
3	8	*	36	10
3	10		66	65
3	12	*	38	11
3	14	*	35	15
3	16	*	16	2
3	-6		161	177
3	-8	*	30	13
3	-10	*	34	5
3	-12	*	37	16
4	0	L	279	329
4	2	*	26	12
4	4		183	184
4	6	*	34	10
4	8		93	86
4	10	*	38	4
4	12		93	95
4	-4		194	204
4	-6	*	26	3
4	-8		76	78
4	-10	*	34	11
4	-12		155	155
4	-14	*	38	9
5	0	*	25	20
5	2		152	145
5	4	*	32	16
5	6		79	74
5	8	*	37	23
5	10	*	38	3
5	-2		45	46
5	-4	*	23	5
5	-6		127	127
5	-8	*	17	17
5	-10		143	149
5	-12	*	36	14
6	0	*	23	2
6	2	*	22	16
6	4		173	167
6	6	*	36	17
6	8		104	97
6	10	*	38	7
6	-2	*	11	0
6	-4		193	193
6	-6	*	15	8
6	-8		141	148
6	-10	*	33	6
6	-12	*	36	4
6	-14	*	38	5
6	-16		90	98
7	0	*	25	1
7	-0	*	29	1
7	2		33	33
7	4	*	35	2
7	6	*	37	24
7	8	*	38	3
7	-2		150	153
7	-4		26	26
7	-6		57	48
7	-8	*	30	21
7	-10	*	15	4
7	-12	*	36	3
7	-14		37	79
8	0		212	218
8	2	*	15	0
8	4		57	55
8	6	*	38	13
8	-2	*	17	1
8	-4		173	170
8	-6	*	29	5
8	-8		104	107
8	-10	*	23	10
8	-12		160	157
8	-14	*	37	14
8	-16		47	62
9	0	*	26	18
9	2		48	48
9	4	*	37	22
9	-2	*	16	10
9	-4	*	30	6
9	-6		94	85
9	-8		28	26
9	-10		86	81
9	-12	*	18	9
10	0	*	31	1
10	2	*	17	8
10	4		121	121
10	6	*	38	13
10	-2	*	15	8
10	-4		164	169
10	-6	*	32	3
10	-8		184	180
10	-10	*	19	4
10	-12	*	32	33
10	-14	*	38	7
10	-16		90	99
11	0	*	20	1
11	2		44	42
11	-2		53	55
11	-4	*	34	15
11	-6		63	65
11	-8	*	17	12
11	-10		28	25
11	-12	*	17	6
11	-14		40	41
12	0		142	147
12	2	*	19	5
12	-2	*	17	9
12	-4		62	54
12	-6	*	35	7
12	-8		96	92
12	-10	*	36	7
12	-12		140	144
12	-14	*	23	18
13	0	*	31	12
13	2		40	48
13	-2	*	25	21
13	-4	*	37	4
13	-6		41	37
13	-8	*	37	24
13	-10		63	65
13	-12	*	18	12
13	-14		44	44
14	0	*	37	1
14	2	*	20	7
14	-2	*	19	1
14	-4		122	121
14	-6	*	38	4
14	-8		105	94
14	-10	*	38	1
14	-12	*	14	8
14	-14	*	22	1
14	-16		68	73
15	0	*	33	4
15	-2		33	55
15	-6		52	55
15	-8	*	39	4
15	-10	*	39	10
15	-12	*	21	10
15	-14		34	38
16	0		61	65
16	-12		101	98
16	-14	*	15	9
16	-16		38	38
18	-16		62	60
		K = 1		
0	1		23	26
0	2	*	20	8
0	4		230	245
0	5		115	114
0	6	*	22	7
0	7		69	62
0	8		180	174
0	9		53	46
0	10	*	30	7
0	11	*	31	4
0	12	*	32	19
0	13	*	31	4
0	14	*	31	9
0	15	*	30	19
1	0	*	15	13
1	1		69	69
1	2		42	49
1	3	*	16	9
1	4		31	29
1	5	*	17	12
1	6		32	49
1	7		30	28
1	8	*	20	18
1	9		58	63
1	10		52	48
1	11	*	14	3
1	12	*	15	2
1	13		31	34
1	14		31	31
1	15	*	26	6
1	2		46	40
1	-1		39	31
1	-2		30	28
1	-3		49	48
1	-4	*	15	0
1	-5		53	60
1	-6		106	102
1	-7		16	15
1	-8	*	16	9
1	-9		43	38
1	-10	*	28	25
1	-11		34	36
1	-12	*	25	18
1	-13		26	22
1	-14		32	31
1	-15	*	24	21
2	1		69	91
2	2	*	11	3
2	3		126	129
2	4		139	150
2	5	*	13	5
2	6	*	15	11
2	7	*	22	15
2	8		96	92
2	9		41	34
2	10	*	18	4
2	11	*	19	13
2	12		95	98
2	13		29	29
2	-1		61	71
2	-2	*	7	7
2	-3		47	47
2	-4		75	86
2	-5		29	31
2	-6	*	15	9
2	-7	*	23	21
2	-8		97	94
2	-9		60	61
2	-10	*	16	7
2	-11	*	27	18
2	-12		127	132
2	-13		29	29
2	-14	*	20	3
2	-15	*	23	16
2	-16		35	26
3	0	*	20	17
3	1		26	23
3	2		129	128
3	3		44	54
3	4	*	21	5
3	5	*	23	17
3	6		31	39
3	7	*	28	10
3	8	*	29	14
3	9	*	31	7
3	10	*	32	16
3	11	*	33	24
3	12		34	6
3	-1		83	82
3	-2		42	40
3	-3		38	35
3	-4	*	17	20
3	-5		42	43
3	-6	U*	21	48
3	-7	*	25	22
3	-8	*	23	16
3	-9		81	75
3	-10		87	79
3	-11	*	29	16
3	-12	*	31	5
4	0	*	22	0
4	1		60	62
4	2	*	16	16
4	3		49	51
4	4		148	154
4	5		54	57
4	6	*	27	1
4	7		37	38
4	8		127	116
4	9		36	35
4	10	*	33	1
4	11	*	34	19
4	12	*	35	4
4	-1		20	20
4	-2		28	28
4	-3	*	17	17
4	-4		220	246
4	-6	*	17	1
4	-7		24	25
4	-8		136	131
4	-9		25	26
4	-10	*	33	10
4	-11	*	25	3
4	-12	*	30	1
5	0	*	22	20
5	1		48	48
5	2	*	19	15
5	3	*	23	2
5	4	*	25	11
5	5	*	27	10
5	6	*	26	25
5	7		37	34
5	8	*	31	4
5	9	*	40	39
5	-1		75	73
5	-2		136	133
5	-3		133	127
5	-4	*	13	14
5	-5		118	115
5	-6		98	100
5	-7		27	22
5	-8	*	19	11
5	-9	*	24	19
5	-10	*	26	9
5	-11		28	34
5	-12	*	23	19
6	0		167	180
6	1		35	32
6	2	*	14	3
6	3		63	58
6	4		80	83
6	5	*	28	2
6	6	*	30	2
6	7	*	31	25
6	8		57	57
6	9	*	34	28
6	10	*	34	6
6	11	*	35	17
6	12		71	68
6	-1		45	46
6	-2	*	15	9
6	-3		55	57
6	-4		151	150
6	-5	*	18	11
6	-6	*	23	20
6	-7	*	20	11
6	-8		95	95
6	-9		64	62
6	-10	*	32	9
6	-11		48	40
6	-12		140	133
7	0	*	23	5
7	1	*	15	9
7	2		67	65
7	3		50	46
7	4	*	28	7
7	5		30	38
7	6		66	66
7	7	*	32	5
7	8	*	33	9
7	9	*	34	6
7	10	*	35	6
7	11	*	35	9
7	12	*	35	8
7	-1	*	27	22
7	-2	*	16	4
7	-3		53	51
7	-4	*	19	16
7	-5	*	19	18
7	-6		62	58
7	-7		64	62
7	-8		29	29
7	-9		65	68
7	-10		74	80
7	-11	*	27	5
7	-12	*	29	5
8	0	*	25	1
8	1		42	41
8	2	*	21	11
8	3		34	32
8	4		127	130
8	5		49	45
8	6	*	32	6
8	7	*	32	29
8	8		69	70
8	9	*	43	8
8	10	*	35	2
8	-1	*	19	8
8	-2	*	18	7
8	-3	*	21	11
8	-4		148	152
8	-5	*	21	15
8	-6	*	17	1
8	-7		42	39
8	-8		170	174
8	-9		30	31
8	-10	*	15	4
8	-11	*	17	14
8	-12	*	29	1
9	0	*	26	16
9	1		55	59
9	2		40	37
9	3	*	30	9
9	4	*	31	9
9	5	*	32	2
9	6	*	33	15
9	7	*	34	19
9	8	*	35	0
9	9	*	35	16
9	-1		52	48
9	-2		68	70
9	-3		57	56
9	-4	*	22	14
9	-5		60	60
9	-6		28	31
9	-7	*	26	17
9	-8	*	20	8
9	-9		42	41
9	-10	*	23	19
9	-11	*	23	18
9	-12	*	29	24
10	0		162	168
10	1		50	40
10	2	*	18	1
10	3		38	30
10	4		51	43
10	5	*	33	3
10	6	*	34	4
10	7	*	35	1
10	-1		51	52
10	-2	*	16	6
10	-3		43	42
10	-4		83	85
10	-5	*	24	12
10	-6	*	24	5
10	-7		24	24
10	-8		90	92
10	-9		54	54
10	-10	*	13	5
10	-11		43	43
10	-12		128	134
10	-13		47	45
11	0	*	29	0
11	1	*	19	4
11	2		32	31

RBFSC4 NELTRON DATA (T=23 C) LNOBSERVEC REFLECTIONS ARE MARKED WITH * AND UNPELIABLE WITH U

K = 0

H	L		FOBS	FCLC
0	2	*	8	1
0	4		52	52
0	6		9	2
0	8		43	40
0	10		24	25
0	12		78	79
0	14	*	10	10
0	16		19	16
0	18		11	11
1	0	*	15	1
1	2		31	33
1	4		12	14
1	6		30	31
1	8		16	16
1	10		36	42
1	12		21	23
1	14	U	28	19
1	16		17	17
1	18		18	15
1	-4	*	5	2
1	-6		44	44
1	-2	*	4	1
1	-8	*	6	3
1	-10	*	6	5
1	-12	*	7	7
1	-14		37	43
1	-16		22	18
1	-18		20	15
2	0	*	3	1
2	2		9	8
2	4		17	16
2	6		15	14
2	8		115	111
2	10		24	21
2	12		14	14
2	14	*	10	3
2	16		13	20
2	-2	*	3	2
2	-4		100	97
2	-6	*	5	1
2	-8	*	9	5
2	-10	*	6	2
2	-12		40	41
2	-14	*	7	5
2	-16	*	10	1
2	-18		10	8
3	0	*	5	4
3	2		42	43
3	4		13	11
3	6		26	28
3	8		13	14
3	10	*	9	0
3	12		15	15
3	14		42	38
3	16	*	13	13
3	-2		31	30
3	-4		13	13
3	-6		104	104
3	-8		11	12
3	-10	*	8	1
3	-12		9	4
3	-14		14	16
3	-16	*	10	0
3	-18		44	49
4	0		47	49
4	2		10	13
4	4		97	94
4	6		24	25
4	8		42	41
4	10		25	25
4	12		39	38
4	14		30	28
4	-2		5	4
4	-4		48	48
4	-6		12	11
4	-8	*	6	1
4	-10		20	19
4	-12		50	49
4	-14	*	7	6
4	-16	*	10	3
4	-18	*	10	3
5	0		19	21
5	2		80	84
5	4		24	25
5	6		30	25
5	8		43	42
5	10		22	24
5	12		16	16
5	14		20	19
5	-2		44	45
5	-4	*	5	4
5	-6		45	45
5	-8	*	8	5
5	-10		104	100
5	-12	*	6	0
5	-14	*	7	6
5	-16	*	10	7
5	-18		30	34
6	0	*	5	1
6	2		32	34
6	4		56	55
6	6		28	28
6	8		15	12
6	10		11	11
6	12		48	38
6	14	*	9	6
6	-2	*	8	5
6	-4		10	10
6	-6	*	9	7
6	-8	*	9	0
6	-10	*	9	7
6	-12		37	36
6	-14	*	6	0
6	-16		43	40
6	-18	*	10	3
7	0		13	13
7	2		22	22
7	4	*	10	6
7	6		20	24
7	8	*	7	6
7	10		13	17
7	12		19	19
7	14	*	9	5
7	-2		84	93
7	-4		8	11
7	-6		25	24
7	-8		26	28
7	-10	*	6	0
7	-12		23	24
7	-14	*	7	3
7	-16	*	10	0
7	-18		10	10
8	0		47	45
8	2	*	6	3
8	4		44	41
8	6		28	27
8	8		37	36
8	10		22	18
8	12		39	40
8	-2	*	11	11
8	-4		86	87
8	-6		14	13
8	-8		42	44
8	-10		31	30
8	-12		56	53
8	-14		26	27
8	-16		67	70
8	-18		23	24
9	0		28	28
9	2		8	11
9	4		39	38
9	6		60	59
9	8		14	14
9	10	*	10	12
9	12		13	12
9	-2		15	16
9	-4	*	9	6
9	-6		32	29
9	-8	*	6	1
9	-10		8	6
9	-12		12	14
9	-14		8	9
9	-16		25	23
9	-18		13	18
10	0	*	6	1
10	2		21	22
10	4		71	74
10	6		26	28
10	8		62	53
10	10	*	9	4
10	-2		25	25
10	-4		55	56
10	-6	*	6	4
10	-8		113	109
10	-10	*	7	4
10	-12		47	47
10	-14		8	3
10	-16		52	50
10	-18	*	14	13
11	0		17	18
11	2		52	52
11	4	*	14	12
11	6	*	13	17
11	8	*	10	5
11	10		10	17
11	-2		13	10
11	-4	*	6	2
11	-6		21	24
11	-8		11	10
11	-10		48	47
11	-12		18	17
11	-14		7	3
11	-16		12	8
11	-18	*	10	1
12	0		54	53
12	2		13	14
12	4	*	10	5
12	6	*	10	4
12	8		29	33
12	-2	*	9	8
12	-4		44	46
12	-6	*	6	1
12	-8		54	52
12	-10		15	16
12	-12		89	86
12	-14		37	36
12	-16	*	10	3
12	-18		25	27
13	0		13	12
13	2		42	41
13	4		17	16
13	6		14	11
13	8	*	9	4
13	-2		50	51
13	-4		7	11
13	-6		34	33
13	-8	*	7	6
13	-10	*	7	3
13	-12		8	12
13	-14		41	45
13	-16		24	23
13	-18		32	31
14	0	*	10	4
14	2		12	17
14	4		18	16
14	6		9	4
14	-2		10	13
14	-4		75	80
14	-6		10	9
14	-8		17	16
14	-10	*	6	3
14	-12	*	7	7
14	-14	*	10	3
14	-16	*	10	12
14	-18	*	10	8
15	0	*	9	2
15	2	*	10	9
15	4	*	9	7
15	-0	*	10	2
15	-2		44	44
15	-4	*	14	15
15	-6		55	55
15	-8	*	10	4
15	-10		25	26
15	-12	*	10	3
15	-14	L	27	15
15	-16	*	10	5
15	-18		38	32
16	0		18	20
16	2	*	9	2
16	4		15	11
16	-2		13	3
16	-4	*	10	3
16	-6	*	10	3
16	-8		34	40
16	-10	*	10	1
16	-12		40	37
16	-14		17	14
16	-16		26	20
16	-18		16	16
17	0		14	15
17	2		18	27
17	-2	*	9	9
17	-4	*	10	0
17	-6	*	14	18
17	-8	*	10	2
17	-10	*	10	8
17	-12	*	10	8
17	-14		45	42
17	-16		16	10
17	-18		24	16
18	0	*	8	1
18	-2	*	9	1
18	-4		16	20
18	-6	*	10	7
18	-8		62	63
18	-10	*	11	3
18	-12		51	47
18	-14	*	10	5
18	-16		15	23
18	-18	*	9	5
19	-2		21	28
19	-4	*	9	8
19	-6		20	17
19	-8	*	10	1
19	-10	*	10	3
19	-12	*	10	6
19	-14		19	22
19	-16	*	9	7
19	-18	*	9	5
20	-6	*	9	7
20	-8		31	36
20	-10	*	9	2
20	-12		40	42
20	-14	*	9	4
20	-16		28	30

K = 1

H	L		FOBS	FCLC
0	1	*	6	4
0	2	*	7	5
0	3	*	7	4
0	4		67	64
0	5		77	73
0	6	*	9	8
0	7		23	26
0	8		77	73
0	9		54	49
0	10	*	10	0
0	11		36	32
0	13	*	10	8
1	0	*	6	0
1	1	*	12	9
1	2	*	7	5
1	3		15	19
1	4	*	26	15
1	5		13	14
1	6		35	41
1	7		18	16
1	8	*	10	8
1	10	*	12	4
1	11		34	31
1	12	*	10	6
1	-1	*	6	1
1	-2		65	63
1	-3	*	13	14
1	-5	*	8	9
1	-7	*	9	5
1	-8	*	8	3
1	-9		36	32
1	-10		30	27
1	-11		26	30
2	0	U	116	129
2	1		34	30
2	2	*	5	1
2	3		78	75
2	4		95	94
2	5	*	9	5
2	6	*	9	4
2	7		14	17
2	8		19	22
2	10	*	12	11
2	9	*	12	5
2	10	*	12	11
2	-1	*	22	12
2	-2	*	7	0
2	-3		11	9
2	-4		10	10
2	-6	*	8	4
2	-7		22	20
2	-8	*	10	3
2	-10	*	10	7
2	-11	*	11	7
3	0		12	13
3	1	*	7	2
3	3	*	8	2
3	4	*	9	1
3	5		28	32
3	6		45	40
3	7		32	37
3	8	*	10	5
3	9	*	11	10
3	10	*	10	3
3	-2	*	7	8
3	-4	*	7	2
3	-5		31	33
3	-6		21	24
3	-7		24	28
3	-8	*	9	1
3	-9		49	45
3	-10		64	59
3	-11	*	10	3
3	-12	*	9	9
3	-13		67	62
4	0	*	6	0
4	1		48	50
4	2	*	8	7
4	3		23	26
4	4	*	12	13
4	5		24	28
4	6	*	10	6
4	7	*	10	4
4	8		27	31
4	-1	*	7	3
4	-2	*	23	12
4	-4		58	65
4	-5	*	8	6
4	-6	*	8	3
4	-7		37	33
4	-8		20	23
4	-9	*	10	6
4	-10	*	10	6
4	-11		29	25
4	-12	*	10	4
5	0	*	8	3
5	1	*	8	6
5	2		31	36
5	3		25	29
5	4	*	9	10
5	5		6	9
5	6		25	25
5	7	*	12	9
5	8	*	9	3
5	-1		50	53
5	-2		45	44
5	-3		71	77
5	-4	*	5	2
5	-5		65	73
5	-6		29	34
5	-7		12	15
5	-8	*	9	1
5	-9	*	9	2
5	-10		34	31
5	-11		28	24
5	-12	*	10	2
6	0		27	29
6	1		16	19
6	2	*	9	5
6	3		17	21
6	4		44	44
6	6	*	12	2
6	7		26	30
6	-1	*	9	1
6	-2	*	9	0
6	-3	*	8	4
6	-4		80	91
6	-5		6	7
6	-6	*	9	11
6	-7	*	9	6
6	-8	*	10	4
6	-10	*	10	0
6	-11		11	15
6	-12		12	15
7	0		11	11
7	1		35	33
7	2	*	8	5
7	3	*	7	7
7	4	*	5	1
7	5		28	23
7	6		55	50
7	-1		32	28